Stoichiometric Producer-Grazer Models

Incorporating the Effects of Excess Food-Nutrient Content

on Grazer Dynamics

by

Angela Peace

A Dissertation Presented in Partial Fulfillment
of the Requirement for the Degree
Doctor of Philosophy

Approved May 2014 by the
Graduate Supervisory Committee:

Yang Kuang, Chair
James J. Elser
Wenbo Tang
Yun Kang
Steven Baer

ARIZONA STATE UNIVERSITY

August 2014

ABSTRACT

There has been important progress in understanding ecological dynamics through the development of the theory of ecological stoichiometry. This fast growing theory provides new constraints and mechanisms that can be formulated into mathematical models. Stoichiometric models incorporate the effects of both food quantity and food quality into a single framework that produce rich dynamics.

While the effects of nutrient deficiency on consumer growth are well understood, recent discoveries in ecological stoichiometry suggest that consumer dynamics are not only affected by insufficient food nutrient content (low phosphorus (P): carbon (C) ratio) but also by excess food nutrient content (high P:C). This phenomenon, known as the *stoichiometric knife edge*, in which animal growth is reduced not only by food with low P content but also by food with high P content, needs to be incorporated into mathematical models. Here we present Lotka-Volterra type models to investigate the growth response of *Daphnia* to algae of varying P:C ratios.

Using a nonsmooth system of two ordinary differential equations (ODEs), we formulate the first model to incorporate the phenomenon of the *stoichiometric knife edge*. We then extend this stoichiometric model by mechanistically deriving and tracking free P in the environment. This resulting full knife edge model is a nonsmooth system of three ODEs. Bifurcation analysis and numerical simulations of the full model, that explicitly tracks phosphorus, leads to quantitatively different predictions than previous models that neglect to track free nutrients. The full model shows that the grazer population is sensitive to excess nutrient concentrations as a dynamical free nutrient pool induces extreme grazer population density changes. These modeling efforts provide insight on the effects of excess nutrient content on grazer dynamics and deepen our understanding of the effects of stoichiometry on the mechanisms governing population dynamics and the interactions between trophic levels.

ACKNOWLEDGEMENTS

I would like to express my deep appreciation and gratitude to my advisor, Dr. Yang Kuang, for providing constant encouragement and guidance, all the way from my undergraduate days to the completion of this doctoral degree. I would also like to thank my committee member, Dr. James J. Elser for his infectious enthusiasm, biological insight, and willingness to allow a mathematician to attempt experiments in his laboratory. I am also grateful to Dr. Yun Kang, Dr. Steven Baer, and Dr. Wenbo Tang, for the friendly guidance and thought-provoking suggestions they provided as members of my committee.

I would like to recognize my colleagues Rebecca Everett and Ilyssa Summer for their optimism and support over the years. I am truly fortunate to have had the opportunity to work alongside such dedicated comrades. Finally, I would like to acknowledge my husband, Tyrus Peace, for his unquestionable loving support all along the way.

TABLE OF CONTENTS

CHAPTER Page

LIST OF TABLES

LIST OF FIGURES

Figure Page

Figure Page

Figure Page

Figure Page

Figure Page

Figure Page

Figure Page

Figure Page

Chapter 1

INTRODUCTION

1.1 The Stoichiometric Framework

Many ecological models have focused on how a single constituent, usually carbon (C) or energy, is transferred between the producer and the grazer trophic levels. A classic example is the Rosenzweig MacArthur variation of the Lotka-Volterra equations,

$$\frac{dx}{dt} = bx\left(1 - \frac{x}{K}\right) - f(x)y \tag{1.1a}$$

$$\frac{dy}{dt} = ef(x)y - dy \tag{1.1b}$$

where $x(t)$ and $y(t)$ are the biomass of the producer and grazer respectively with units of C. Parameter b is the producer intrinsic growth rate and d is the grazer loss rate. Parameter e is the constant production efficiency, converting producer biomass into grazer biomass; $e < 1$ due to the second law of thermodynamics. K is the constant producer carrying capacity with units of C. Function $f(x)$ is the grazer ingestion rate, usually taken to be a Holling type functional response. Here the dynamics simply describe the amount of carbon in each species and the flux of carbon between them. The producer carrying capacity, K, is arbitrarily defined as a constant in terms of carbon.

These assumptions on the chemical homogeneity of both trophic levels may lead to serious consequences for modeling predictions. Consider, for example, the data presented by Urabe *et al.* (2002) in Figure 1.1. These are data of green algae *Scenedesmus acutus* (producer) and *Daphnia* (grazer) populations under different light treatments. Under low light the species look to be coexisting around an equilibrium

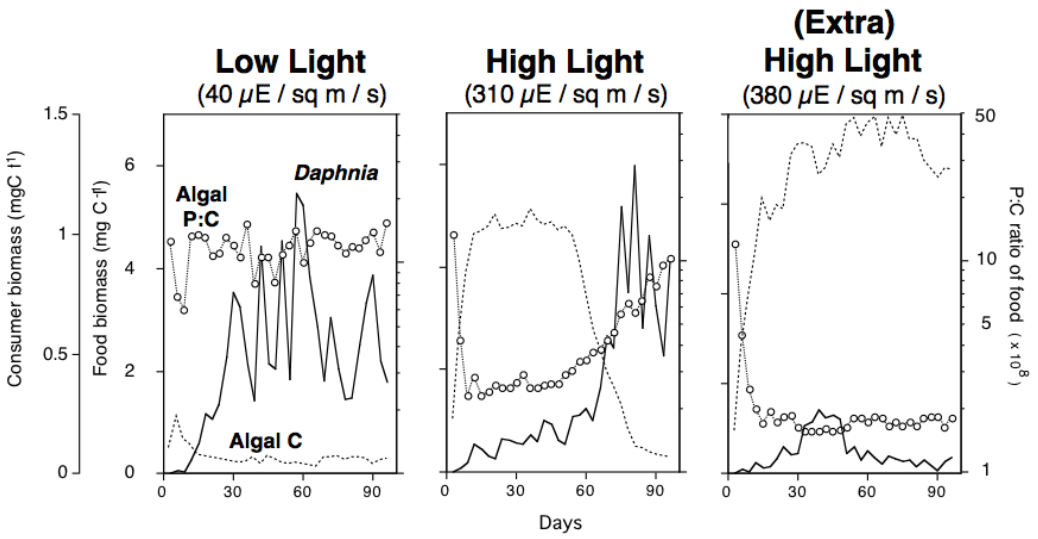

Figure 1.1: Data presented in Urabe *et al.* (2002) of green algae *Scenedesmus acutus* (producer) and *Daphnia* (grazer) populations under different light treatments. The algal P:C data, or food quality, is also given. Under low light the algae population is low in quantity but high in quality (high P:C ratio). Here the Daphnia population is in high abundance since their food is of good quality. Under high light the populations appear to be cyclical. Under extra high light the algae population is high in quantity but low in quality (low P:C ratio). Here the *Daphnia* population is in low abundance, even near extinction, despite the available food abundance. This is due to low food quality.

value. Under high light the species look to be in a cyclical regime. These are two scenarios that System (1.1) can capture. Interesting dynamics occur when the system is under extra high light. Here the algae population prospers and is in high abundance. However, despite this large quantity of available food, the *Daphnia* population is not able to prosper and is in low abundance, near extinction. This scenario is where System (1.1) breaks down and is unable make correct predictions. This is an issue of

food quality, which is where single currency models like System (1.1) fail. Figure 1.1 also shows data for the algal phosphorus to carbon ratio (P:C). This ratio represents the *quality*, of the algae. Under low light the algae population is low in quantity but high in quality (high P:C ratio). Here the Daphnia population is in high abundance since their food is good quality. Under extra high light the algae population is high in quantity but low in quality (low P:C ratio). Here the *Daphnia* population is in low abundance, even near extinction, despite the abundance of available food. This is due to low food quality.

Single currency models are commonly utilized despite the fact that all organism are composed of several chemical elements including carbon, nitrogen (N), and phosphorus (P) and the relative abundance of these chemical elements vary considerably between species and trophic levels. Interestingly A.J. Lotka explored the importance of the underlying elemental basis of life and knew the importance of multiple constituents in living systems (Lotka (1925); Elser *et al.* (2012)). Despite the known importance of chemical heterogeneity in nature, it has not been until recently that this importance has been studied by theoretical ecologists. Recent advances towards the understanding of ecological interactions have been made through the development of the theory of ecological stoichiometry (Sterner and Elser (2002)). This theory considers the balance of multiple chemical elements and how the relative abundance of essential elements such as C, N, P in organisms affects ecological dynamics. Ecologists have made important progress and have collected a large amount of data from both lab experiments and field sites to support ecological stoichiometry (Andersen (1997); Sterner and Elser (2002); Urabe and Sterner (1996); Elser *et al.* (1996, 1998); Elser and Urabe (1999); Elser *et al.* (2000, 2001); Urabe *et al.* (2002); McCauley *et al.* (2008); Hessen *et al.* (2013)).

The fast growing empirical study of ecological stoichiometry provides new con-

straints and mechanisms that can be formulated into mathematical models. As a result, stoichiometric models incorporate the effects of both food quantity and food quality into a single framework that produces rich dynamics.

Section 1.2 discusses some basic modeling approaches that are used to incorporate stoichiometric effects into producer and grazer growth functions. Section 1.3 presents motivations and goals of this research.

1.2 Building a Stoichiometric Model

1.2.1 Producer Growth Functions

Logistic Growth

It has long been known that the growth of any producer population depends on environmental conditions and must be bounded by finite resources. Verhulst (1838, 1845) defined the carrying capacity of an ecosystem to incorporate the idea of finite resources into ecological population models. His famous *logistic growth curve* takes the following form:

$$\mu_x = bx\left(1 - \frac{x}{K}\right) \tag{1.2}$$

where μ_x is the specific growth rate and b is the intrinsic growth rate of producer x. The carrying capacity is simply K. This represents all environmental factors that may bound the density of the producer population and has units C. Loladze *et al.* (2000) considered the consequences of determining the upper bound of a population density by a single constant when developing the LKE model (presented in section 2.1). They proposed a modification to Eq. (1.2) that allows producer growth to be limited by available C or available P. This *stoichiometric logistic growth curve* takes

the following form:

$$\mu_x = bx\left(1 - \frac{x}{\min\left\{K, \frac{P_a}{q}\right\}}\right) \tag{1.3}$$

where P_a is the total amount of phosphorus available for producer growth and q is the producer's minimal P:C ratio. Here they have redefined the carrying capacity to be determined by K, a term representing available C or light intensity, or $\frac{P_a}{q}$, a term representing growth limited by available P. The use of the minimum function follows directly from Justin Leibig's law of the minimum, which states that an organism's growth will be limited by whichever single resource is in lowest supply relative to the organism's needs (Sterner and Elser (2002)).

Droop's Cell Quota Growth

There is a difference between nutrient uptake and nutrient-controlled growth. Nutrient-controlled growth depends on nutrients inside the cell. Michael Droop defined the cell quota, Q, as the total cell nutrient per unit biomass (Droop (1968)). This definition allows the growth rate to depend on an internal nutrient pool. While analyzing measurements from vitamin B_{12}-limited chemostat cultures of *Monochrysis lutheri*, Droop discovered a simple relationship between specific growth rate (μ_x) and the cell quota (Q):

$$\mu_x = \mu_m\left(1 - \frac{q}{Q}\right) \tag{1.4}$$

where q is the smallest amount of internal nutrient on which the cell can exist and μ_m is the maximum specific growth rate, an unreachable asymptote defined with $\frac{1}{Q} = 0$ (Droop (1968); Tett and Droop (1988)).

Since carbon makes up a large proportion of total biomass and there is generally little variation in the carbon to volume ratio, carbon is often used as the measure of biomass. The cell quota is then defined as the ratio of a specific nutrient to carbon. A

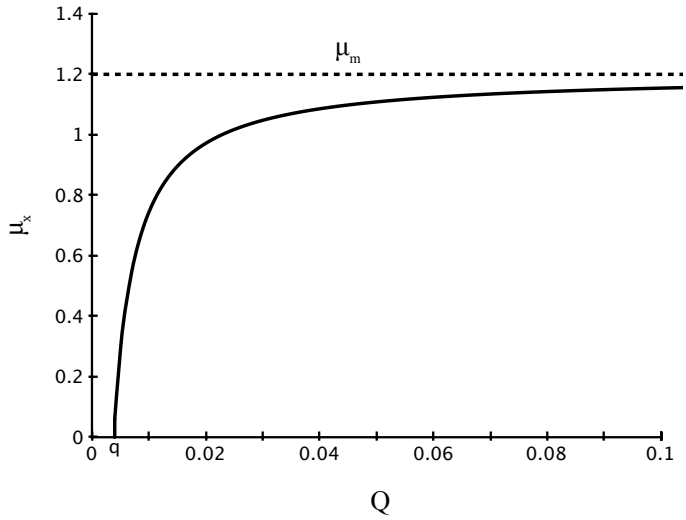

Figure 1.2: Droop cell quota function, Eq. (1.4). This shows the relationship between specific growth rate (μ_x) and the cell quota (Q). Here $\mu_m = 1.2$, $q = 0.004$

classic example is used when modeling phosphorus limited algae. Here the cell quota is the phosphorus to carbon ratio, Q=P:C of the algae. It is very natural to use cell quota dynamics in stoichiometric models, since this formulation allows the growth rate to depend on internal nutrient concentrations. Allowing Q to vary, depending on the available nutrients in the environment, brings stoichiometry into the model.

The cell quota could be defined using any other element that is essential to growth. One can take a threshold approach and follow Leibig's law of the minimum. This leads to the assumption that only one factor is in control at any one time, or only one nutrient limits growth at any given time. The limiting nutrient is the nutrient for which the respective normalized quota is the smallest. Thingstad (1987) combined Droop's growth equation Eq. (1.4) and Leibig's law of the minimum into an expression for growth rate, which depends on three nutrients:

$$\mu_x = \mu_m \left(1 - \max\left\{\frac{q_C}{Q_C}, \frac{q_N}{Q_N}, \frac{q_P}{Q_P}\right\}\right) \tag{1.5}$$

where q_C, q_N, q_P are the minimal cell quotas and Q_C, Q_N, Q_P are the cell quotas for

carbon, nitrogen, and phosphorus respectively. Here these quotas are the nutrient to cell number ratios.

Logistic Growth vs. Droop's Cell Quota Growth

Kuang *et al.* (2004) mechanistically formulated a tractable stoichiometric plant-herbivore model using Droop's cell quota growth expression. They showed that the classical logistic model can be mechanistically derived from the Droop equation. Following their approach, we can see the similarities between these two approaches. Consider a simple cell quota population model,

$$x' = \mu_m \left(1 - \frac{q}{Q}\right) x - Dx \tag{1.6}$$

where x is the biomass of the producer given in units C, μ_m is the maximum specific growth rate, q is minimal cell quota, and D is the producer specific loss rate. Let Q be the P:C ratio of the producer, a stoichiometric variable term. Let P_a be the amount of P in the producer population available for growth. Then $Q = \frac{P_a}{x}$ and the equation becomes:

$$x' = \mu_m \left(1 - \frac{q}{\frac{P_a}{x}}\right) x - Dx \tag{1.7a}$$

$$= \mu_m \left(1 - \frac{x}{\frac{P_a}{q}}\right) x - Dx \tag{1.7b}$$

$$= (\mu_m - D)x \left(1 - \frac{x}{\frac{\mu_m - D}{\mu_m}\frac{P_a}{q}}\right) \tag{1.7c}$$

The growth term above now resembles the Logistic growth expression Eq. (1.2) with net growth rate $b = \mu_m - D$ and a carrying capacity defined in terms of phosphorus, $K = \frac{\mu_m - D}{\mu_m}\frac{P_a}{q}$. Kuang *et al.* (2004) explained this expression for the carrying capacity. The theoretical carrying capacity in terms of phosphorus is $\frac{P_a}{q}$, however the actual upper limit that the producer biomass can attain is the smaller expression $\frac{\mu_m - D}{\mu_m}\frac{P_a}{q}$.

The theoretical maximal carrying capacity ($\frac{P_a}{q}$) can never actually be reached since the population's loss rate will keep it below its maximum.

If we assume that the producer loss rate (D) is negligibly small compared to its maximal growth rate (μ_m) then $\frac{\mu_m - D}{\mu_m} \approx 1$. Taking this assumption and applying Leibig's law to Eq. (1.7c) to allow growth to be limited by carbon as well as phosphorus yields the following:

$$x' = (\mu_m - D)x \left(1 - \frac{x}{\min\left\{K, \frac{P_a}{q}\right\}} \right) \tag{1.8}$$

which is comparable to Eq. (1.3).

1.2.2 Grazer Growth Functions

The Rosenzweig MacArthur variation of the Lotka-Volterra equations (System 1.1) uses the simple expression for the growth of the grazer:

$$\mu_y = ef(x)y \tag{1.9}$$

where constant e is the production efficiency, converting producer biomass into grazer biomass, and $f(x)$ is the grazer ingestion rate, usually taken to be a Holling type II functional response. Loladze *et al.* (2000) questioned the validity of a constant production efficiency, e. In order to incorporate the effects of food quality, the grazer production efficiency should be reduced when the producer food quality becomes low. Following an approach presented by Andersen (1997), Loladze *et al.* (2000) assumed the producer is optimal food for the grazer if its P:C ratio is equal to or greater than the P:C ratio of the grazer, in the LKE model (presented in section 2.1). After a modification to the production efficiency, the grazer growth expression takes the following form:

$$\mu_y = \hat{e} \min\left(1, \frac{Q}{\theta}\right) f(x)y \tag{1.10}$$

where $\hat{e} < 1$ is the maximal production efficiency and θ is the grazer P:C ratio. This new expression for production incorporates the effects of low nutrient food content on grazer dynamics.

Comparing the producer quota (Q) to the grazer quota (θ) is a typical way to incorporate food quality into grazer growth and bring stoichiometry into the model. Indeed, ecological stoichiometry is based on the observation that there are stoichiometric mismatches between trophic levels that profoundly affect trophic efficiency and nutrient fluxes (Hessen *et al.* (2013)).

One important feature in many stoichiometric models is the use of minimum functions to incorporate stoichiometry. The minimum functions act as switches as growth is limited by different nutrients. This approach of only one resource limiting at a time is called the threshold approach and is often used when formulating stoichiometric models, making them nonsmooth systems. The threshold approach follows directly from Justin Leibig's law of the minimum, which states that an organism's growth will be limited by whichever single resource is in lowest supply relative to the organism's needs (Sterner and Elser (2002)). It may be important to note that the law of the minimum applies to an individual organism and our models are at the scale of a population, therefore, our uses of minimum functions present approximations of the population dynamics. Loladze *et al.* (2000) stated that the main qualitative results of their stoichometric nonsmooth model are not affected by changing the minimum functions to their smoother analogs. When dealing with threshold functions, like the minimum functions that arise in many stoichiometric models, the analysis must be split into two parts. However, the two cases will often be simple compared to their smooth analogs.

Special precautions must be taken when analyzing nonsmooth dynamics. For example, Dulac's criterion is very useful in smooth dynamical systems when ruling

out the existence of limit cycles in regions of the plane. However the classical Dulac's criterion requires the vector field to be C^1, which is not the case with these nonsmooth functions. Fortunately, Sanchez (2005) generalizes Dulac's criterion for locally Lipshitz-continuous planar systems that need not be C^1. This generalized Dulac's criterion was used in a global model analysis by (Li *et al.* (2011)).

Nonsmooth dynamical systems have been receiving increasing attention recently. Makarenkov and Lamb (2012) discuss the need to develop new mathematical methods to study the dynamics of nonsmooth systems, which are motivated by real world applications. These types of systems arise in engineering and mechanics, neuroscience, hydrodynamics, as well as in ecological modeling. Makarenkov and Lamb (2012) give a nice survey on the current directions of research on nonsmooth systems with an emphasis on bifurcation theory that includes 400 citations.

1.3 Motivation and Goals

Throughout recent years a wide variety of stoichiometric producer-grazer population models have been proposed and studied. These models vary from two-dimensional producer-grazer models that consider only two chemical constituents to more complicated models that incorporate multiple species and multiple constituents (Nisbet *et al.* (1991); Andersen (1997); Muller *et al.* (2001); Grover (2002, 2003, 2004); Loladze *et al.* (2000); Kuang *et al.* (2004); Miller *et al.* (2004); Fan *et al.* (2005); Sui *et al.* (2007); Wang *et al.* (2008); Stech *et al.* (2012a); Peace *et al.* (2013); Wang *et al.* (2012)). A literature review of stoichiometric producer grazer models is presented in Chapter 2. These models introduce food quality by incorporating the effects of nutrient deficiencies on grazer growth.

It is clear that low nutrient food content causes a nutrient deficiency in grazers, the consequences of which are relatively well understood and modeled (Loladze *et al.*

(2000); Elser *et al.* (2001); Demott *et al.* (1998); Frost *et al.* (2006)). However, recent reported empirical data suggest that grazer dynamics are also affected by *excess* food nutrient content (Boersma and Elser (2006); Elser *et al.* (2006)).

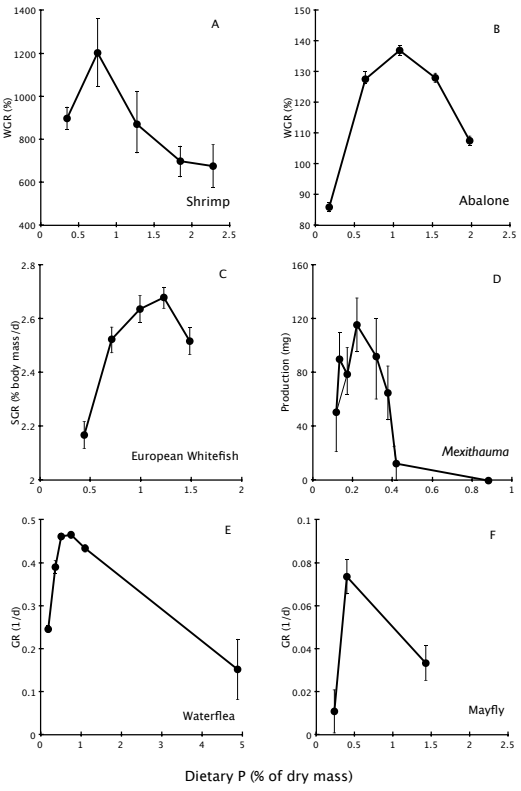

Figure 1.3: Empirical data showing the *stoichiometric knife edge* reported by Boersma and Elser (2006). The x-axis is P content of the food and the y-axis is growth rate, given by GR (instantaneous growth rate), SGR (specific growth rate in percentage body mass per day), or WGR (mass gain rate: increase in body mass).

This phenomenon, called the *stoichiometric knife edge*, reflects a reduction in animal growth caused not only by food with low P content but also by food with excessively high P content. The effects of excess nutrients have recently been receiving attention and there are several examples reporting the knife edge phenomenon for a variety of grazers (*Daphnia*, snails, insects, fish) (Elser *et al.* (2012); Boersma and Elser (2006); Elser *et al.* (2006, 2005)), Figure 1.3. Unfortunately there is still little known about the general shape of the relationship between grazer growth rate and food P:C ratio. The shape of this curve may vary among different grazers. The recent data on this phenomenon motivate us to rethink our notion of optimal food. The *stoichiometric knife edge* implies that optimal food should no longer be considered as food with sufficient nutrient content, which just accounts for avoiding deficien-

cies, but instead as food with a balanced nutrient content, avoiding both deficient and excess nutrient food content.

Understanding the issues of excess nutrients is especially important as human activities, such as mining phosphorus for agricultural uses, continue to alter the global P cycle. Human induced nutrient loads can be several magnitudes higher relative to natural levels (Elser and Bennett (2011); Smith and Schindler (2009)). P concentrations of freshwater systems worldwide are estimated to be at least 75% greater than preindustrial levels (Bennett *et al.* (2001); Gaxiola *et al.* (2011)). Empirical data shows that up to 10% of aquatic habitats have measurements of high algal P:C, in the range where grazer growth begins to decline due to excess P (Sterner *et al.* (2008)).

While the effects of low food nutrient content have been incorporated into stoichiometric food web models, the models presented in this paper are the first to incorporate the effects of excess nutrient content. We consider an ecological system of algae (producer) and *Daphnia* (grazer). One of the main goals of developing these models is to gain insight on the effects of excess nutrient content on grazer dynamics. We hope to better our understanding of the effects of stoichiometry on the mechanisms governing population dynamics and the interactions between trophic levels.

Chapter 2 presents a literature review on the existing stoichiometric producer-grazer models. The existing models incorporate the effects of low nutrient food content on grazer dynamics. Chapter 3 presents and analyzes a Lotka-Volterra type model to investigate the growth response of *Daphnia* to algae of varying P:C ratios. This model incorporates the effects of low and excess nutrient food content on grazer growth. The model developed in Chapter 3 captures the mechanism of the *stoichiometric knife edge*. Chapter 4 extends this model by mechanistically deriving and tracking P in the producer and free P in the environment in order to investigate the growth response of Daphnia to algae of varying P:C ratios. Bifurcation analysis and numerical

simulations of the full model, which explicitly tracks phosphorus, lead to quantitatively different predictions than previous models that neglect to track free nutrients. The full model shows that the fate of the grazer population is very sensitive to excess nutrient concentrations.

Chapter 2

REVIEW OF THE DYNAMICS OF SOME BASIC STOICHIOMETRIC MODELS

Since the development of the theory of ecological stoichiometry (Sterner and Elser (2002)), a wide variety of stoichiometric models have been proposed and analyzed. Some are simple yet mathematically tractable systems of two species that consider two currencies while others are more complicated and incorporate multiple species and multiple currencies. Some make the assumption that grazer stoichiometries are fixed, while others relax this assumption. Some models make simplifying assumptions on nutrient levels in the environment while others explicitly track nutrients in the media. In this chapter we present an overview of stoichiometric models that have been developed and analyzed.

Section 2.1 starts off with stoichiometric producer-grazer models that incorporate the effects of low nutrient content on population dynamics. Here the producer is assumed to have a variable nutrient to carbon ratio while that of the grazer is fixed. Rather than explicitly tracking nutrient levels in the environment, these models assume all available nutrients are in the producer and grazer populations. This assumption leads to a fully tractable system of two ordinary differential equations that provides a good structure for stoichiometric modeling. Section 2.2 presents stoichiometric models that consider free nutrients in the environment. These models lead to different quantitative predictions than previous models. Section 2.3 presents variations to the stoichiometric modeling schemes presented in Sections 2.1 and 2.2, which further investigate the possible dynamics of stoichiometric producer-grazer models. These models help address whether commonly seen stoichiometric effects are robust to modeling variations such as increasing the number of species and/or nutrients,

discretization in time, allowing for non-homeostatic grazers, and an alternative smooth modeling approach.

2.1 Nutrient Quality Limited Growth Models

Andersen (1997) was one of the first to introduce stoichiometric effects on grazer growth in mathematical models. He modifies the density dependence of the producer growth rate and the grazer's growth efficiency while using a Holling type I functional response. Introducing a stoichiometric density dependence adjusts the shape of the producer nullcline and the stability properties of the system. Andersen uses Leibig's law with a minimum function to represent the constraint on grazer growth, caused by low nutrient food content of the producer. This constraint dramatically changes the shape of the grazer nullcline from the simple single currency models. In Andersen's model the grazer nullcline is made up of two branches; a vertical branch similar to single currency Lotka-Volterra models where food quantity determines growth and a sloped branch where food quality determines growth (Andersen (1997); Andersen *et al.* (2004)).

Following Andersen's approach, Loladze *et al.* (2000) formulate a very nice tractable two-dimensional Lotka-Volterra type model to capture the dynamics of the data presented in Figure 1.1. This model, called the LKE model (Elser *et al.* (2012)), incorporates stoichiometry into the transfer of 2 currencies (C,P) between producer and grazer. It provides a foundation that many future stoichiometric models build upon. It utilizes the fact that both producer and grazer are chemically heterogeneous organisms. Specifically, it tracks the amount of two essential elements, C and P, in each trophic level. It allows the P:C ratio of the producer to vary above a minimum value, which effectively brings food quality into the model. The LKE model makes the following assumptions:

A1: *The total mass of phosphorus in the entire system is fixed, i.e., the system is closed for phosphorus with a total of P (mgP/L).*

A2: *P:C ratio in the producer varies, but it never falls below a minimum q (mgP/mgC); the grazer maintains a constant P:C, θ (mgP/mgC).*

A3: *All phosphorus in the system is divided into two pools: phosphorus in the grazer and phosphorus in the producer.*

In order to extend System (1.1) to incorporate stoichiometry following these assumptions, Loladze *et al.* (2000) modified two terms: the producer carrying capacity and the grazer production efficiency. Using the *stoichiometric logistic growth curve* Eq. (1.3), they modified the carrying capacity to be the minimum function

$$\min\left(K, \frac{P-\theta y}{q}\right). \tag{2.1}$$

This allows the carrying capacity to be determined by K, a term representing available C or light intensity, or $\frac{P-\theta y}{q}$, a term representing growth limited by available P. Since P is the total amount of phosphorus, $P-\theta y$ is the phosphorus available for producer growth according to the above assumptions. To incorporate the effects of food quality, the grazer production efficiency is reduced when the producer P:C value becomes low. Using the approach described in Eq (1.10), the LKE model assumes the producer is optimal food for the grazer if its P:C ratio is equal to or greater than the P:C of the grazer. They modified the production efficiency to be the minimum function

$$\hat{e}\min\left(1, \frac{(P-\theta y)/x}{\theta}\right). \tag{2.2}$$

where $\hat{e} < 1$ is the maximal production efficiency and $Q = \frac{P-\theta y}{x}$ is the producer's P:C ratio. This new expression for production incorporates the effects of low nutrient food content on grazer dynamics. Incorporating these modifications to System (1.1) results

in the LKE model, given below.

$$\frac{dx}{dt} = bx\left(1 - \frac{x}{\min(K, (P-\theta y)/q)}\right) - f(x)y \tag{2.3a}$$

$$\frac{dy}{dt} = \hat{e}\min\left(1, \frac{(P-\theta y)/x}{\theta}\right) f(x)y - dy \tag{2.3b}$$

Here $x(t)$ and $y(t)$ are the biomass of the producer and grazer respectively, measured in terms of C. Parameter b is the maximum growth rate of the producer, K is the producer carrying capacity in terms of C or light intensity, P is the total phosphorus in the system, θ is the grazer's constant P:C, q is the producer's minimal P:C, $\hat{e}$ is the maximum production efficiency, and d is the grazer loss rate. The grazer's ingestion rate, $f(x)$ is taken to be a monotonic increasing and differentiable function, $f'(x) \geq 0$. $f(x)$ is saturating with $\lim_{x\to\infty} f(x) = \hat{f}$.

Parameter		Value
P	Total Phosphorus	0.025 mgP / L
$\hat{e}$	Maximal production efficiency	0.8
b	Maximal growth rate of producer	1.2 days^{-1}
d	Grazer loss rate	0.25 days^{-1}
θ	Grazer constant P:C	0.03 (mgP)/(mgC)
q	Producer minimal P:C	0.0038 (mgP)/(mgC)
$\hat{f}$	Maximal ingestion rate of the grazer	0.81 days^{-1}
a	Half saturation of the grazer ingestion response	0.25 mg C / L
K	Producer carrying capacity	0.25-2.0 mg C / L

Table 2.1: Model parameters for the LKE model (System 2.3). All parameters are biologically realistic values obtained from (Andersen (1997) and Urabe and Sterner (1996)).

Loladze *et al.* (2000) provide good details on the analysis of the LKE model. They prove boundedness and invariance of the system as well as investigate the complex dynamics that lead to multiple positive equilibria and show that bistability and deterministic extinction of the grazer are possible. The analysis includes numerical simulations (Figure 2.1) and a phase plane analysis (Figure 2.2). The stoichiometric constraints of the model dramatically changes the shape of the grazer nullcline from the simple single currency models. Similar to Andersen's model (Andersen (1997)), the grazer nullcline is made up of two branches dividing the phase space into two regions. The vertical branch lies in a region where food quantity determines growth and the sloped branch lies in a region where food quality determines growth. They also present a simple graphical test to determine local stability of interior equilibria.

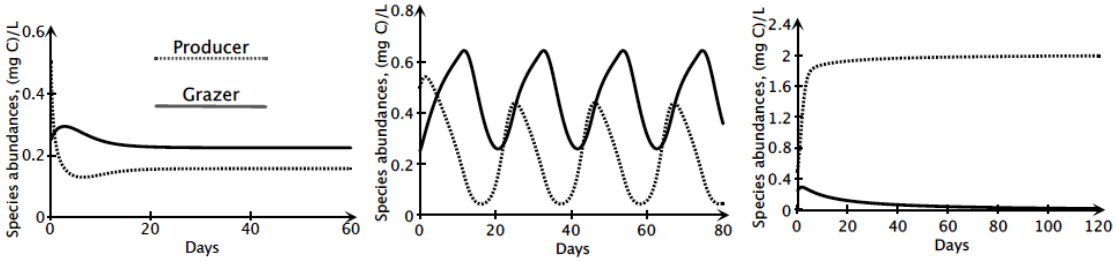

(a) Low Light (K=0.25 mgC/l) (b) High Light (K=0.75 mgC/l) (c) Extra High (K=2 mgC/l))

Figure 2.1: Simulations of the LKE model using Holling type II functional response $f(x) = \frac{\hat{f}x}{a+x}$ and parameters found in Table 1 for varying light intensity K. Compare these to the data presented in Figure 1.1. Under low light the population densities stabilize around a stable equilibrium where x is low in quantity but high in quality. Increasing K destabilizes the equilibrium and under high light the populations are cyclical. Under extra high light x is high in quantity but low in quality, which leads to deterministic extinction of y.

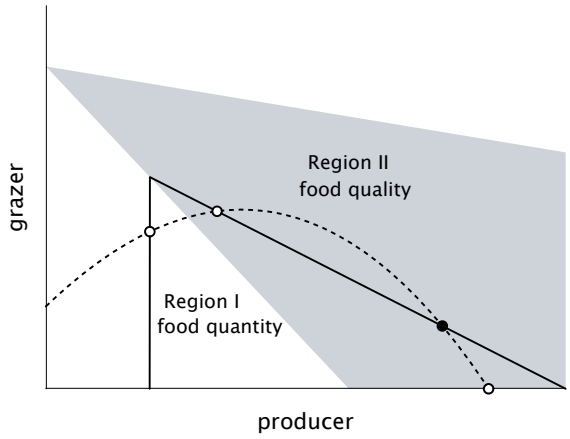

Figure 2.2: Phase plane for the LKE model (System 2.3). All solutions remain in the trapezoidal shaped region. The producer nullcline is hump shaped, similar to the classical Lotka-Volterra model (System 1.1). The grazer nullcline is made up of two branches; a vertical branch and sloped branch. These two branches divide the phase plane into two regions: region I, where grazer growth is determined by food quantity and region II, where grazer growth is determined by food quality. The effects of food quality in region II bend the grazer nullcline down.

An energy enrichment bifurcation analysis of the LKE model unveils interesting dynamical behaviors. Using K as the bifurcation parameter, Loladze *et al.* (2000), show the system exhibits a Hopf bifurcation, limit cycles, homoclinic bifurcation, and a saddle-node bifurcation, see Figure 2.3.

These energy enrichment bifurcation dynamics are common to several stoichiometric producer-grazer models (Loladze *et al.* (2000); Kooijman *et al.* (2004); Fan *et al.* (2005); Lin *et al.* (2012); Loladze *et al.* (2004); Diehl (2007)). Under low energy levels, the grazer is unable to survive due to low food quantity. Energy enrichment induces a switch in stability as the grazer population is able to coexist with the producer. Further energy enrichment brings periodic coexistence. However, even higher energy enrichment induces the collapse of the periodic solutions. Models with this bifurcation

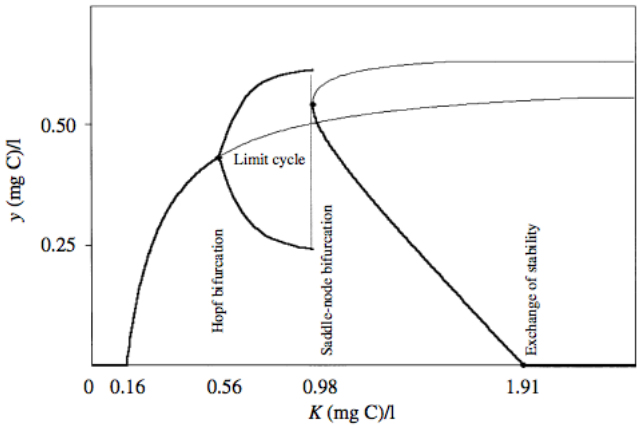

Figure 2.3: Bifurcation diagram for the LKE model (System 2.3) presented by 2.3, using Holling type II functional response $f(x) = \frac{\hat{f}x}{a+x}$ and parameters found in Table 1 with K as the bifurcation parameter. Here bold and thin lines correspond to stable and unstable equlibria, respectively. For low values of K, the grazer is unable to survive due to low food quantity. As K increases, the grazer population increases. As K continues to increase the system reaches a Hopf bifurcation and limit cycles emerge. These limit cycles are abruptly halted once K increases to the saddle-node bifurcation. Post the saddle-node bifurcation, the grazer population starts to decline and eventually reaches deterministic extinction. High values of K result in a low algal P:C ratio, which is low quality food for the grazer. The decline in grazer population caused by low food quality is a result of the stoichiometric constraints incorporated into the model.

behavior exhibit the "*paradox of energy enrichment*" (Loladze *et al.* (2000); Diehl (2007)), as increasing energy increases producer productivity and density but results in a decrease in grazer density. This decrease in grazer density is due to low food quality.

Stech *et al.* (2012a) presented and analyzed a simple model in order to gain insight into the causes of the observed energy-induced dynamics in stoichiometric

producer-grazer models. This simple system takes the following form:

$$\frac{dx}{dt} = g(x,K)x - f(x)y \tag{2.4a}$$

$$\frac{dy}{dt} = \hat{e}\mu\left(\frac{P}{x}\right)f(x)y - dy \tag{2.4b}$$

where x and y are the producer and grazer population respectively. Function $g(x,K)$ is the producer growth rate, a general function dependent on the ambient energy levels, K, $f(x)$ is the grazer's ingestion rate, $\hat{e}$ its maximal conversion efficiency, and d its death rate. The general function $\mu\left(\frac{P}{x}\right)$ is a stoichiometric constraint on grazer's growth, where P is the fixed total amount of nutrients in the system. Using this simplistic model, Stech *et al.* (2012a) concluded that the collapse of the grazer population under high energy enrichment is caused by the dilution of nutrients in the producer population (low producer nutrient:carbon ratio) and does not rely on other nutrient related processes.

Li *et al.* (2011) presented further analysis of the LKE model including a global analysis for the LKE model using a Holling type I functional response and a bifurcation analysis of the light dependent carrying capacity, K for the LKE model using a mass-action functional response. In order to globally analyze the system with a Holling type II functional response, $f(x) = \frac{cx}{a+x}$, they fixed all parameters of the LKE model (System 2.3) with values found in Table I except for the bifurcation parameter K. The model then becomes:

$$\frac{dx}{dt} = \frac{6}{5}x\left(1 - \frac{x}{\min(K, \frac{25}{4} - 10y)}\right) - \frac{16xy}{5+20x} \tag{2.5a}$$

$$\frac{dy}{dt} = \frac{4}{5}\min\left(x, \frac{5}{8} - y\right)\frac{16y}{5+20x} - \frac{1}{4}y. \tag{2.5b}$$

They divided the analysis into the following cases according to the parameter K in order to analyze the system.

- Case 1: $0 < K \leq 25/156$

- Case 2: $25/156 < K \leq 89/156$
- Case 3: $89/156 < K \leq 0.585185$
- Case 4: $0.585185 < K \leq 0.654664$
- Case 5: $0.654664 < K < 2$

This robust analysis unveils even more interesting dynamical behaviors of the LKE model including many different types of bifurcations and a region of bistability (see Figure 2.4).

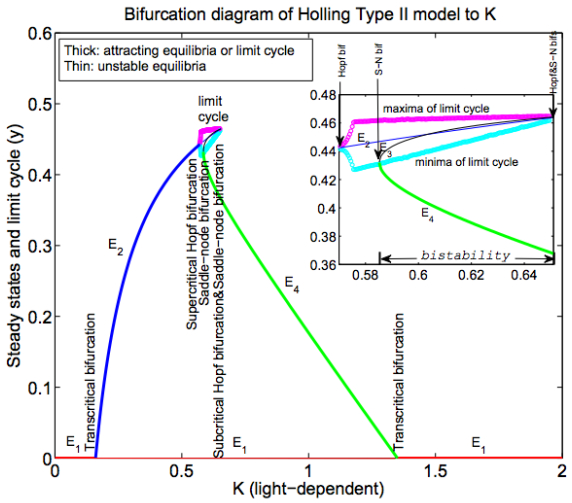

Figure 2.4: Bifurcation anlaysis of the LKE model (System 2.3) presented by Li *et al.* (2011) using Holling type II functional response $f(x) = \frac{cx}{a+x}$ and parameters found in Table 1 with K as the bifurcation parameter. This thorough investigation provides details on the complex dynamics, showcasing multiple internal equilibria, limit cycles, bistability, and supercritical, subcritical, saddle-node, and transcritical bifurcations.

As K varies, the system exhibits both supercritical and subcritical Hopf bifurcations, a saddle-node bifurcation, and a transcritical bifurcation. This bifurcation analysis in Li *et al.* (2011) provides additional information to the bifurcation analysis given by

Loladze *et al.* (2000), which suggests that the dynamical behaviors of stoichiometric models are highly sensitive to parameter values.

2.2 Expanded Nutrient Limited Growth Models That Track Free Nutrients

The LKE model, System (2.3), assumes phosphorus is either in the producer or the grazer and does not allow for free nutrients to be in the environment. This assumption is based on the fact that algae take up nutrients very quickly. This is not the case when nutrient pools in the environment are important to the dynamics of the system, as seen in terrestrial settings, for example. It is a tempting assumption to make since it reduces the system down to two equations rather than three. It is worth noting that this assumption is not always appropriate. There have been some models that explicitly track free nutrients as well as nutrients inside the producer and grazer populations (Kuang *et al.* (2004); Wang *et al.* (2008)).

Kuang *et al.* (2004) mechanistically formulated a tractable model of plant-herbivore population dynamics. They consider variable P content of a plant that follows Droop growth and an herbivore whose growth can be limited by plant food quality. Here they make the first two assumptions made by the LKE model (A1, A2), but rather than making the third assumption, they allow for phosphorus to be in the environment. Then they arrive at a system of 3 ODEs

$$\frac{dx}{dt} = \mu_m \left(1 - \frac{q}{Q}\right) x - Dx - f(x)y \tag{2.6a}$$

$$\frac{dy}{dt} = \hat{e} \min\left(1, \frac{Q}{\theta}\right) f(x)y - dy \tag{2.6b}$$

$$\frac{dQ}{dt} = \alpha P_f - \mu_m(Q - q) \tag{2.6c}$$

where x and y are the producer and grazer population, respectively. Q is the producer's variable P:C quota and θ is the grazer's constant P:C quota. D and d are the death rates of the producer and grazer, respectively. Function $f(x)$ is the grazer functional

response, μ_m is the producer's maximal growth rate, q is the producer's minimal P:C, $\hat{e}$ is the grazer's production efficiency in terms of carbon, α is the producer's P uptake rate and P_f is the free phosphorus in the environment. Since total phosphorus (P_t) is fixed the following equations holds:

$$P_t = P_f + Qx + \theta y \tag{2.7}$$

Kuang *et al.* (2004) use the fact that the time scale of cell metabolic processes is much faster than that of population growth in order to make a quasi-steady-state argument to simplify the system down to 2 ODEs by approximating $\frac{dQ}{dt} \approx 0$. After rearranging terms and allowing growth to be limited by C or P following Leibigs law, they arrive at the following simple two ODE model:

$$\frac{dx}{dt} = (\mu_m - D)x \left[1 - \max\left(\frac{x}{K}, \frac{x + \mu_m \alpha^{-1}}{[(\mu_m - D)/\mu_m]\,[\mu_m \alpha^{-1} + (P_t - \theta y)/q]}\right)\right] - f(x)y \tag{2.8a}$$

$$\frac{dy}{dt} = \hat{e} \min\left(1, \frac{Q}{\theta}\right) f(x)y - dy. \tag{2.8b}$$

They show that the LKE model is a special case of the above model. The third assumption taken by the LKE model (A3) can be applied to this model by setting P_f=0 and $\alpha = \infty$, then System (2.8) is equivalent to the LKE model (System (2.3)). They present a numerical experiment where they vary the carrying capacity, K, and compare the dynamics of System (2.8) with those of the LKE model. Both models demonstrate similar qualitative dynamics. For low and high values of K, the solutions to these models are almost identical, however for intermediate values of K the solutions are quantitively different. This shows that the mechanism for P uptake has a true influence on the dynamics, and thus stoichiometric details really matter for quantitative predictions.

Kuang et al. also show that without the grazer, System (2.8) reduces down to the

form of the classical logistic equation,

$$\frac{dx}{dt} = (\mu_m - D)x\left(1 - \frac{x}{[(\mu_m - D)/\mu_m]P_t/q}\right) \tag{2.9}$$

where the carrying capacity is given as $[(\mu_m - D)/\mu_m]P_t/q$. This model highlights the important implication that the classical logistic model can be mechanistically derived from the Droop equation.

While the simple nutrient limiting models from Section 2.1 are mathematically tractable they may make some unrealistic simplifying assumptions. These models do not explicitly track P in the producer or in the environment. System (2.8) from Kuang *et al.* (2004) provides a more mechanistic interpretation of the stoichiometric producer-grazer systems, while still being mathematically tractable. Wang *et al.* (2008) present another extension of the LKE model by explicitly tracking P in the producer and in the environment. Their model takes the following form,

$$\frac{dx}{dt} = rx\left(1 - \frac{x}{\min\{K, p/q\}}\right) - f(x)y \tag{2.10a}$$

$$\frac{dy}{dt} = \hat{e}\min\left\{1, \frac{p/x}{\theta}\right\} f(x)y - \hat{d}y \tag{2.10b}$$

$$\frac{dp}{dt} = g(P) - \frac{p}{x}f(x)y - dp \tag{2.10c}$$

$$\frac{dP}{dt} = -g(P)x + dp + \theta\hat{d}y + \left(\frac{p}{x} - \hat{e}\min\{\theta, \frac{p}{x}\}\right) f(x)y \tag{2.10d}$$

where p is the density of phosphorus in the producer, P is the density of free phosphorus in the media, r is the producer's intrinsic growth rate, d is the phosphorus loss rate in the producer, and $\hat{d}$ is the loss rate of the grazer. They assume the total phosphorus in the system is fixed and are able to reduce System (2.10) down from

four ODES to three ODEs,

$$\frac{dx}{dt} = rx\left(1 - \frac{x}{\min\{K, p/q\}}\right) - f(x)y \tag{2.11a}$$

$$\frac{dy}{dt} = \hat{e}\min\left\{1, \frac{p/x}{\theta}\right\} f(x)y - \hat{d}y \tag{2.11b}$$

$$\frac{dp}{dt} = g(P) - \frac{p}{x}f(x)y - dp \tag{2.11c}$$

where P is simply the total phosphorus minus the phosphorus in the producer and grazer populations. Wang *et al.* (2008) provide analysis of this model, including positive invariance and boundedness, stability of boundary equilibria, and numerical bifurcation analysis and simulations. They found quantitative differences between their model and the LKE model. Similar to the model presented by Kuang *et al.* (2004) (System (2.8)), the LKE model is a limiting case of System (2.11) as well. However, unlike the LKE model, System (2.11) can easily be extended to include the dynamics of multiple species.

2.3 Model Variations

2.3.1 Discrete Models

Many continuous stoichiometric producer-grazer models seem to exhibit distinctive features. Firstly, grazers can become extinct deterministically when producers are high in quantity but low in quality. Secondly, producer-grazer oscillations are suddenly halted as producer quality decreases. Fan *et al.* (2005) and Sui *et al.* (2007) examine the discrete analogs of continuous stoichiometric models in order to determine if stoichiometric effects are just artifacts of continuous time models. Furthermore, it is also crucial to determine if new stoichiometric effects arise in discrete systems.

Fan *et al.* (2005) consider the discrete analog of the LKE model, System (2.3),

$$x(n+1) = x(n)\exp\left\{b - \frac{bx(n)}{\min\{K,(P-\theta y(n))/q\}} - \frac{f(x(n))y(n)}{x(n)}\right\} \tag{2.12a}$$

$$y(n+1) = y(n)\exp\left\{\hat{e}\min\left\{1, \frac{P-\theta y(n)}{\theta x(n)}\right\} f(x(n)) - d\right\} \tag{2.12b}$$

They provide analysis on this discrete model showing boundedness of solutions, an investigation of equilibria stability, and numerical bifurcations. Fan *et al.* (2005) conclude that the continuous LKE model and this discrete model exhibit the same qualitative phenomenas, confirming the robostness of underlying stoichiometric effects. Chaos can arise in System (2.12), due to the variation in food quality. Similar to the LKE model, producer-grazer oscillations are suddenly halted as producer quality decreases. The discrete model also includes a novel stoichiometric effect, as decreasing producer quality can also halt chaotic dynamics.

Sui *et al.* (2007) analyze and compare System (2.8), presented by Kuang *et al.* (2004), to its discrete analog.

$$x(n+1) = x(n)\exp\left\{b\left[1 - \max\left\{\frac{x(n)}{K}, \frac{x(n)+\mu_m\alpha^{-1}}{\frac{b}{\mu_m}\left(\mu_m\alpha^{-1} + \frac{P_n-\theta y(n)}{q}\right)}\right\}\right] - \frac{f(x(n))y(n)}{x(n)}\right\} \tag{2.13a}$$

$$y(n+1) = y(n)\exp\left\{\hat{e}\min\left\{1, \frac{Q(n)}{\theta}\right\} f(x(n)) - d\right\} \tag{2.13b}$$

After comparing the dynamics exhibited by System (2.8) and System (2.13), they concluded that stoichiometric effects of low food quality on grazers are robust to discretization of time.

2.3.2 Nonhomeostatic Grazer Models

Most stoichiometric producer-grazer models assume the grazer has a constant nutrient to carbon ratio. This is called a *strict homeostasis* assumption. These

models allow variable stoichiometry in autotrophs but assume heterotrophs have a fixed stoichiometry. This assumption is based on the fact that, although grazer stoichiometries are variable, the range of variation is small compared to the range of producer stoichiometries. Wang *et al.* (2012) investigated how the *strict homestasis* assumption, used in stoichiometric algae-zooplankton models, affects the dynamics. They developed a single nutrient (R) closed system that models producer and grazer populations, as well as, explicitly models both producer and grazer varying quotas. Growth terms for each species follow Droop's equation, so the model is written as,

$$\frac{dA}{dt} = \mu_A \left(1 - \frac{Q_A^{min}}{Q_A}\right) A - d_A A - f(A)H \tag{2.14a}$$

$$\frac{dQ_A}{dt} = \rho_A(Q_A, R) - \mu_A \left(1 - \frac{Q_A^{min}}{Q_A}\right) Q_A \tag{2.14b}$$

$$\frac{dH}{dt} = \mu_H \left(1 - \frac{Q_H^{min}}{Q_H}\right) H - d_H H \tag{2.14c}$$

$$\frac{dQ_H}{dt} = f(A)Q_A - \mu_H \left(1 - \frac{Q_H^{min}}{Q_H}\right) Q_H - \sigma_H(A, Q_A, Q_H) \tag{2.14d}$$

where Q_A (Q_A^{min}) and Q_H (Q_H^{min}) are the quotas (minimum quotas) for the producer A and grazer H, respectively. ρ_A is the producer nutrient:C uptake rate and σ_H is the grazer nutrient recycling rate. μ_A, μ_H are maximal growth rates, d_A, d_H are the death rates, and $f(A)$ is the grazer's functional response.

They used this model to define a "hard dynamical threshold" by changing the strength of grazer homeostasis until a bifurcation occurred. This analysis gives insight into when the *strict homeostasis* assumption is reasonable to make. They extended the model to incorporate two nutrients and found similar results. The hard dynamical threshold strongly depends on grazer traits of mortality and growth rates and is independent of producer stoichiometric variation. Wang *et al.* (2008) concluded that the *strict homeostasis* assumption is safe for many herbivores; however, it can lead to issues for herbivores with small mortality rates.

2.3.3 Competition Models

Loladze *et al.* (2004) developed a stoichiometric model of two grazers and one producer that tracks carbon and phosphorus. The formulation of this model is an extension of the LKE model, to include a second grazer,

$$\frac{dx}{dt} = rx\left(1 - \frac{x}{K, \frac{P-\theta_1 y_1 - \theta_2 y_2}{q}}\right) - f_1(x)y_1 - f_2(x)y_2 \tag{2.15a}$$

$$\frac{dy_1}{dt} = e_1 \min\left\{1, \frac{(P - \theta_1 y_1 - \theta_2 y_2)/x}{\theta_1}\right\} f_1(x)y_1 - d_1 y_1 \tag{2.15b}$$

$$\frac{dy_2}{dt} = e_2 \min\left\{1, \frac{(P - \theta_1 y_1 - \theta_2 y_2)/x}{\theta_2}\right\} f_2(x)y_2 - d_2 y_2 \tag{2.15c}$$

where θ_1 and θ_2 are the constant P:C ratios of two predators y_1 and y_2 respectively. Functions $f_1(x)$ and $f_2(x)$ are ingestion rates, e_1 and e_2 are the maximum production efficiencies, and d_1 and d_2 are the death rates of the grazers. They provide an analysis that includes positive invariance and boundedness, as well as, an investigation of equilibria stability via numerical simulations and bifurcations. Notably, a stable equilibrium of the coexistence of all three species is possible. This contradicts the competitive exclusion principle, which states that at most n species can coexist on n resources, a phenomenon not observed in the diversity of nature (Volterra (1926); Gause (1934); Hardin (1960); MacArthur and Levins (1964); Levin (1970)). In System (2.15) bad food quality weakens producer-grazer interactions by limiting C flow across these trophic levels. This weakening promotes coexistence. The results presented in Loladze *et al.* (2004) suggest that ecological stoichiometry may play an important role in explaining biodiversity.

Xie *et al.* (2010) derive a discrete analog of System 2.15,

$$x(n+1) = x(n)\exp\left\{b - \frac{bx(n)}{\min\{K, (P-\theta_1 y_1(n) - \theta_2 y_2(n))/q\}} - \sum_{i=1}^{2} \frac{f_i(x(n))y_i(n)}{x(n)}\right\} \tag{2.16a}$$

$$y_1(n+1) = y_1(n)\exp\left\{\hat{e}_1 \min\left\{1, \frac{P-\theta_1 y_1(n) - \theta_2 y_2(n)}{\theta_1 x(n)}\right\} f_1(x(n)) - d_1\right\} \tag{2.16b}$$

$$y_2(n+1) = y_2(n)\exp\left\{\hat{e}_2 \min\left\{1, \frac{P-\theta_1 y_1(n) - \theta_2 y_2(n)}{\theta_2 x(n)}\right\} f_2(x(n)) - d_2\right\} \tag{2.16c}$$

where θ_i is the P:C ratio, $\hat{e}_i$ is the conversion efficiency, d_i is death rate, and $f_i(x)$ is the grazing functional response for grazer i. Analysis of this discrete model suggest that stoichiometric mechanisms are robust to time discretization. While the two models (System 2.15 and System 2.16) share similar dynamics, Xie *et al.* (2010) noted some important differences found in their analysis. Coexistence of both grazers in the continuous System 2.15 is only possible at a stable equilibrium. In the discrete System 2.16 coexistence is possible at a stable equilibrium as well as during limit cycles. Analysis also shows that chaotic dynamics and a strange attractor can arise for biologically plausible parameters.

Lin *et al.* (2012) formulated a stoichiometric model of two producers and one grazer that tracked carbon and one additional nutrient. Here, they track free nutrients levels in the environment. The goal of this model was to examine enrichment-induced changes in the system. To do this, they investigated bifurcations when varying producer growth rates and the total amount of the nutrient. Unlike many other stoichiometric producer-grazer models, here they assume that producer growth is independent of nutrient levels. In order to investigate enrichment effects, they directly

increase producer growth rates. Their model takes the following form,

$$\frac{dx_1}{dt} = \left(g_1(x_1, x_2) - d_{x1} - \frac{cy}{a + x_1 + x_2} \right) x_1 \tag{2.17a}$$

$$\frac{dx_2}{dt} = \left(g_2(x_1, x_2) - d_{x2} - \frac{cy}{a + x_1 + x_2} \right) x_2 \tag{2.17b}$$

$$\frac{dy}{dt} = \min \left\{ \hat{e}, \left(\frac{x_1 Q_1 + x_2 Q_2}{x_1 + x_2} \right) \frac{1}{\theta} \right\} \frac{c(x_1 + x_2)y}{a + x_1 + x_2} - d_y y \tag{2.17c}$$

$$\frac{dQ_1}{dt} = \left(B_1(P - \theta y - Q_1 x_1 - Q_2 x_2) - Q_1 \right) g_1(x_1, x_2) \tag{2.17d}$$

$$\frac{dQ_2}{dt} = \left(B_2(P - \theta y - Q_1 x_1 - Q_2 x_2) - Q_2 \right) g_2(x_1, x_2) \tag{2.17e}$$

where g_1 and g_2 are the growth rates of competing producers x_1 and x_2. The grazer population is modeled by y. The grazer's maximum ingestion rate is c and the half saturation constant of this ingestion rate is a. Parameters d_{x1}, d_{x2}, and d_y are the death rates, θ is the grazer's constant nutrient:C ratio, Q_1 and Q_2 are the variable nutrient:C ratios of the producers, B_1 and B_2 are the producer's nutrient uptake rates, and P is the constant total nutrient density. They found similar qualitative dynamics as previous one producer -one grazer stoichiometric models, like the LKE model. They found that, similar to these models, adding stoichiometric constraints prevents enrichment from causing large amplitude oscillations. The introduction of a competing producer leads to new equlibria, limit cycles, and bifurcations. When considering competition, they observed that the producer with the lower growth rate will die out via a transcritical bifurcation. Lin *et al.* (2012) provide further evidence that stoichiometry can drastically change population dynamics, specifically in a system where a grazer preys on more than one producer.

Miller *et al.* (2004) also investigated a stoichiometric model with two producers and one grazer, but they assumed the producers reside on different patches, whereas, the grazer can travel between the patches. They assume that nutrients in the environment available for uptake had constant concentrations. Grazer growth may be limited

by the nutrient content of the producers, whose own growths could be limited by environmental nutrient concentrations and self-crowding. Miller *et al.* (2004) used their model to examine extinction dynamics. They observed a "stoichiometric extinction effect" where a system with producers of different quality, that reside separately in two patches, while a grazer disperses between the patches, can actually lead to the extinction of one of the producers. This offers yet more evidence that stoichiometry may provide a mechanism for deterministic extinction.

2.3.4 Multiple Nutrient Models

James P. Grover produced a series of models (Grover (2002, 2003, 2004)) that highlight the importance of grazer nutrient recycling on stability and competitive outcomes. Grover (2002) presented a model with two producers competing for two nutrients (N, P) and one grazer that recycles both nutrients. Unlike most stoichiometric models, he assumed each species had fixed nutrient:carbon ratios. He assumed grazer nutrient recycling rates depend on the fixed grazer nutrient:carbon ratio. He was then able to investigate how nutrient recycling, or sequestering, affects competitive and invasion outcomes of the two producers. Despite the simplicity and the fixed stoichiometric ratios employed, this model emphasizes the important role that stoichiometric constraints have on determining coexistence vs. competitive exclusion.

Grover (2003) presented another model with nutrient recycling but employed variable stoichiometric ratios. This model incorporates one producer (B bacteria) and one grazer (Z flagellate) in which three nutrients (N,P,C) can limit the growth of both populations in a chemostat setting.

$$\frac{dB}{dt} = \mu_B B - DB - m_B - aBZ \tag{2.18a}$$

$$\frac{dZ}{dt} = \mu_Z Z - DZ - m_Z Z \tag{2.18b}$$

Where μ_B, μ_Z represent the per capita reproduction rates, D is the chemostat dilution rate, m_B, m_Z are the per capita mortality rates, and a is the attack or clearance rate of the grazer. Unlike many stoichiometric models, no homeostatic assumption was made, as this model allowed both the producer and grazer nutrient:carbon ratios to vary. Grazer nutrient recycling or sequestering rates depend on the varying grazer nutrient:carbon ratios. In order to allow all three nutrients to limit the growth rates of both populations J.P. Grover followed the approach used by Thingstad (1987) to formulate per capita reproduction rates. This combines the Droop equation and Liebig's law of the minimum into an expression for growth rate,

$$\mu_i = \mu_i^{\max}\left[1 - \max_j\left(\frac{Q_{j,i}^{\min}}{Q_{j,i}}\right)\right] \tag{2.19}$$

for species i=B, Z and nutrient j=N,P,C. Here $Q_{j,i}$ represents the quota (cellular nutrient content) of nutrient j in species i. $Q_{j,i}^{\min}$ is the minimum quota for reproduction (Droop (1974)). $\mu_i^{\max}$ is the apparent maximal growth rate achieved asymptotically for an infinite quota. Producer nutrient uptake ($V_{j,B}$) follows Michaelis-Menten kinetics and decreases linearly with quota,

$$V_{j,B} = V_{j,B}^{\max}\left(\frac{[j]}{K_{j,B} + [j]}\right)\left(\frac{Q_{j,B}^{\max} - Q_{j,B}}{Q_{j,B}^{\max} - Q_{j,B}^{\min}}\right) \tag{2.20}$$

for j=N,P,C. Here $V_{j,B}^{\max}$ is the producer maximal uptake rate, $K_{j,B}$ is a half-saturation constant, $Q_{j,B}^{\max}$ is the producer maximum quota, and $[j]$ is the concentration of element j. Grazer nutrient assimilation is modeled,

$$A_{j,Z} = ae_jBQ_{j,B}\left(\frac{Q_{j,Z}^{\max} - Q_{j,Z}}{Q_{j,Z}^{\max} - Q_{j,Z}^{\min}}\right) \tag{2.21}$$

for j= N,P,C. Here $Q_{j,Z}^{\max}$ is the grazer maximum quota and e_j is the maximal assimilation efficiency ($e_N = e_P = 1$, $e_C < 1$ to account for metabolic costs). The quota

dynamics are modeled,

$$\frac{dQ_{j,B}}{dt} = V_{j,B} - \mu_B Q_{j,B} - R_{j,B} \tag{2.22a}$$

$$\frac{dQ_{j,Z}}{dt} = aBQ_{j,B} - \mu_Z Q_{j,Z} - R_{j,Z} \tag{2.22b}$$

for j = N, C, P. Here $R_{j,i}$ are the nutrient recycling and respiration rates given below;

$$R_{N,B} = R_{P,B} = 0 \tag{2.23a}$$

$$R_{C,B} = \rho^g \mu_B Q_{C,B} + \rho^m (Q_{C,B} - C^{\min}_{C,B}) \tag{2.23b}$$

$$R_{j,Z} = aBQ_{j,B}\left[1 - e_j\left(\frac{Q^{\max}_{j,Z} - Q_{j,Z}}{Q^{\max}_{j,Z} - Q^{\min}_{j,Z}}\right)\right] \tag{2.23c}$$

where ρ^g and ρ^m are coefficients from growth-related and maintenance respiration, respectively. Lastly, the dissolved nutrient concentrations are modeled explicitly,

$$\frac{d[j]}{dt} = D([j]_{in} - [j]) - BV_{j,B} + ZY_{j,Z} + m_z ZQ_{j,Z} + m_B BQ_{j,B} \tag{2.24}$$

for j=N,P,C. Nutrient recycling is represented by $Y_{j,Z}$, where $Y_{N,Z} = R_{N,Z}$ and $Y_{P,Z} = R_{P,Z}$. $Y_{C,Z} = 0$ since respired C is assumed to leave the system.

This model effectively examines the dynamics of several nutrient elements simultaneously. The expressions for growth (eq. 2.19), nutrient uptake (eq. 2.20), and nutrient assimilation (eq. 2.21) are all formulated based on Droop cell quota dynamics (Droop (1974); Thingstad (1987)). This model makes it clear that grazer nutrient recycling rates, which depend on grazer stoichiometric ratios, can play a critical role in determining the stability of producer-grazer systems and their responses to enrichment.

Grover (2004) extends the previous model by adding a competing producer population. He then investigates competitive outcomes in relation to supplies of limiting nutrients and the grazer's preference for attacking different producers. This three species extended model showed that competition outcomes are also strongly related to grazer nutrient recycling. These papers (Grover (2003, 2004)) have nicely detailed

models that explicitly model producer and grazer populations, the nutrient quotas for each species, and track free nutrient concentrations dissolved in the environment. While these details are important not to overlook, these systems end up quite large (11-15 ODES) and most analysis is limited to simulations.

2.3.5 Dynamic Energy Budget Theory Smooth Approach

Despite continuous advances in analyzing nonsmooth dynamics, having a switch in a model is mathematically inconvenient. Also an organism residing in an environment near the threshold may undergo continual switching of the limiting resource, which can add unnecessary taxes to its growth. An alternative smooth approach to stoichiometric modeling has been developed using dynamic energy budget theory and the concept of synthesizing units (Nisbet *et al.* (2000); Muller *et al.* (2001); Kooijman *et al.* (2004, 2007); Kooijman (2009)). Dynamic energy budget theory is based on energy and mass balances and provides a framework to deal with stoichiometric restrictions. A synthesizing unit converts a given number of varying types of substrates to produce products while meeting stoichiometric constraints (Kooijman (1998, 2000); Muller *et al.* (2001)). Common examples of synthesizing units are enzymes.

Muller *et al.* (2001) used synthesizing units to describe grazer growth in a stoichiometric producer-grazer model. Here the mass of the producer is assumed to consist of two parts; structural biomass and nutrient reserves. Following their approach but changing parameter symbols to better compare with other models presented in this manuscript, let x denote the producer structure, m the producer nutrient reserve density, and y the grazer biomass. Let the grazer have constant P:C ratio of θ and the producer structure have constant P:C ratio of q. The producer cell quota, Q, varies as the proportion of producer reserves to structure varies depending on environmental conditions. Here $Q = m + q$. Yield coefficients are used to represent the flux of

producer structure and reserves to grazer biomass in the expression of grazer growth. Using synthesizing units the stoichiometric producer-grazer model developed by Muller *et al.* (2001) takes the following form,

$$\frac{dx}{dt} = bx\left(1 - \frac{q}{Q}\right) - f(x)y \tag{2.25a}$$

$$\frac{dy}{dt} = \left[\frac{1}{r} + \frac{1}{f(x)\left(\gamma_{xc} + m\gamma_{mc}\right)} + \frac{1}{f(x)\left(\gamma_{xp} + m\gamma_{mp}\right)} - \frac{1}{f(x)\left(\gamma_{xc} + \gamma_{xp} + m(\gamma_{mc} + \gamma_{mp})\right)}\right]^{-1} y - dy \tag{2.25b}$$

where b is the producer specific growth rate and, γ_{xc} and γ_{xp} are yield coefficients for assimilating carbon and phosphorus from the producer structure, x. Parameters γ_{mc} and γ_{mp} are yield coefficients for assimilating carbon and phosphorus from the producer reserves, m. Parameter r is the maximum specific grazer biomass synthesis rate and d is the grazer loss rate. The four yield coefficients are non-negative and are bounded by the constraints below,

$$\gamma_{xp} \leq \frac{q}{\theta}, \qquad \gamma_{xc} \leq 1, \qquad \gamma_{mp} \leq \frac{1}{\theta}, \qquad \gamma_{mc} \leq 1.$$

In the context of synthesizing units, one substrate can have a stronger limiting effect than the other. In the growth expression in equation (3.1a) the dominant limiting factor is determined by comparing $f(x)(\gamma_{xc} + m\gamma_{mc})$ with $f(x)(\gamma_{xp} + m\gamma_{mp})$. Phosphorus is the limiting factor for grazer growth when

$$f(x)(\gamma_{xc} + m\gamma_{mc}) > f(x)(\gamma_{xp} + m\gamma_{mp}).$$

Numerically, the behavior of a synthesizing unit is similar to Leibig's law of the minimum except for a narrow region near the threshold where several substrates can limit growth simultaneously (Kooijman *et al.* (2004)). Here the transition from one limiting factor to the other is smooth. Biologically this makes sense since nutrients

can be low in the environment but not yet limit grazer growth due to the amount of nutrients in the producer reserves.

Dynamic energy budget theory offers a framework for stoichiometric modeling, whose structure is more mechanistic than the threshold approach. While this approach has the mathematical benefit of offering smooth models, it adds complexity and introduces more parameters that may be difficult to measure, such as the yield coefficients above. Analytical analysis is limited by the complex terms that arise, such as the grazer's growth expression in equation (3.1a). Analytical analysis of nonsmooth models, using the threshold approach, must be split into different cases, however these cases are often simple, relative to their smooth analogs. Smooth models developed using the dynamic energy budget and synthesizing unit approach have given qualitatively similar results to nonsmooth models developed using the threshold approach Loladze *et al.* (2000); Andersen *et al.* (2004); Moe *et al.* (2005).

Stech *et al.* (2012b) developed and analyzed a general stoichiometric producer-grazer model consisting of three ODEs, in order to investigate the bifurcation dynamics observed in stoichiometric models. To keep the model general they do not specify the producer growth, nutrient uptake, or grazer growth functions, but they use generalized versions of functions following the dynamic energy budget approach and synthesizing unit concept. Here they showed the general model exhibits similar qualitative bifurcation dynamics under energy enrichment as previous stoichiometric producer-grazer models, however, the quantitative dynamics depend on the function structures. Stech *et al.* (2012c) reduce the system of 3 ODEs in Stech *et al.* (2012b) with a quasi-steady-state approximation to form a general system of 2 ODEs. The quasi-steady-state reduction and general function forms, following the dynamics energy budget and synthesizing units approach, allowed for more complex analytical analysis to be done. They rigorously showed that high energy (low producer nutrient:carbon

ratio) drives the system to a globally attracting equilibrium. They concluded that the energy enrichment induced loss of periodic coexistence, commonly exhibited in stoichiometric producer-grazer models, is robust to modeling variations.

Chapter 3

STOICHIOMETRIC KNIFE EDGE MODEL

3.1 Stoichiometric Knife Edge Phenomenon

The model presented in Elser *et al.* (2012) and Peace *et al.* (2013) is the first to incorporate the effects of excess nutrient content. It describes an ecological system of algae (producer) and *Daphnia* (grazer), building on the structure of the LKE model. The model aims to capture the dynamics of the *stoichiometric knife edge*. Plath and Boersma (2001) suggested that *Daphnia* may follow a simple feeding rule: *eat until you get enough P, then stop.* See Figure 3.1. High P content of food causes the animal to strongly decrease their ingestion rate, perhaps leading to insufficient C intake and thus decreased growth rate. In other words, the satiation level of *Daphnia* is dictated by P concentration in the algae.

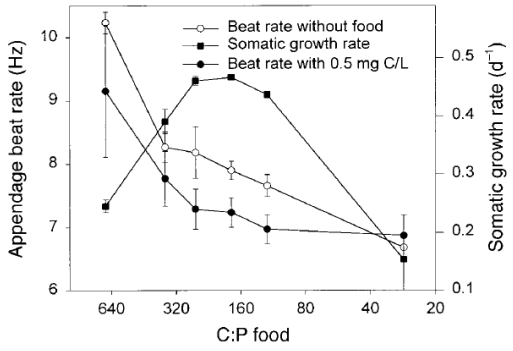

Figure 3.1: Data presented in Plath and Boersma (2001) of appendage beat (feeding) rate of *Daphnia Magna* under different P food content. The x-axis depicts food C:P (molar). Here "Beat rate with 0.5 mg C/L" refers to the 0.5 mg of algae in the medium during beat rate measurements and "Beat rate without food" refers to measurements taken without algae in the medium.

This feeding behavior is one possible mechanism that may cause the observed reduction in grazer growth rate and is taken as an assumption in this model. The *stoichiometric knife edge* model makes the following assumptions.

A1: *The total mass of phosphorus in the entire system is fixed, i.e., the system is closed for phosphorus with a total of P (mgP/L).*

A2: *P:C ratio in the producer varies, but it never falls below a minimum q (mgP/mgC); the grazer maintains a constant P:C, θ (mgP/mgC).*

A3: *All phosphorus in the system is divided into two pools: phosphorus in the grazer and phosphorus in the producer.*

A4: *The grazer ingests P up to the rate required for its maximal growth but not more.*

The first three above assumptions are identical to the assumptions of the LKE Model. The fourth assumption claims the ingestion rate of the grazer depends on the P content of the producer, as well as, the total food abundance.

3.2 Model Formulation

Peace *et al.* (2013) describe the construction of the stoichometric knife edge model. We started with the LKE model and incorporated the above assumption, A4, in order to include the dynamics of the stoichometric knife edge. This assumption leads to a new expression for the grazer ingestion rate. Since $f(x)$ is the grazer ingestion rate and Q is the P quota of the producer; the grazer will ingest P at rate $f(x)Q$ if its ingestion is never capped by a maximum P intake rate. However, the grazer's maximal possible growth rate expressed in P units is $\hat{f}\theta$, where $\hat{f}$ is the maximum of $f(x)$. Using these two quantities, we define the grazer satiation level (GSL) as the ratio of $f(x)Q$ to $\hat{f}\theta$.

If $GSL < 1$, then the grazer ingests at its usual $f(x)$ rate. But if $GSL \geq 1$, then the grazer ingests at the rate $\frac{\hat{f}\theta}{Q}$. This way the grazer's rate of P ingestion is capped at $(\frac{\hat{f}\theta}{Q})Q = \hat{f}\theta$. This leads to a new specific ingestion rate as follows:

$$u(x,y) = \left\{ \begin{array}{ll} f(x) & \text{for } f(x)Q < \hat{f}\theta \\ \frac{\hat{f}\theta}{Q} & \text{for } f(x)Q > \hat{f}\theta \end{array} \right\} = \min\{f(x), \frac{\hat{f}\theta}{Q}\}$$

The grazer's production efficiency is also modified to incorporate the effect of mandatory C losses to metabolic costs, mainly to respiration, on the post-ingested food quality. Similar to the LKE model, the grazer growth rate may be limited by P; however, if P is in excess, the growth rate may be limited by the amount of available C. Q is actually the P:C ratio of the producer before ingestion. A portion of this ingested C is required for metabolic costs such as respiration. Parameter $\hat{e}$ is the maximal production efficiency in terms of carbon so that $\frac{Q}{\hat{e}}$ is the P:C ratio of the post-ingested producer representing the amount of P and C available for growth.

When $\frac{Q}{\hat{e}} < \theta$, there is no excess P and the grazer's growth rate is determined by the P content of the producer. The grazer ingests $u(x,y)Q$ units of P, and the grazer's growth rate, $g(x,y)$, satisfies $g(x,y)\theta = u(x,y)Q$. On the other hand, when $\frac{Q}{\hat{e}} > \theta$, there is excess P. In this situation, the grazer's growth is no longer limited by P, but by the amount of available C. The grazer ingests $u(x,y)$ units of C and $u(x,y)\hat{e}$ units of C are available for growth. The growth rate then satisfies $g(x,y) = u(x,y)\hat{e}$. The grazer's biomass growth rate is defined as follows:

$$\begin{aligned} g(x,y) &= \left\{ \begin{array}{ll} \frac{Q}{\theta}u(x,y) & \text{for } \frac{Q}{\hat{e}} < \theta \\ \hat{e}u(x,y) & \text{for } \frac{Q}{\hat{e}} > \theta \end{array} \right\} = \min\{\hat{e}, \frac{Q}{\theta}\}u(x,y) \\ &= \min\left\{\hat{e}, \frac{Q}{\theta}\right\} \min\left\{f(x), \frac{\hat{f}\theta}{Q}\right\} \end{aligned}$$

Since $\hat{e}f(x) < \hat{f}$, we see that

$$g(x,y) = \min\left\{\hat{e}f(x), \frac{Q}{\theta}f(x), \hat{e}\frac{\hat{f}\theta}{Q}, \hat{f}\right\} = \min\left\{\frac{Q}{\theta}f(x), \hat{e}\frac{\hat{f}\theta}{Q}, \hat{e}f(x)\right\}.$$

Biologically, this translates into three cases in which growth is determined by: energy limitation ($\hat{e}f(x)$), P limitation ($\frac{Q}{\theta}f(x)$), and P in excess ($\hat{e}\hat{f}\frac{\theta}{Q}$).

The result is the *stoichiometric knife edge* model:

$$\frac{dx}{dt} = bx\left(1 - \frac{x}{\min\{K, (P-\theta y)/q\}}\right) - \min\left\{f(x), \frac{\hat{f}\theta}{Q}\right\} y \tag{3.1a}$$

$$\frac{dy}{dt} = \min\left\{\hat{e}f(x), \frac{Q}{\theta}f(x), \hat{e}\hat{f}\frac{\theta}{Q}\right\} y - dy \tag{3.1b}$$

where $Q = \frac{P-\theta y}{x}$.

3.3 Model Analysis

3.3.1 Boundedness and Positive Invariance

The following lemmas provide a basic analysis of the model verifying the boundedness and invariance of the solution.

Lemma 3.3.1. *The model, given in System 3.1 is well defined as $x \to 0$*

Proof. Since,

$$\begin{aligned}\frac{dx}{dt} &= bx(1 - \frac{x}{\min\{K, \frac{P-\theta y}{q}\}}) - \min\{f(x), \frac{\hat{f}\theta}{Q}\}y \\ &= bx(1 - \frac{x}{\min\{K, \frac{P-\theta y}{q}\}}) - \min\{f(x), \frac{\hat{f}\theta x}{P-\theta y}\}y,\end{aligned}$$

$x'(t)$ is well defined at $x \to 0$.

$$\frac{dy}{dt} = \begin{cases} \hat{e}f(x)y - dy & \text{if} \quad \hat{e}f(x) < \frac{Q}{\theta}f(x), \hat{e}f(x) < \hat{e}\hat{f}\frac{\theta}{Q} \\ \frac{Q}{\theta}f(x)y - dy = \frac{f(x)}{x}\frac{(P-\theta y)}{\theta}y - dy & \text{if} \quad \frac{Q}{\theta}f(x) < \hat{e}f(x), \frac{Q}{\theta}f(x) < \hat{e}\hat{f}\frac{\theta}{Q} \\ \hat{e}\hat{f}\frac{\theta}{Q}y - dy = \hat{e}\hat{f}\frac{\theta x}{P-\theta y}y - dy & \text{if} \quad \hat{e}\hat{f}\frac{\theta}{Q} < \hat{e}\hat{f}, \hat{e}\hat{f}\frac{\theta}{Q} < \frac{Q}{\theta}f(x) \end{cases}$$

$y'(t)$ is well defined at $x \to 0$. □

Lemma 3.3.2. *Solutions with initial conditions in the open rectangle* $\{(x,y) : 0 < x < k = \min\{K, \frac{P}{q}\}, 0 < y < \frac{P}{\theta}\}$ *remain there for all future time.*

Proof. Assume there exists a time t_1 such that a trajectory with initial conditions in the rectangle $(0,k) \times (0, \frac{P}{\theta})$ crosses a boundary of the rectangle for the first time. The following cases prove the lemma by contradiction.

Case 1 left boundary: $x(t_1) = 0$. Let $\overline{f} = f'(0) = \lim_{x \to 0} \frac{f(x)}{x}$ and $\overline{y} = \max_{t \in [0,t_1]} y(t) < \frac{P}{\theta}$

$$\begin{aligned} x' &= [b(1 - \frac{x}{\min\{K, \frac{P-\theta y}{q}\}}) - \min\{\frac{f(x)}{x}, \frac{\hat{f}\theta}{P - \theta y}\}y]x \\ &\geq [b(1 - \frac{x}{\min\{K, \frac{P-\theta y}{q}\}}) - \min\{\overline{f}, \frac{\hat{f}\theta}{P - \theta y}\}y]x \\ &\geq [b(1 - \frac{k}{\min\{K, \frac{P-\theta \overline{y}}{q}\}}) - \min\{\overline{f}, \frac{\hat{f}\theta}{P - \theta \overline{y}}\}\overline{y}]x \\ &= \alpha x. \end{aligned}$$

Where α is a constant. Thus $x(t) \geq x(0)e^{\alpha t}$. This implies that $x(t_1) \geq x(0)e^{\alpha t_1} > 0$. This contradicts $x(t_1) = 0$ and proves that no such trajectory can reach this boundary.

Case 2 right boundary: $x(t_1) = k$.

$$\begin{aligned} x' &= bx(1 - \frac{x}{\min\{K, \frac{P-\theta y}{q}\}}) - \min\{f(x), \frac{\hat{f}\theta}{Q}\}y \\ &\leq bx(1 - \frac{x}{\min\{K, \frac{P-\theta y}{q}\}}) \\ &\leq bx(1 - \frac{x}{\min\{K, \frac{P}{q}\}}) \\ &= bx(1 - \frac{x}{k}) \end{aligned}$$

Then $x(t) < k$ by the standard comparison argument, thus no trajectory can reach this boundary.

Case 3 bottom boundary: $y(t_1) = 0$.

$$\begin{aligned} y' &= \min\{\hat{e}f(x), \frac{Q}{\theta}f(x), \hat{e}\hat{f}\frac{\theta}{Q}\}y - dy \\ &\geq -dy \end{aligned}$$

This implies that $y(t_1) \geq y(0)e^{-dt_1} > 0$. This contradicts $y(t_1) = 0$ and proves that no such trajectory can reach this boundary.

Case 4 top boundary: Assume $y(t_1) = \frac{P}{\theta}$, and $0 < y(t) < \frac{P}{\theta}$ for $0 \leq t < t_1$. Then

$$\begin{aligned} y' &= \min\{\hat{e}f(x), \frac{Q}{\theta}f(x), \hat{e}\hat{f}\frac{\theta}{Q}\}y - dy \\ &\leq \min\{\hat{e}f(x), \frac{Q}{\theta}f(x), \hat{e}\hat{f}\frac{\theta}{Q}\}y \\ &\leq \frac{Q}{\theta}f(x)y = \frac{\frac{P}{\theta} - y}{x}f(x)y \\ &= \frac{f(x)}{x}(\frac{P}{\theta} - y)y \\ &\leq \bar{f}(\frac{P}{\theta} - y)y \\ &= \bar{f}\frac{P}{\theta}y(1 - \frac{y}{P/\theta}) \end{aligned}$$

The standard comparison argument yields a contradiction, $y(t) < \frac{P}{\theta}$ for $0 \leq t \leq t_1$. $\square$

Lemma 3.3.3. *Solutions with initial conditions in the open trapezoid (or triangle if $K \geq \frac{P}{q}$) $\{(x, y) : 0 < x < k = \min\{K, \frac{P}{q}\}, 0 < y < \frac{P}{\theta}, qx + \theta y < P\}$ remain there for all future time.*

Proof. Based on the previous Lemma, we only have to prove $qx + \theta y < P$ for all future time. Assume that $qx(t_1) + \theta y(t_1) = P$ and $qx(t) + \theta y(t) < P$ for $0 \leq t < t_1$. Then

$x(t_1) = \frac{P-\theta y(t_1)}{q}$ and $Q(t_1) = \frac{P-\theta y(t_1)}{x(t_1)} = q$. It is easy to see that $qx'(t_1) + \theta y'(t_1) \geq 0$.

$$\begin{aligned}
x'(t_1) &= bx(t_1)(1 - \frac{x(t_1)}{\min\{K, \frac{P-\theta y(t_1)}{q}\}}) - \min\{f(x(t_1)), \frac{\hat{f}\theta x(t_1)}{P-\theta y(t_1)}\}y(t_1) \\
&\leq bx(t_1)(1 - \frac{x(t_1)}{\frac{P-\theta y(t_1)}{q}}) - \min\{f(x(t_1)), \frac{\hat{f}\theta}{q}\frac{x(t_1)}{\frac{P-\theta y(t_1)}{q}}\}y(t_1) \\
&= bx(t_1)(1 - \frac{x(t_1)}{x(t_1)}) - \min\{f(x(t_1)), \frac{\hat{f}\theta}{q}\frac{x(t_1)}{x(t_1)}\}y(t_1) \\
&= -\min\{f(x(t_1)), \frac{\hat{f}\theta}{q}\}y(t_1)
\end{aligned}$$

$$\begin{aligned}
y'(t_1) &= \min\{\hat{e}f(x(t_1)), \frac{Q(t_1)}{\theta}f(x(t_1)), \hat{e}\hat{f}\frac{\theta}{Q(t_1)}\}y(t_1) - dy(t_1) \\
&= \min\{\hat{e}, \frac{Q(t_1)}{\theta}\}\min\{f(x(t_1)), \frac{\hat{f}\theta}{Q(t_1)}\}y(t_1) - dy(t_1) \\
&= \min\{\hat{e}, \frac{q}{\theta}\}\min\{f(x(t_1)), \frac{\hat{f}\theta}{q}\}y(t_1) - dy(t_1) \\
&< \frac{q}{\theta}\min\{f(x(t_1)), \frac{\hat{f}\theta}{q}\}y(t_1)
\end{aligned}$$

$$\begin{aligned}
qx'(t_1) + \theta y'(t_1) &< -q\min\{f(x(t_1)), \frac{\hat{f}\theta}{q}\}y(t_1) + q\min\{f(x(t_1)), \frac{\hat{f}\theta}{q}\}y(t_1) \\
&= 0
\end{aligned}$$

This contradicts the assumption $qx'(t_1) + \theta y'(t_1) \geq 0$. □

These lemmas prove the solutions of System 3.1 are confined to a bounded region; that is, initial conditions that are outside of this boundary are biologically meaningless.

To investigate the equilibria we first rewrite System 3.1 in the following form.

$$\frac{dx}{dt} = xF(x, y) \tag{3.2a}$$

$$\frac{dy}{dt} = yG(x, y) \tag{3.2b}$$

where

$$F(x,y) = b\left(1 - \frac{x}{\min\{K,(P-\theta y)/q\}}\right) - \min\left\{\frac{f(x)}{x}, \frac{\hat{f}\theta}{P-\theta y}\right\} y \tag{3.3a}$$

$$G(x,y) = \min\left\{\hat{e}f(x), \frac{Q}{\theta}f(x), \hat{e}\hat{f}\frac{\theta}{Q}\right\} - d \tag{3.3b}$$

Setting System 3.2 equal to zero yields the following Jacobian.

$$J = \begin{vmatrix} F(x,y) + xF_x(x,y) & xF_y(x,y) \\ yG_x(x,y) & G(x,y) + yG_y(x,y) \end{vmatrix}$$

3.3.2 Boundary Equilibria

There are two equilibria on the boundary, $E_0 = (0,0)$ and $E_1 = (k,0)$. The local stability of $E_0 = (0,0)$ is determined by the Jacobian in the following form,

$$J(E_0) = \begin{vmatrix} b & 0 \\ 0 & -d \end{vmatrix}.$$

The determinant is negative and the eigenvalues have different signs. Therefore E_0 is always an unstable saddle. The local stability of $E_1 = (k,0)$ is determined by the Jacobian in the following form,

$$J(E_1) = \begin{vmatrix} -b & kF_y(k,0)) \\ 0 & G(k,0) \end{vmatrix}.$$

The stability of E_1 depends on the sign of $G(k,0)$. If $G(k,0)$ is positive, then E_1 is an unstable saddle. If $G(k,0)$ is negative, then E_1 is a locally asymptotically stable node.

3.3.3 Interior Equilibria

To investigate the interior equilibria the phase plane is divided into three biologically significant regions by the two lines $\hat{e} = \frac{q}{\theta}$ and $f(x) = \frac{\hat{f}\theta}{Q}$. Figure 3.2c shows the three regions. Region I is defined by $\hat{e} < \frac{Q}{\theta}$ and $f(x) < \frac{\hat{f}\theta}{Q}$. This represents the cases where

P is neither limiting nor in excess. Region II is defined by $\hat{e} > \frac{Q}{\theta}$; here, growth is limited by a deficiency of P. Region III is defined by $\hat{e} < \frac{Q}{\theta}$ and $f(x) > \frac{\hat{f}\theta}{Q}$, where P is in excess and reduces grazer growth.

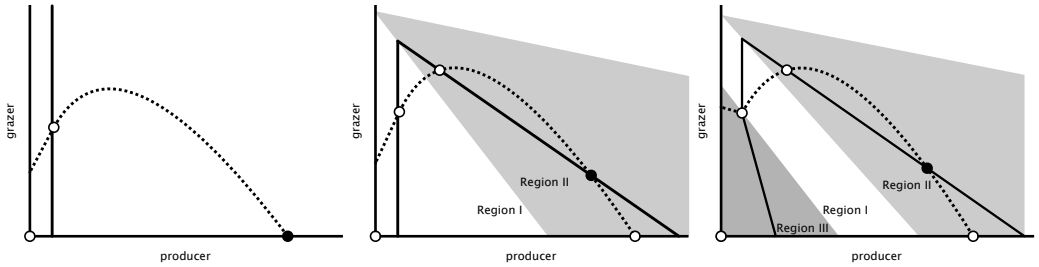

(a) Rosenzweig-MacArthur (b) LKE (c) Knife edge Modification

Figure 3.2: Phase planes for the (a) classical Rosenzweig-MacArthur, (b) stoichiometric LKE model, and (c) *stoichiometric knife edge* model. Here we compare the grazer nullclines for these three models. The classical Rosenzweig-MacArthur grazer nullcline is a vertical line. The stoichiometric LKE model breaks the grazer nullcline into two segments. This divides the phase plane into two regions; region I, where grazer growth is determined by food quantity and region II, where grazer growth is determined by food with limiting nutrients. Finally the modified model takes into account excess food nutrient content. The grazer nullcline is divided into three segments, breaking the phase plane into three regions. This new region III is where grazer growth is limited by excess food nutrient content.

Loladze *et al.* (2000) developed a simple graphical test that determines the local stability of the interior equilibria of the LKE system using the slopes of the nullclines determined by the sign of the partial derivatives of F and G. ($-F_x/F_y$ defines the slope of the producer nullcline and $-G_x/G_y$ defines the slope of the grazer nullcline.) Peace *et al.* (2013) presents similar results for this model. The partial derivatives of F

and G satisfy,

$$F_x = \frac{\partial F}{\partial x} = \begin{cases} -\frac{b}{\min(K, \frac{P-\theta y}{q})} - (\frac{f(x)}{x})'y & \text{if} f(x) < \frac{\hat{f}\theta}{Q} \\ -\frac{b}{\min(K, \frac{P-\theta y}{q})} < 0 & \text{if } f(x) > \frac{\hat{f}\theta}{Q} \end{cases}$$

$$F_y = \frac{\partial F}{\partial y} = \begin{cases} -\frac{f(x)}{x} < 0 & \text{if } f(x) < \frac{\hat{f}\theta}{Q}, K < \frac{P-\theta y}{q} \\ -\frac{Ph}{(P-\theta y)^2} < 0 & \text{if} f(x) > \frac{\hat{f}\theta}{Q}, K < \frac{P-\theta y}{q} \\ -\frac{bxq\theta}{(P-\theta y)^2} - \frac{f(x)}{x} < 0 & \text{if} f(x) < \frac{\hat{f}\theta}{Q}, K > \frac{P-\theta y}{q} \\ -\frac{bxq\theta}{(P-\theta y)^2} - \frac{Ph}{(P-\theta y)^2} < 0 & \text{if} f(x) > \frac{\hat{f}\theta}{Q}, K > \frac{P-\theta y}{q} \end{cases}$$

$$G_x = \frac{\partial G}{\partial x} = \begin{cases} \hat{e}f'(x) > 0 & \text{if } \hat{e}f(x) < \frac{Q}{\theta}f(x), \hat{e}f(x) < \hat{e}\hat{f}\frac{\theta}{Q} \\ \frac{P-\theta y}{\theta}(\frac{f(x)}{x})' < 0 & \text{if } \frac{Q}{\theta}f(x) < \hat{e}f(x), \frac{Q}{\theta}f(x) < \hat{e}\hat{f}\frac{\theta}{Q} \\ \hat{e}\hat{f}\frac{\theta}{P-\theta y} > 0 & \text{if } \hat{e}\hat{f}\frac{\theta}{Q} < \hat{e}f(x), \hat{e}\hat{f}\frac{\theta}{Q} < \frac{Q}{\theta}f(x) \end{cases}$$

$$G_y = \frac{\partial G}{\partial y} = \begin{cases} 0 & \text{if } \hat{e}f(x) < \frac{Q}{\theta}f(x), \hat{e}f(x) < \hat{e}\hat{f}\frac{\theta}{Q} \\ -\frac{f(x)}{x} < 0 & \text{if } \frac{Q}{\theta}f(x) < \hat{e}f(x), \frac{Q}{\theta}f(x) < \hat{e}\hat{f}\frac{\theta}{Q} \\ \frac{\hat{e}\hat{f}x\theta^2}{(P-\theta y)^2} > 0 & \text{if } \hat{e}\hat{f}\frac{\theta}{Q} < \hat{e}f(x), \hat{e}\hat{f}\frac{\theta}{Q} < \frac{Q}{\theta}f(x) \end{cases}$$

We denote an interior equilibrium as $E^* = (x^*, y^*)$, where $F(x^*, y^*) = 0 = G(x^*, y^*)$. The Jacobian at (x^*, y^*) is

$$J(E^*) = \begin{vmatrix} x^*F_x(x^*, y^*) & x^*F_y(x^*, y^*)) \\ y^*G_x(x^*, y^*) & y^*G_y(x^*, y^*) \end{vmatrix}.$$

The stability can be determined from the signs of the determinant, $x^*y^*(F_xG_y - F_yG_x)$ and the trace, $x^*F_x + y^*G_y$. The analysis is done for each of the regions separately.

1. Suppose (x^*, y^*) lies in region I, $\hat{e} < \frac{Q}{\theta}$ and $f(x) < \frac{\hat{f}\theta}{Q}$. Here $F_y < 0$, $G_x > 0$, and $G_y = 0$. The determinant is positive.

$$\text{sign(Det(J))=sign}(-F_yG_x) > 0.$$

$$\text{sign(Tr(J))=sign}(F_x)=\text{sign}(-F_x/F_y).$$

Since $-F_x/F_y$ is the slope of the producer nullcline, (x^*, y^*) is locally asymptotically stable if the producer nullcline is declining. If the nullcline is increasing then the equilibrium is a repeller.

2. Suppose (x^*, y^*) lies in region II, $\hat{e} > \frac{Q}{\theta}$. Here $F_y < 0$, $G_x < 0$, and $G_y < 0$.

$$\text{sign(Det(J))=sign}(F_xG_y - F_yG_x)=\text{sign}(\tfrac{F_xG_y - F_yG_x}{F_yG_y})=\text{sign}(-\tfrac{G_x}{G_y} - (-\tfrac{F_x}{F_y}))$$

If $-\frac{G_x}{G_y} < -\frac{F_x}{F_y}$, then the slope of the grazer nullcline is less that the slope of the producer nullcline, then the determinant is negative and (x^*, y^*) is a saddle. If the grazer nullcline has a larger slope, then the determinant is positive.

$$F_xG_y - F_yG_x > 0 \Rightarrow F_x < \tfrac{F_yG_x}{G_y} < 0 \Rightarrow Tr(J) = x^*F_x + y^*G_y < 0$$

The eigenvalues for the Jacobian have negative real parts. Thus (x^*, y^*) is locally asymptotically stable.

3. Suppose (x^*, y^*) lies in region III, $\hat{e} < \frac{Q}{\theta}$ and $f(x) > \frac{\hat{f}\theta}{Q}$. Here $F_x < 0$, $F_y < 0$, $G_x > 0$, and $G_y > 0$.

$$\text{sign(Det(J))=sign}(\tfrac{F_y G_x - F_x G_y}{F_y G_y})\text{=sign}(-\tfrac{F_x}{F_y} - (-\tfrac{G_x}{G_y}))$$

If $-\frac{F_x}{F_y} < -\frac{G_x}{G_y}$, then the slope of the producer nullcline is less that the slope of the grazer nullcline, then the determinant is negative and (x^*, y^*) is a saddle. If the producer nullcline has a larger slope, then the determinant is positive. The stability depends on the sign of the trace:

$$\text{sign(Tr(J))=sign}(x^* F_x + y^* G_y).$$

If $x^* F_x + y^* G_y > 0$, then the eigenvalues for the Jacobian have positive real parts and (x^*, y^*) is a repeller. If $x^* F_x + y^* G_y < 0$, then the eigenvalues for the Jacobian have negative real parts and (x^*, y^*) is locally asymptotically stable. Further analysis of the flow diagram shows this equilibrium is a stable spiral. The direction field on the grazer nullcline, $G(x, y) = 0$, is in the x-direction and depends on the sign of $F(x, y)$. On the grazer nullcline $x' = 0$ at (x^*, y^*), $x' > 0$ below the producer nullcline $F(x, y) = 0$, and $x' < 0$ above the producer nullcline $F(x, y) = 0$. The direction field on the producer nullcline is in the y-direction and depends on the sign of $g(x, y)$. On the producer nullcline $y' = 0$ at (x^*, y^*), $y' > 0$ to the right of the grazer nullcline $G(x, y) = 0$, and $y' < 0$ to the left of the grazer nullcline $G(x, y) = 0$. See Figure 3.3 for the flow diagram.

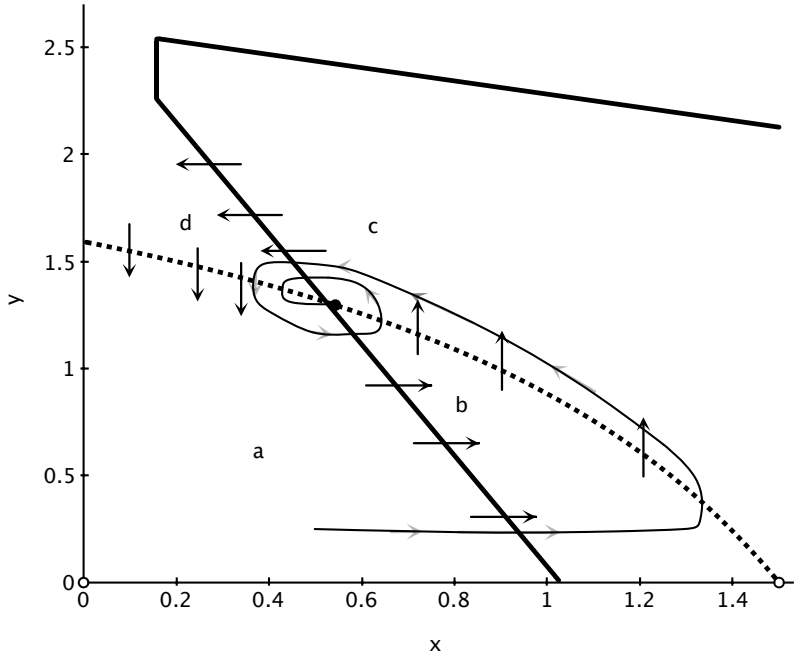

Figure 3.3: This direction field analysis shows that a trajectory in region **a** must flow into region **b**, then into region **c**, then into region **d**, and finally back into region **a** as it approaches the locally asymptotically stable equilibrium (x^*, y^*). Therefore (x^*, y^*) is a stable spiral. The dynamics of the system experience damped oscillations as the solution approaches (x^*, y^*).

A summary of the stability of the biologically significant equilibria is presented in the following theorem.

Theorem 3.3.1. *There are two boundary equilibria. The origin is a saddle, the other equilibrium $E_1 = (k, 0)$ depends on the sign of G(k,0). If G(k,0) is positive this boundary equilibrium is a saddle, if G(k,0) is negative it is a locally asymptotically stable node. The stability of any interior equilibrium $E^* = (x^*, y^*)$ depends on the slopes of the producer and grazer nullclines. If $(x^*, y^*) \in$ Region I, it is locally asymptotically stable if the producer nullcline is declining and unstable if it is increasing. If $(x^*, y^*) \in$ Region II and the producer nullcline has a shallower slope than the grazer nullcline, it*

is locally asymptotically stable; otherwise, if the producer nullcline has a steeper slope, it is a saddle. If $(x^*, y^*) \in$ *Region III and the producer nullcline has a shallower slope than the grazer nullcline, it is a saddle. If the producer nullcline has a steeper slope, the stability of* (x^*, y^*) *depends on the sign of* $x^* F_x + y^* G_y$*. If it is stable, it is a stable spiral and the system undergoes damped oscillations as it approaches* (x^*, y^*)*.*

3.4 Numerical Experiments

All simulations used the Holling type II function $f(x) = \frac{\hat{f}x}{a+x}$ for the ingestion rate and the parameter values listed in Table 3.1. These values were also used by Loladze *et al.* (2000) and chosen as biologically realistic values obtained from Andersen (1997) and Urabe and Sterner (1996).

Parameter		Value
P	Total Phosphorus	0.03-0.2 mgP / L
$\hat{e}$	Maximal production efficiency	0.8
b	Maximal growth rate of producer	1.2 days^{-1}
d	Grazer loss rate	0.25 days^{-1}
θ	Grazer constant P:C	0.03 (mgP)/(mgC)
q	Producer minimal P:C	0.0038 (mgP)/(mgC)
$\hat{f}$	Maximal ingestion rate of the grazer	0.81 days^{-1}
a	Half saturation of the grazer ingestion response	0.25 mg C / L
K	Producer carrying capacity	1.5 mg C / L

Table 3.1: Model parameters for the knife edge model (System 3.1). All parameters are biologically realistic values obtained from Andersen (1997) and Urabe and Sterner (1996) and used in Loladze *et al.* (2000)

In the numerical experiments P levels are increased in an ecologically meaningful range from 0.03 to 0.2 mg P / L. When P=0.03 mg P / L the population densities are at an equilibrium (Figure 3.4a). However, when P=0.05 mg P / L, the population densities no longer tend to a specific value but oscillate around an unstable equilibrium (Figure 3.4b). When P=0.08 mg P / L, the oscillations disappear and the population densities stabilize around a stable equilibrium (Figure 3.4c). Finally, for P=0.2 mg P / L, the producer density approaches a stable positive value, but the grazer population becomes extinct (Figure 3.4d). Figure 3.5 shows corresponding phase portraits for these numerical runs. The overall dynamics are similar to those of the original LKE model. However, large amounts of phosphorus in the system (P=0.2 mg P / L) cause the grazer population to head to deterministic extinction despite the large amounts of food available. This is the result of the reduction in growth due to an excess of phosphorus in their food.

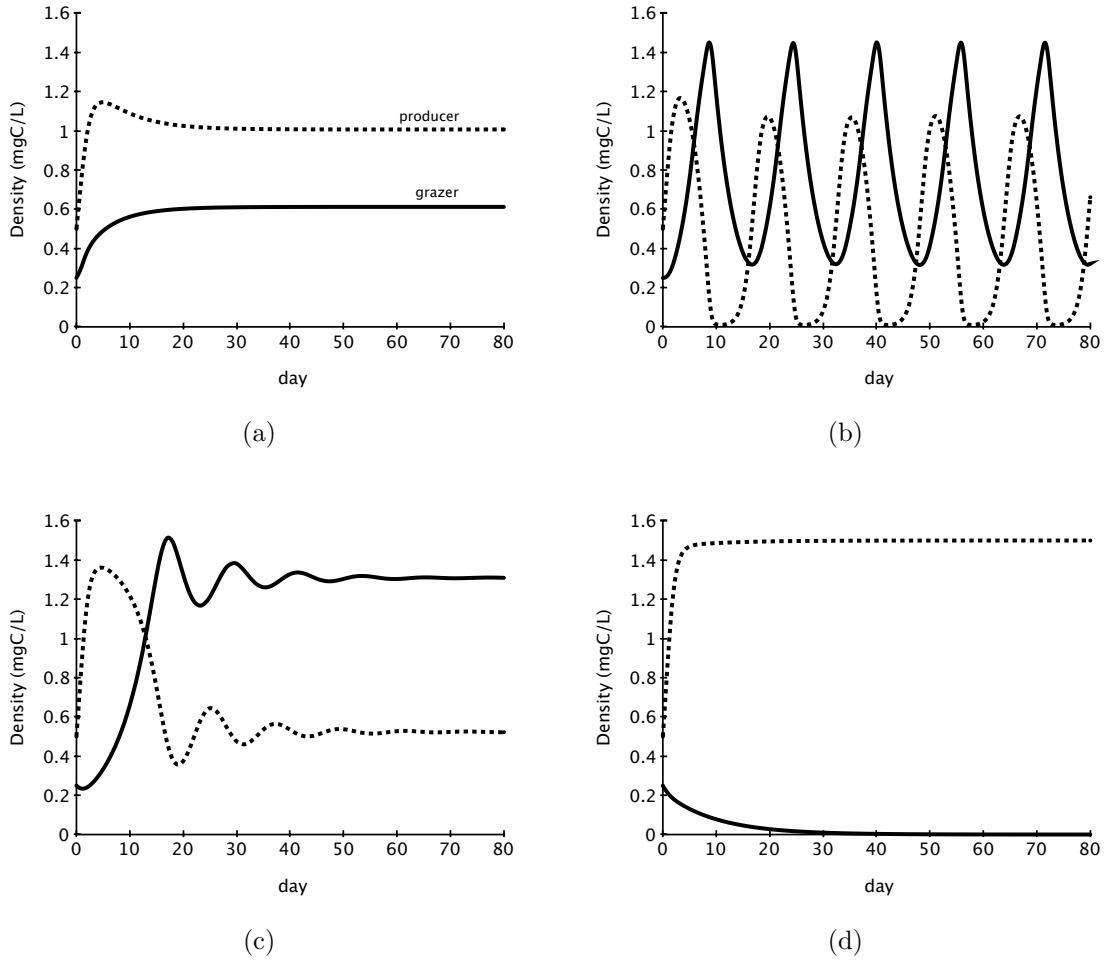

Figure 3.4: Numerical simulations performed using parameters found in Table 3.1 and varying values for P, (a) low total phosphorus P=0.03 mg P / L, (b) P=0.05 mg P / L, (c) P= 0.08 mg P / L, (d) excess phosphorus P=0.2 mg P / L. Panels (a) and (c) show positive stable equilibria while panel (b) captures oscillations around an unstable equilibrium. Panel (d) shows the grazer going towards extinction despite high food abundance. The extinction is caused by reduction of grazer growth due to high producer P:C.

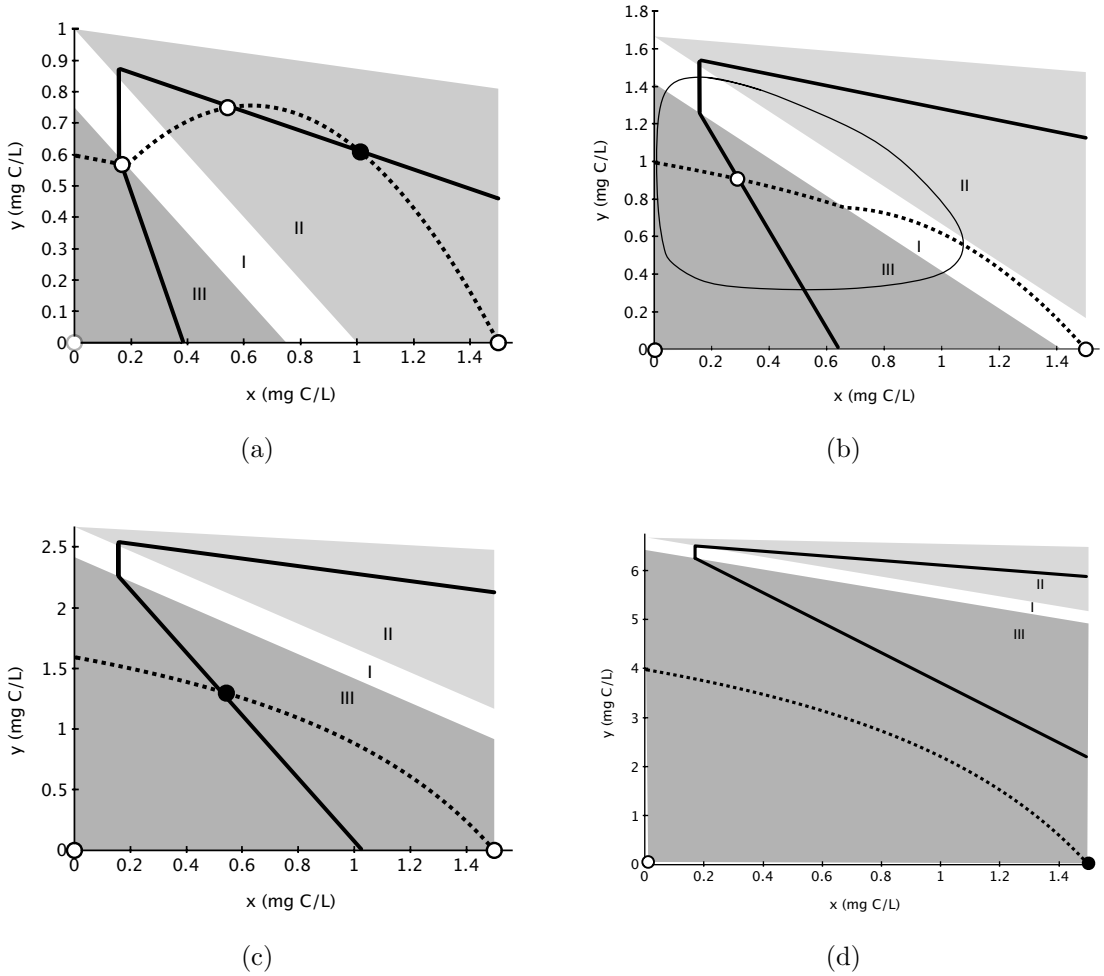

Figure 3.5: Phase planes corresponding to the numerical simulations in Figure 3.5, using parameters found in Table 3.1 and varying values for P, (a) low total phosphorus P=0.03 mg P / L, (b) P=0.05 mg P/ L, (c) P= 0.08 mg P/ L, (d) excess phosphorus P=0.2 mg P / L. The three different regions are depicted: P is not deficient or in excess in Region I, P is limiting in Region II, and P is in excess in Region III. Open circles denote unstable equilibria and filled in circles denote stable equilibria.

3.5 Discussion

Ecological stoichiometry stresses the importance of incorporating the effects of food quality into food web models. While there is a clear understanding of why grazer growth is low when food nutrient content is low, there has been little insight into the consequences of reduced grazer growth when food nutrient content is high. This proposed modification of the LKE Model was the first model to incorporate the knife edge phenomenon into grazer dynamics. The dynamical consequences of the knife edge for grazers can be seen in Figures 3.4d and 3.5d. Excess P causes grazer growth to decrease and eventually leads to grazer extinction despite the high food abundance. The effects of the knife edge can also be seen in the bifurcation diagram depicted in Figure 3.6. Here total phosphorus is used as a bifurcation parameter. As phosphorus is introduced into the system, a limit cycle emerges via a saddle-node bifurcation, then this limit cycle collapses via a Hopf bifurcation, grazer density begins to decrease, and eventually reaches deterministic extinction. To address the robustness of Figure 3.6 we investigated how sensitive this bifurcation diagram is to changes in parameter values. The overall shape of the diagram is robust. However, changes in parameter values can shift the location of the Hopf and saddle-node bifurcation points along the total P axis. For example increasing b, the maximal growth rate of the producer, increases the Hopf and saddle-node bifurcation points, and shifts the diagram to the right. Increasing θ, grazer P:C, or K, producer carrying capacity, decreases the Hopf and saddle-node bifurcation points, and shifts the diagram to the left.

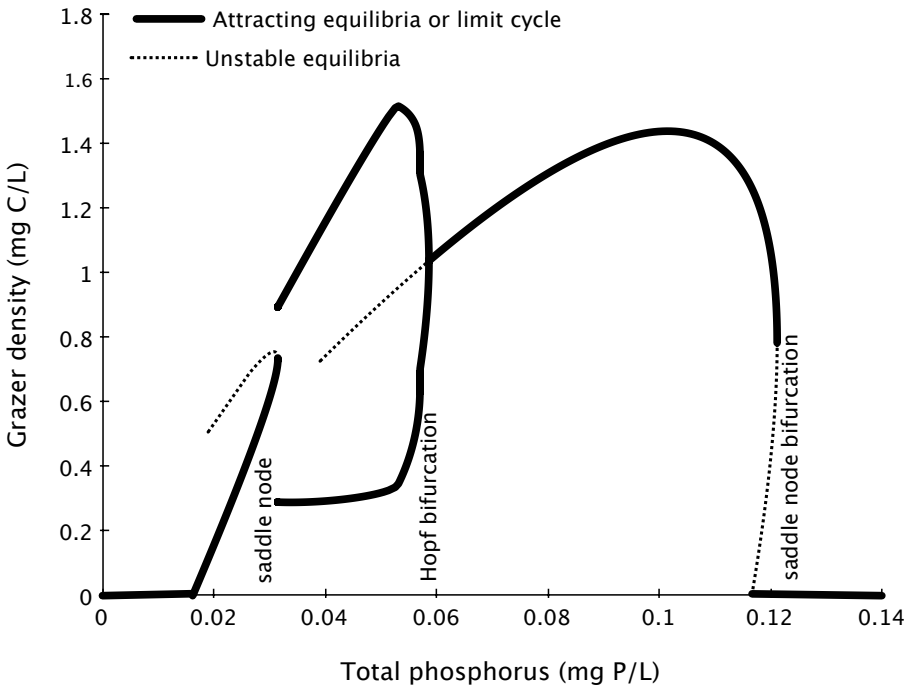

Figure 3.6: A bifurcation diagram of the locally asymptotically stable grazer density where total phosphorus is the bifurcation parameter. Parameter values are in Table 3.1 where P varies from 0 to 0.13 mg P /L. For P less than 0.016 mg P / L the grazer cannot persist due to starvation. As P increases from 0.016 mg P / L to 0.031 mg P / L the grazer equilibrium increases. At P=0.031 mg P / L this stable equilibrium is lost at a saddle-node bifurcation. There is a limit cycle as P increases from 0.031 mg P / L to 0.058 mg P / L. When P reaches 0.058 mg P / L, the limit cycle disappears and a new stable equilibrium appears at a Hopf bifurcation. Eventually as P increases, the grazer equilibrium begins to decreases until P=0.118 mg P / L where the grazer can no longer persist due to excess P. Data was generated via simulation using XPP/AUTO, details of which can be found in Appendix A.2.

The shape of the knife edge produced by these equations is captured in Figure 3.7, where the grazer growth function, $g(x, y)$ is plotted against the P quota of the

producer, Q. The left side of the curve depicts growth limitation by P and the right side shows growth decreasing due to excess P, as growth becomes limited by C because of reduced feeding rates. The shape of this curve depends on $\hat{f}\theta$, the maximum units of P ingested by each unit of grazer biomass per unit time. High values of $\hat{f}$ raise the height of the knife curve. High values of θ broaden the plateau at the peak of the grazer growth function. In reality, the value of $\hat{f}\theta$ and the shape of this curve will depend on the animal species being studied and require more detailed investigations.

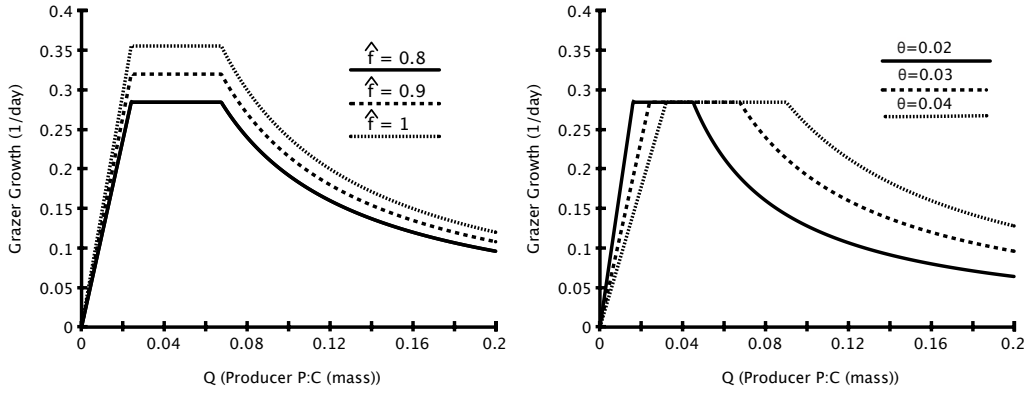

(a) (b)

Figure 3.7: Theoretical knife edge curve showing predicted dependence of grazer growth rate on producer P content for different values of $\hat{f}$ (a) and θ (b) using parameter values from Table 3.1. The grazer growth rate is low both when food P content is low, where growth is limited by P and when food P content is high, where P is in excess and growth is limited by C. $\hat{f}$; defined as the maximum grazer ingestion rate, controls the height of the peak of the knife curve. θ, the grazer P:C ratio controls the breadth of the plateau at the peak of the knife curve.

The theoretical knife curve (Figure 3.7,) as parameterized here shows that grazer growth begins to decline once the producer P:C exceeds 0.05-0.07. A relevant question

is how frequently available food for zooplankton reaches levels this high. This can be assessed by considering the data compiled by Sterner *et al.* (2008), who assembled data from published and unpublished sources consisting of 2,855 observations of carbon and phosphorus ratios in suspended particulate matter from small lakes, great lakes, and coastal and offshore oceans. They found that up to 10% of the data from each habitat had measurements of P:C near 0.05. Therefore, P:C values where grazer growth begins to decline due to excess P are indeed ecologically meaningful and are not infrequently observed in nature. The above model is parameterized for *Daphnia*, which have an unusually high P:C ratio ($\theta = 0.03$ (Andersen (1997); Urabe and Sterner (1996))) compared to other species of zooplankton. In this model the effects of excess P occur when the P:C of the post ingested algae is greater than the P:C of the zooplankton ($\frac{Q}{\hat{e}} > \theta$). Since other species of zooplankton have P:C ratios lower than *Daphnia* the effects of the knife edge will be seen for lower values of seston P:C; therefore such P:C values may be even more common than the 10% noted above. The issue of excess nutrients, and specifically nitrogen (N) and phosphorus excesses, becomes particularly relevant as human activities profoundly increase the inputs of these two elements into man managed and natural ecosystems. In some instances, the human-induced N and P loads can be several orders of magnitude higher relative to natural levels (Elser and Bennett (2011); Smith and Schindler (2009)), thus, creating ecosystem-wide states of nutrient excesses that would likely be manifested in low C:P and C:N ratios.

Chapter 4

EXPANDED STOICHIOMETRIC KNIFE EDGE MODEL THAT TRACKS FREE NUTRIENTS

4.1 Tracking Phosphorus in the Stoichiometric Knife Edge Model

Recall that the model presented in the previous section made the following assumptions.

A1: *The total mass of phosphorus in the entire system is fixed, i.e., the system is closed for phosphorus with a total of P (mgP/L).*

A2: *P:C ratio in the producer varies, but it never falls below a minimum q (mgP/mgC); the grazer maintains a constant P:C, θ (mgP/mgC).*

A3: *All phosphorus in the system is divided into two pools: phosphorus in the grazer and phosphorus in the producer.*

A4: *The grazer ingests P up to the rate required for its maximal growth but not more.*

Assumption 3 presents a problem for this model. It is assumed that all available P is in the algae; however, if the algae population is low, Q becomes unrealistically large. To improve this model more work is needed to investigate this extreme scenario of excess P with low algal density and define a maximum for the producer P quota. One possible approach to address this problem is to introduce a maximum value for Q. A modified model with a bounded quota is presented below. This modified model takes the same form as System (3.1) but places an upper bound on Q. Define $\hat{Q}$ as

the maximum P:C ratio of the producer. Then Q in System (3.1) takes the following form.

$$Q = \min\{\hat{Q}, \frac{P - \theta y}{x}\}$$

Assumption 2 is replaced with the following.

A2: *P:C ratio in the producer varies between a minimum q (mgP/mgC) and a maximum $\hat{Q}$ (mgP/mgC); the grazer maintains a constant P:C, θ (mgP/mgC).*

Assumption 3 is no longer needed, as the system allows for free P to be in the medium, outside of the grazers and producers. Simulations of the modified model are presented in Figure 4.1 using the parameter values in Table 3.1 and $\hat{Q} = 0.07$ for varying values for P. These parameter values are the same as used in the simulations of System (3.1) found in Figure 3.4. The dynamics are similar for these two models but there are some important differences worth noting as seen in panels (b), (c), and (d) of these Figures. In both models we see periodic oscillations around an unstable positive coexistence equilibrium for P=0.05 mg P / L depicted in panel (b). However Figure 4.1b shows oscillations where grazer density reaches smaller values. Figure 3.4c shows damped oscillations towards a positive stable equilibrium whereas Figure 4.1c shows large oscillations where the grazer density is at near zero values for a significant period of time and is very vulnerable to stochastic extinction. Figure 3.4d shows deterministic extinction caused by reduction of grazer growth due to high producer P:C. Figure 4.1d does not depict grazer extinction for the case of extreme excess P, but oscillations make the grazer vulnerable to stochastic extinction. This modified model, which places an upper bound on Q, appears to be more sensitive to high levels of P as the grazer density nears extinction during oscillations.

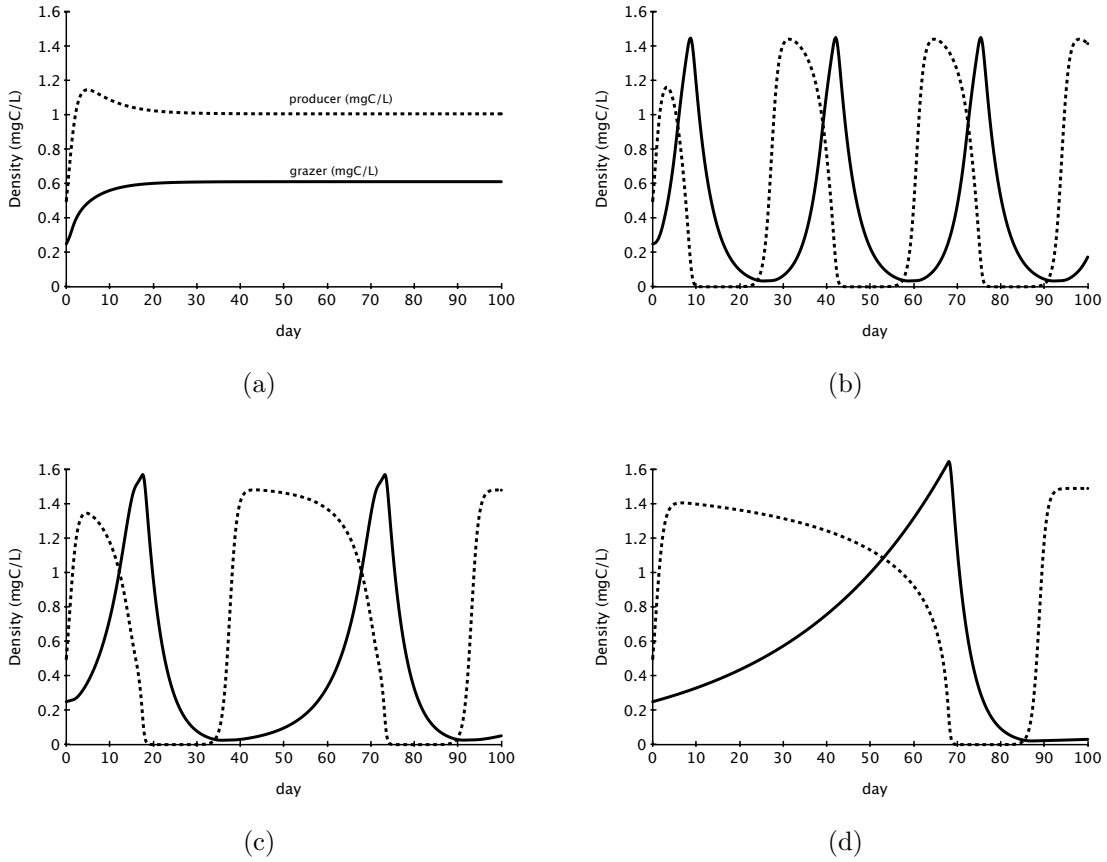

Figure 4.1: Numerical simulations of the modified system performed using parameters found in Table 3.1 and $\hat{Q} = 0.07$ for varying values for P, (a) low total phosphorus P=0.03 mg P / L, (b) P=0.05 mg P / L, (c) P= 0.08 mg P / L, (d) excess phosphorus P=0.2 mg P / L. Grazer and producer densities (mg C / L) are given by solid and dashed lines respectively. Panel (a) shows a positive stable equilibrium while panels (b), (c), and (d) capture oscillations around unstable equilibria. As P increases, these oscillations become large in amplitude and the grazer density approaches near zero values where the grazer is very vulnerable to stochastic (but not deterministic) extinction.

This approach of simply capping the quota is ad hoc. It would be more rigorous to explicitly track phosphorus as it travels from the environment and into the producer and grazer populations. Doing so would require an additional equation to handle free P concentrations. A three dimensional ODE model is formulated in this section in order to track free P in the *stoichiometric knife edge* model following the procedure used by Wang *et al.* (2008).

4.2 Model Formulation

Let P_a describe the P in the algae, P_z the P in the zooplankton, P_f the free P in the medium. We assume that total phosphorus, P, is constant.

$$P = P_a + P_z + P_f \tag{4.1}$$

Notice that P_a/x describes the producer cell quota. The following equations track the phosphorus in the algae and the free phosphorus.

$$\frac{dP_a}{dt} = \underbrace{v(P_f, Q)x}_{\text{P uptake}} - \underbrace{\frac{P_a}{x} \min\left\{ f(x), \frac{\hat{f}\theta}{P_a/x} \right\} y}_{\text{P loss due to grazing}} \tag{4.2}$$

$$\frac{dP_f}{dt} = \underbrace{-v(P_f, Q)x}_{\text{producer P uptake}} + \underbrace{\theta d y}_{\substack{\text{P from} \\ \text{grazer} \\ \text{death}}} + \underbrace{\min\left\{ f(x), \frac{\hat{f}\theta}{P_a/x} \right\} y \left(\frac{P_a}{x} - \min\left\{ \hat{e}, \frac{P_a/x}{\theta} \right\} \theta \right)}_{\text{P recycled by grazer}} \tag{4.3}$$

Here $v(P_f, Q)$ is the P uptake rate of the producer. This depends on the amount of available free phosphorus (P_f) as well as the producer quota (Q). As P_f increases v should increase towards a maximum saturation level, as in a Holling type function response. Since Q is bounded above, v decreases as Q increases towards its maximum.

v shall take the form following Diehl (2007),

$$v(P_f, Q) = \frac{\hat{c}P_f}{\hat{a} + P_f} \frac{\hat{Q} - Q}{\hat{Q} - q} \tag{4.4}$$

where $\hat{Q}$ is the maximum Quota, $\hat{c}$ is the maximum phosphorus per carbon uptake rate of the producer, and $\hat{a}$ is the phosphorus half saturation constant of the producer.

There is a small modification in the producer equation. Under assumption 3, the previous model assumes $P - \theta y$ is the amount of P available for producer growth. To modify this to allow free P in the water, the amount of P available for producer growth is denoted Qx. Therefore the producer equation becomes

$$\frac{dx}{dt} = bx\left(1 - \frac{x}{\min(k, (Qx)/q)}\right) - \min\left\{f(x), \frac{\hat{f}\theta}{Q}\right\} y. \tag{4.5}$$

Also note that

$$\frac{dx}{dt} = bx \min\left\{1 - \frac{x}{k}, 1 - \frac{x}{Qx/q}\right\} - \min\left\{f(x), \frac{\hat{f}\theta}{Q}\right\} y \tag{4.6a}$$

$$= bx \min\left\{1 - \frac{x}{k}, 1 - \frac{q}{Q}\right\} - \min\left\{f(x), \frac{\hat{f}\theta}{Q}\right\} y \tag{4.6b}$$

Letting $Q = P_a/x$ we can write an equation that describes how the producer P quota changes over time.

$$\frac{dQ}{dt} = v(P_f, Q) - b \min\left\{Q(1 - \frac{x}{k}), (Q - q)\right\} \tag{4.7}$$

We then arrive at the following model.

$$\frac{dx}{dt} = bx \min\left\{1 - \frac{x}{k}, 1 - \frac{q}{Q}\right\} - \min\left\{f(x), \frac{\hat{f}\theta}{Q}\right\} y \tag{4.8a}$$

$$\frac{dy}{dt} = \min\left\{\hat{e}f(x), \frac{Q}{\theta}f(x), \hat{e}\hat{f}\frac{\theta}{Q}\right\} y - dy \tag{4.8b}$$

$$\frac{dQ}{dt} = v(P_f, Q) - b \min\left\{Q(1 - \frac{x}{k}), (Q - q)\right\} \tag{4.8c}$$

$$\frac{dP_f}{dt} = -v(P_f, Q)x + \theta dy + \min\left\{f(x), \frac{\hat{f}\theta}{Q}\right\} y \left(Q - \min\left\{\hat{e}, \frac{Q}{\theta}\right\}\theta\right) \tag{4.8d}$$

The assumption that total P in the system is constant allows this model to be reduced to three ODEs. P is indeed constant, to see this conservation law note that total phosphorus can be expressed as $P = Q(t)x(t) + \theta y(t) + P_f(t)$. Then, since $\hat{e}f(x) < \hat{f}$ the following holds true.

$$\frac{dP}{dt} = Q'(t)x(t) + Q(t)x'(t) + \theta y'(t) + P_f'(t) \tag{4.9}$$

$$= \min\left\{\hat{e}f(x), \frac{Q}{\theta}f(x), \hat{e}\hat{f}\frac{\theta}{Q}\right\}\theta y - \min\left\{f(x), \frac{\hat{f}\theta}{Q}\right\}\min\left\{\hat{e}, \frac{Q}{\theta}\right\}\theta y \tag{4.10}$$

$$= \min\left\{\hat{e}f(x), \frac{Q}{\theta}f(x), \hat{e}\hat{f}\frac{\theta}{Q}\right\}\theta y - \min\left\{\hat{e}f(x), \frac{Q}{\theta}f(x), \frac{\hat{e}\hat{f}\theta}{Q}, \hat{f}\right\}\theta y \tag{4.11}$$

$$= 0 \tag{4.12}$$

Thus P is indeed constant and we can formulate an expression for the free phosphorus, $P_f(t) = P - Q(t)x(t) - \theta y(t)$. The model may be reduced down to three equations.

$$\frac{dx}{dt} = bx\min\left\{1 - \frac{x}{k}, 1 - \frac{q}{Q}\right\} - \min\left\{f(x), \frac{\hat{f}\theta}{Q}\right\}y \tag{4.13a}$$

$$\frac{dy}{dt} = \min\left\{\hat{e}f(x), \frac{Q}{\theta}f(x), \hat{e}\hat{f}\frac{\theta}{Q}\right\}y - dy \tag{4.13b}$$

$$\frac{dQ}{dt} = v(P - Qx - \theta y, Q) - b\min\left\{Q(1 - \frac{x}{k}), (Q - q)\right\} \tag{4.13c}$$

4.3 Model Analysis

Here we present a basic analysis of the model verifying the boundedness and positivity of the solutions. We also locate boundary equilibria and develop some criteria to determine their stability. Interior equilibria are investigated numerically in Section 4.4.1. For the following analysis we denote $K = \min\{k, \frac{P}{q}\}$.

4.3.1 Positive Invariance

Theorem 4.3.1. *Solutions to system (4.13) with initial conditions in the set*

$$\Omega = \left\{(x, y, Q) : 0 \leq x \leq K = \min\left\{k, \frac{P}{q}\right\}, 0 \leq y, q \leq Q \leq \hat{Q}, Qx + \theta y \leq P\right\} \tag{4.14}$$

will remain there for all forward time.

Proof. Let $S(t) = (x(t), y(t), Q(t))$ be a solution of 4.13 with $S(0) \in \Omega$. Assume there exists a time $t_1 > 0$ such that $S(t_1)$ touches or crosses a boundary of Ω for the first time. The following cases prove the lemma by contradiction.

Case 1: $Q(t_1) = q$

Then for every $t \in [0, t_1]$,

$$\begin{aligned} Q' &= v(P - Qx - \theta y, Q) - b \min\left\{Q(1 - \frac{x}{k}), Q - q\right\} \\ &\geq -b \min\left\{Q(1 - \frac{x}{k}), Q - q\right\} \\ &\geq -b(Q - q). \end{aligned}$$

This implies that $Q(t) \geq q + (Q(0) - q)e^{-bt} > q$. This contradicts $Q(t_1) = q$ and proves that $S(t_1)$ can not cross this boundary.

Case 2: $x(t_1) = 0$

Let $\overline{f} = f'(0) = \lim_{x \to 0} \frac{f(x)}{x}$ and $\overline{y} = \max_{t \in [0, t_1]} y(t) < \frac{P}{\theta}$. Then for every $t \in [0, t_1]$,

$$\begin{aligned} x' &= bx \min\left\{1 - \frac{x}{k}, 1 - \frac{q}{Q}\right\} - \min\left\{f(x), \frac{\hat{f}\theta}{Q}\right\} y \\ &\geq -f(x)y \geq -\bar{f}\bar{y}x \equiv \alpha x \end{aligned}$$

This implies that $x(t_1) \geq x(0)e^{\alpha t_1} > 0$, where α is a constant. This contradicts $x(t_1) = 0$ and proves that $S(t_1)$ does not reach this boundary.

Case 3: $y(t_1) = 0$

Then for every $t \in [0, t_1]$,

$$\begin{aligned} y' &= \min\left\{\hat{e}f(x), \frac{Q}{\theta}f(x), \hat{e}\hat{f}\frac{\theta}{Q}\right\} y - dy \\ &\geq -dy. \end{aligned}$$

This implies that $y(t_1) \geq y(0)e^{-dt_1} > 0$. This contradicts $y(t_1) = 0$ and proves that $S(t_1)$ does not reach this boundary.

Case 4: $Qx + \theta y = P$

Since $v(P - Q(t_1)x(t_1) - \theta y(t_1)) = 0$

$$\begin{aligned} \left.\frac{d(Qx+\theta y)}{dt}\right|_{t_1} &= Q'(t_1)x(t_1) + Q(t_1)x(t_1)' + \theta y'(t_1) \\ &= -Q(t_1)\min\left\{f(x(t_1)), \frac{\hat{f}\theta}{Q(t_1)}\right\} y(t_1) \\ &\qquad + \theta \min\left\{\hat{e}f(x(t_1)), \frac{Q(t_1)}{\theta}f(x(t_1)), \hat{e}\hat{f}\frac{\theta}{Q(t_1)}\right\} y(t_1) - \theta d y(t_1) \\ &= -y(t_1)\min\left\{f(x(t_1)), \frac{\hat{f}\theta}{Q(t_1)}\right\}\left(Q(t_1) - \theta\min\left\{\hat{e}, \frac{Q(t_1)}{\theta}\right\}\right) - \theta d y(t_1) \\ &\leq 0. \end{aligned}$$

Thus, $S(t_1)$ can not cross this boundary.

Case 5: $x(t_1) = K$

Then for every $t \in [0, t_1]$,

$$\begin{aligned} x' &= bx \min\left\{1 - \frac{x}{k}, 1 - \frac{q}{Q}\right\} - \min\left\{f(x), \frac{\hat{f}\theta}{Q}\right\} y \\ &\leq bx \min\left\{1 - \frac{x}{k}, 1 - \frac{q}{Q}\right\} \\ &= bx\left(1 - \frac{x}{\min\left\{k, \frac{Qx}{q}\right\}}\right) \\ &\leq bx\left(1 - \frac{x}{\min\left\{k, \frac{P}{q}\right\}}\right) \\ &= bx\left(1 - \frac{x}{K}\right). \end{aligned}$$

Then $x(t_1) \leq K$ by a standard comparison argument, thus $S(t_1)$ can not cross this boundary.

Case 6: $Q(t_1) = \hat{Q}$

Since $v(P - Q(t_1)x(t_1) - \theta y(t_1), Q(t_1)) = 0$

$$\begin{aligned} Q' &= -b \min\left\{Q(1.\frac{x}{k}), Q - q\right\} \\ &< 0. \end{aligned}$$

Thus $S(t_1)$ can not cross this boundary. □

4.3.2 Boundary Equilibria

Consider the system,

$$x' = xF(x, y, Q) = 0 \tag{4.15a}$$

$$y' = yG(x, y, Q) = 0 \tag{4.15b}$$

$$Q' = H(x, y, Q) = 0 \tag{4.15c}$$

There are two equilibria on the boundary; E_0 for extinction of both the producer and the grazer and E_1 for extinction of just the grazer. $E_0 = (x_0, y_0, Q_0) = (0, 0, Q_0)$ where Q_0 satisfies $v(P, Q_0) = b(Q_0 - q)$. Although $Q_0 > 0$, this equilibrium still represents the case for producer and grazer extinction because $x_0, y_0 = 0$. $E_1 = (x_1, y_1, Q_1) = (k, 0, \min\{\frac{P}{k}, \hat{Q}\})$ if $1 - \frac{x}{k} < 1 - \frac{q}{Q}$ and $E_1 = (\frac{P}{q}, 0, q)$ if $1 - \frac{x}{k} > 1 - \frac{q}{Q}$. The following theorems give results on the stability of these extinction equilibria.

The Jacobian of the above system (4.15) is

$$J = \begin{vmatrix} F(x,y,Q) + xF_x(x,y,Q) & xF_y(x,y,Q) & xF_Q(x,y,Q) \\ yG_x(x,y,Q) & G(x,y,Q) + yG_y(x,y,Q) & yG_Q(x,y,Q) \\ H_x(x,y,Q) & H_y(x,y,Q) & H_Q(x,y,Q) \end{vmatrix}.$$

Theorem 4.3.2. *The producer and grazer extinction equilibrium, E_0, is unstable.*

Proof. To prove that E_0 is unstable, it is sufficient to show the system linearized at this equilibrium has an eigenvalue whose real part is positive. This is seen in the following Jacobian,

$$J(E_0) = \begin{vmatrix} b\left(1 - \frac{q}{Q_0}\right) & 0 & 0 \\ 0 & G(0,0,Q_0) & 0 \\ H_x(0,0,Q_0) & H_y(0,0,Q_0) & H_Q(0,0,Q_0) \end{vmatrix},$$

where $b\left(1 - \frac{q}{Q_0}\right) > 0$. □

Lemma 4.3.1. *The grazer extinction equilibrium $E_1 = (x_1, y_1, Q_1)$ takes the following form for the cases below.*

$$E_1 = (x_1, y_1, Q_1) = \begin{cases} \left(k, 0, \min\left\{\frac{P}{k}, \hat{Q}\right\}\right) & \text{if } 1 - \frac{x}{k} < 1 - \frac{q}{Q} \\ \left(\frac{P}{q}, 0, q\right) & \text{if } 1 - \frac{x}{k} > 1 - \frac{q}{Q} \end{cases} \tag{4.16}$$

and these two forms of E_1 cannot coexist.

Proof. We consider two cases ($1 - \frac{x}{k} < 1 - \frac{q}{Q}$ and $1 - \frac{x}{k} > 1 - \frac{q}{Q}$).

Case 1: $1 - \frac{x}{k} < 1 - \frac{q}{Q}$

In this case, (Eq. 4.13a) becomes

$$\frac{dx}{dt} = bx\left(1 - \frac{x}{k}\right) - \min\left\{f(x), \frac{\hat{f}\theta}{Q}\right\} y \tag{4.17}$$

and $x_1 = k$. (Eq. 4.13c) becomes

$$\frac{dQ}{dt} = v(P - Qx - \theta y, Q) - bQ\left(1 - \frac{x}{k}\right) \tag{4.18}$$

therefore $v(P - Q_1 k, Q_1) = 0$. There are two cases to consider here ($\frac{P}{k} > \hat{Q}$ and $\frac{P}{k} < \hat{Q}$). If $\frac{P}{k} > \hat{Q}$ then $Q_1 = \hat{Q}$ to remain in Ω. Since $P \geq Q_1 x_1 = Q_1 k$, the case when $\frac{P}{k} < \hat{Q}$ results in $\hat{Q} > \frac{P}{k} \geq Q_1$, thus $Q_1 = \frac{P}{k}$. The two cases are summarized below

$$Q_1 = \left\{ \begin{array}{ll} \hat{Q} & \text{if } \frac{P}{k} > \hat{Q} \\ \frac{P}{k} & \text{if } \frac{P}{k} < \hat{Q} \end{array} \right\} = \min\left\{\frac{P}{k}, \hat{Q}\right\}. \tag{4.19}$$

Case 2: $1 - \frac{x}{k} > 1 - \frac{q}{Q}$

In this case, (Eq. 4.13a) becomes

$$\frac{dx}{dt} = bx\left(1 - \frac{q}{Q}\right) - \min\left\{f(x), \frac{\hat{f}\theta}{Q}\right\} y \tag{4.20}$$

and $Q_1 = q$. (Eq. 4.13c) becomes

$$\frac{dQ}{dt} = v(P - Qx - \theta y, Q) - bQ\left(1 - \frac{q}{Q}\right) \tag{4.21}$$

therefore $v(P - qx_1, q) = 0$ and thus $x_1 = \frac{P}{q}$.

To show that the two equilibrium forms cannot coexist, we need to show that they satisfy two opposite conditions.

In case 1: $1-\frac{x}{k}<1-\frac{q}{Q}$ and $E_1=\left(k,0,\min\left\{\frac{P}{k},\hat{Q}\right\}\right)$, therefore

$$0<1-\frac{q}{\min\left\{\frac{P}{k},\hat{Q}\right\}}$$
$$\implies \min\left\{\frac{P}{k},\hat{Q}\right\}>q.$$

Here

$$\frac{P}{k}\geq\min\left\{\frac{P}{k},\hat{Q}\right\}>q.$$

In case 2: $1-\frac{x}{k}>1-\frac{q}{Q}$ and $E_1=\left(\frac{P}{q},0,q\right)$, therefore

$$1-\frac{P}{qk}>0$$
$$\implies \frac{P}{k}<q.$$

The two cases follow opposite conditions. Actually, when $\frac{P}{k}=q$, the two forms of E_1 collide to $(k,0,q)$. □

Theorem 4.3.3. *The grazer extinction equilibrium, E_1, is locally asymptotically stable if*

$$\min\left\{\hat{e}f(x_1),\frac{Q_1}{\theta}f(x_1),\hat{e}\hat{f}\frac{\theta}{Q_1}\right\}<d.$$

Proof. Assume that $\min\left\{\hat{e}f(x_1),\frac{Q_1}{\theta}f(x_1),\hat{e}\hat{f}\frac{\theta}{Q_1}\right\}<d$. To prove that E_1 is stable we consider two cases ($1-\frac{x}{k}<1-\frac{q}{Q}$ and $1-\frac{x}{k}>1-\frac{q}{Q}$). We look at the linearized system and use the Routh-Hurwitz criterion.

Case 1: $1-\frac{x}{k}<1-\frac{q}{Q}$

Here $E_1=\left(k,0,\min\left\{\frac{P}{k},\hat{Q}\right\}\right)$ by Lemma 4.3.1 and the Jacobian takes the following form,

$$J(E_1)=\begin{vmatrix} -b & kF_y\left(k,0,\min\left\{\frac{P}{k},\hat{Q}\right\}\right) & 0 \\ 0 & \min\left\{\hat{e}f(k),\frac{\min\left\{\frac{P}{k},\hat{Q}\right\}}{\theta}f(k),\hat{e}\hat{f}\frac{\theta}{\min\left\{\frac{P}{k},\hat{Q}\right\}}\right\}-d & 0 \\ H_x\left(k,0,\min\left\{\frac{P}{k},\hat{Q}\right\}\right) & H_y\left(k,0,\min\left\{\frac{P}{k},\hat{Q}\right\}\right) & \frac{dv}{dQ}\big|_{E_1} \end{vmatrix}.$$

Let $\alpha_1 = \min\left\{\hat{e}f(k), \frac{\min\left\{\frac{P}{k},\hat{Q}\right\}}{\theta}f(k), \hat{e}\hat{f}\frac{\theta}{\min\left\{\frac{P}{k},\hat{Q}\right\}}\right\} - d < 0$ and $\alpha_2 = \frac{dv}{dQ}\big|_{E_1} < 0$. Then the Jacobian simplifies to

$$J(E_1) = \begin{vmatrix} -b & kF_y\left(k, 0, \min\left\{\frac{P}{k}, \hat{Q}\right\}\right) & 0 \\ 0 & \alpha_1 & 0 \\ H_x\left(k, 0, \min\left\{\frac{P}{k}, \hat{Q}\right\}\right) & H_y\left(k, 0, \min\left\{\frac{P}{k}, \hat{Q}\right\}\right) & \alpha_2 \end{vmatrix}.$$

The characteristic equation may be written

$$(-b-\lambda)(\alpha_1-\lambda)(\alpha_2-\lambda) = 0$$

The eigenvalues of $J(E_1)$ are $-b, \alpha_1, \alpha_2$, which are all negative.

Case 2: $1 - \frac{x}{k} > 1 - \frac{q}{Q}$

Here $E_1 = (\frac{P}{q}, 0, q)$ by Lemma 4.3.1 and the Jacobian takes the following form,

$$J(E_1) = \begin{vmatrix} 0 & \frac{P}{q}F_y(\frac{P}{q}, 0, q) & \frac{Pb}{q^2} \\ 0 & \min\left\{\hat{e}f(\frac{P}{q}), \frac{\hat{q}}{\theta}f(\frac{P}{q}), \hat{e}\hat{f}\frac{\theta}{q}\right\} - d & 0 \\ \frac{dv}{dx}\big|_{E_1} & H_y(\frac{P}{q}, 0, q) & \frac{dv}{dQ}\big|_{E_1} - b \end{vmatrix}.$$

Let $\alpha_1 = \min\left\{\hat{e}f(\frac{P}{q}), \frac{\hat{q}}{\theta}f(\frac{P}{q}), \hat{e}\hat{f}\frac{\theta}{q}\right\} - d < 0$, $\alpha_2 = \frac{dv}{dQ}\big|_{E_1} - b < 0$, $\alpha_3 = \frac{dv}{dx}\big|_{E_1} < 0$. Then the Jacobian simplifies down to

$$J(E_1) = \begin{vmatrix} 0 & \frac{P}{q}F_y(\frac{P}{q}, 0, q) & \frac{Pb}{q^2} \\ 0 & \alpha_1 & 0 \\ \alpha_3 & H_y(\frac{P}{q}, 0, q) & \alpha_2 \end{vmatrix}.$$

The characteristic equation may be written

$$\lambda^3 + \lambda^2(-\alpha_1 - \alpha_2) + \lambda(\alpha_1\alpha_2 - \frac{Pb}{q^2}\alpha_3) + \frac{Pb}{q^2}\alpha_1\alpha_3.$$

Since $\alpha_1, \alpha_2, \alpha_3 < 0$ we find that $-\alpha_1 - \alpha_2 > 0$, $\frac{Pb}{q^2}\alpha_1\alpha_3 > 0$, and $(-\alpha_1 - \alpha_2)(\alpha_1\alpha_2 - \frac{Pb}{q^2}\alpha_3) > \frac{Pb}{q^2}\alpha_1\alpha_3$. These are the conditions of the Routh-Hurwitz criterion that guarantee all the eigenvalues of $J(E_1)$ have strictly negative real parts. Thus E_1 is locally asymptotically stable for both cases. □

Theorem 4.3.4. *The grazer extinction equilibrium, E_1, is globally asymptotically stable if*

$$\min\left\{\hat{e}f(K), \frac{\hat{Q}}{\theta}f(K), \hat{e}\hat{f}\frac{\theta}{q}\right\} < d.$$

Proof. The set Ω is positively invariant under System (4.13) by Lemma 4.3.1. Let

$$\alpha = \min\left\{\hat{e}f(K), \frac{\hat{Q}}{\theta}f(K), \hat{e}\hat{f}\frac{\theta}{q}\right\} - d < 0. \tag{4.22}$$

For all $(x, y, Q) \in \Omega$ the expression for y' may be expressed as

$$\begin{aligned}\frac{y'}{y} &= \min\left\{\hat{e}f(x), \frac{Q}{\theta}f(x), \hat{e}\hat{f}\frac{\theta}{Q}\right\} - d \\ &\leq \min\left\{\hat{e}f(K), \frac{\hat{Q}}{\theta}f(K), \hat{e}\hat{f}\frac{\theta}{q}\right\} - d \\ &= \alpha\end{aligned}$$

This implies that $\lim_{t\to\infty} y(t) = 0$. In autonomous System (4.13), $y(t)$ converges to 0. We may consider the behavior of System (4.13) on the plane $y = 0$ with the limit system

$$\frac{dx}{dt} = bx\min\left\{1 - \frac{x}{k}, 1 - \frac{q}{Q}\right\} \tag{4.23a}$$

$$\frac{dQ}{dt} = v(P - Qx, Q) - b\min\left\{Q(1 - \frac{x}{k}), (Q - q)\right\}, \tag{4.23b}$$

defined on the domain

$$\bar{\Omega} = \left\{(x, Q)|0 < x < K, q < Q < \hat{Q}\right\} \tag{4.24}$$

System (4.23) is the limiting system of the asymptotically autonomous System (4.13) under the constraint $\min\left\{\hat{e}f(K), \frac{\hat{Q}}{\theta}f(K), \hat{e}\hat{f}\frac{\theta}{q}\right\} - d$. Results from Markus (1956) and Thieme (1992) allow us to compare solutions of an autonomous system with those of the asymptotically autonomous limit system. System (4.23) has one equilibrium $\bar{E}_1 = (\bar{x}_1, \bar{Q}_1)$ and this equilibrium is globally asymptotically stable. To show this global stability we consider two cases ($1 - \frac{x}{k} < 1 - \frac{q}{Q}$ and $1 - \frac{x}{k} > 1 - \frac{q}{Q}$) where we

look at the linearized system and then consider the existence of periodic orbits.

Case 1: $1-\frac{x}{k}<1-\frac{q}{Q}$

Here $\bar{E}_1=\left(k,\min\left\{\frac{P}{k},\hat{Q}\right\}\right)$ and the Jacobian takes the form,

$$J(\bar{E}_1)=\begin{vmatrix} -b & 0 \\ \frac{dv}{dx}\big|_{\bar{E}_1}+\frac{b\min\left\{\frac{P}{k},\hat{Q}\right\}}{k} & \frac{dv}{dQ}\big|_{\bar{E}_1} \end{vmatrix}.$$

The eigenvalues are $-b<0$ and $\frac{dv}{dQ}\big|_{\bar{E}_1}<0$.

Case 2: $1-\frac{x}{k}>1-\frac{q}{Q}$

Here $\bar{E}_1=(\frac{P}{q},q)$ and the Jacobian takes the form,

$$J(\bar{E}_1)=\begin{vmatrix} 0 & b\frac{P}{q^2} \\ \frac{dv}{dx}\big|_{\bar{E}_1} & \frac{dv}{dQ}\big|_{\bar{E}_1}-b \end{vmatrix}.$$

Here $\text{trace}(J(\bar{E}_1))=\frac{dv}{dQ}\big|_{\bar{E}_1}-b<0$ and $\det(J(\bar{E}_1))=-b\frac{P^2}{q^2}\frac{dv}{dx}\big|_{\bar{E}_1}>0$. In both cases $\bar{E}_1$ is locally asymptotically stable. To show that no periodic orbits exist in $\bar{\Omega}$ consider

$$(xQ)'=xv(P-Qx,Q)>0.$$

The inequality shows that xQ has no maximum (or minimum), hence there can not be any periodic solutions. Since $\bar{\Omega}$ is simply connected and is positively invariant under System (4.23) and contains no periodic orbits, by the Poincaré-Bendixson Theorem, all solutions of System (4.23) starting in $\bar{\Omega}$ will converge to $\bar{E}_1$. Thus $\bar{E}_1$ is globally asymptotically stable. The $\omega-$limit set of a forward bounded solution of the autonomous System (4.13) consists of the equilibrium of its limit autonomous System (4.23) (Thieme (1992)). Thus the $\omega-$limit set of System (4.13) is $\{E_1\}$. The grazer only extinction equilibrium E_1 is globally asymptotically stable,

$$\text{if } 1-\tfrac{x}{k}<1-\tfrac{q}{Q} \quad \text{then} \quad \lim_{t\to\infty}(x(t),y(t),Q(t))=\left(k,0,\min\left\{\frac{P}{k},\hat{Q}\right\}\right),$$
$$\text{if } 1-\tfrac{x}{k}>1-\tfrac{q}{Q} \quad \text{then} \quad \lim_{t\to\infty}(x(t),y(t),Q(t))=\left(\frac{P}{q},0,q\right).$$

□

4.4 Numerical Experiments

This section describes the results of numerical experiments and a numerical bifurcation analysis on interior equilibria. All simulations use the Holling type II function $f(x) = \frac{\hat{f}x}{a+x}$ for the grazer ingestion rate. Parameter values are listed in Table 4.1. All parameters are biologically realistic values obtained from Andersen (1997) and Urabe and Sterner (1996) and used by Loladze *et al.* (2000) and Peace *et al.* (2013). The values of $\hat{c}$ and $\hat{a}$ are used in Wang *et al.* (2008) and are within the same orders of magnitude as those found in Andersen (1997) and Diehl (2007).

In our numerical experiments we increase P in an ecologically meaningful range from 0.03 to 0.2 mg P/L. P is the total amount of phosphorus in the system and affects the P:C ratio of the producer (Q) and thus the growth dynamics of the grazer. Figure 4.2 shows numerical simulations of the full model for varying values of P using initial conditions: $x_0 = 0.5$, $y_0 = 0.25$, and $Q_0 = (P - \theta y_0)/x_0$. As P increases, the system exhibits stable coexistence equilibria, periodic cycles, and grazer extinction equilibria. Values of P that lead the system into limit cycles can affect the grazer's chance of survival. The cycles are large in amplitude which results in the grazer population spending significant periods of time with low populations near extinction, where they are sensitive to stochastic extinction. The amplitude of these limits cycles are much larger than those on the 2D knife model, System (3.1), that does not explicitly track free phosphorus in the media (Peace *et al.* (2013)).

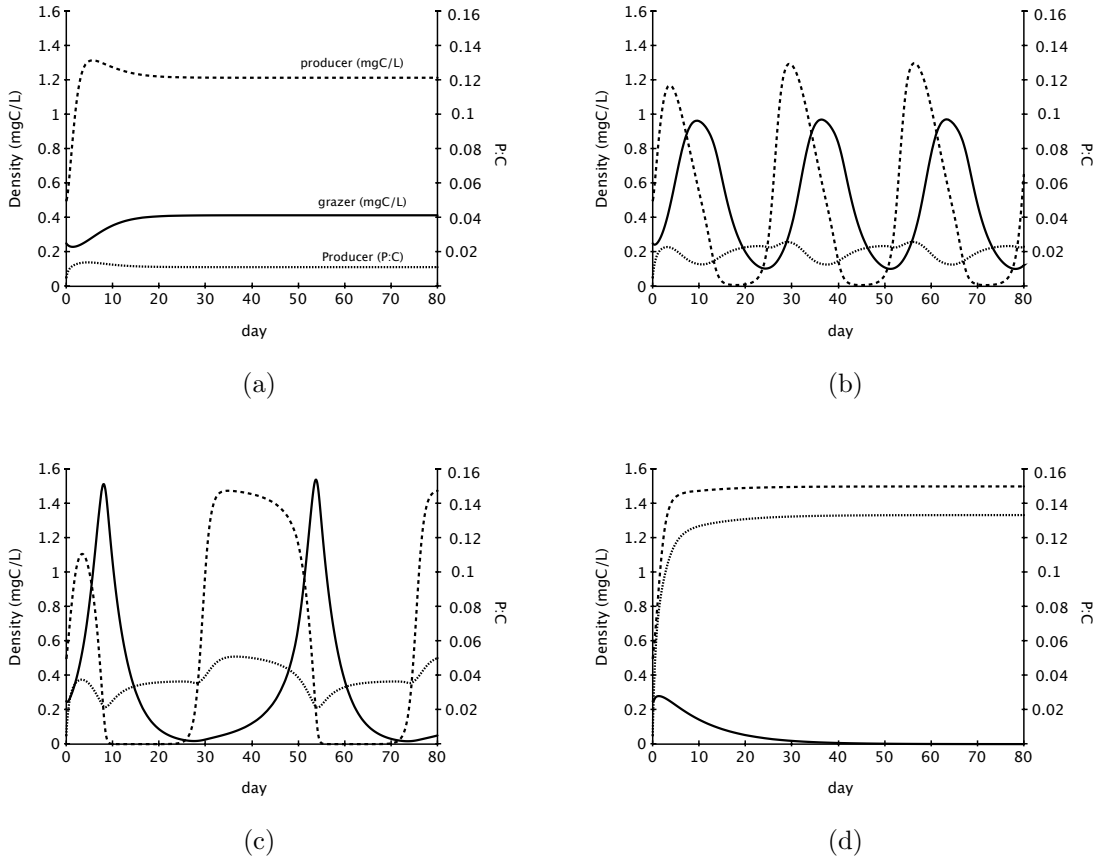

Figure 4.2: Numerical simulations of the full model presented in System (4.13) performed using parameters found in Table 4.1 and varying values of P, (a) low total phosphorus P=0.03 mg P / L, (b) P=0.05 mg P / L, (c) P= 0.08 mg P / L, (d) excess phosphorus P=0.2 mg P / L. $x_0 = 0.5$ mg C / L, $y_0 = 0.25$ mg C / L, $Q_0 = \min\{(P - \theta y_0)/x_0, \hat{Q}\}$ were used as initial conditions. Grazer and producer densities (mg C / L) are given by solid and big-dashed lines respectively and Q, producer cell quota (P:C), is given by small-dotted lines. Panel (a) shows a positive stable equilibrium while panels (b) and (c) capture oscillations around unstable equilibria. These oscillations have an unstable grazer density, almost nearing extinction. Panel (d) shows the grazer going towards extinction despite high food abundance. The extinction is caused by reduction of grazer growth due to high producer P:C.

Parameter		Value
P	Total Phosphorus	0.03-0.2 mg P/L
b	Maximal growth rate of producer	1.2/d
d	Grazer loss rate	0.25/d
θ	Grazer constant P:C	0.03 mg P/mg C
q	Producer minimal P:C	0.0038 mg P/mg C
$\hat{e}$	Maximal production efficiency	0.8 (unitless)
k	Producer carrying capacity	1.5 mg C/L
$\hat{f}$	Maximal ingestion rate of the grazer	0.81/d
a	Half saturation of the grazer ingestion	0.25 mg C/L
$\hat{c}$	Producer maximum P per C uptake rate	0.2 mg P/mg C/d
$\hat{a}$	Producer P half saturation constant	0.008 mg P/L
$\hat{Q}$	Maximum quota	2.5 mg P/mg C
$f(x)$	Grazer ingestion rate	$\left(\frac{\hat{f}x}{a+x}\right)$ /d

Table 4.1: Model parameters for the Full Knife Edge Model, System (4.13). All parameters are biologically realistic values obtained from Andersen (1997) and Urabe and Sterner (1996) and used by Loladze *et al.* (2000) and Peace *et al.* (2013). The values of $\hat{c}$ and $\hat{a}$ are used in Wang *et al.* (2008) and are within the same orders of magnitude as those found in Andersen (1997) and Diehl (2007).

4.4.1 Numerical Bifurcation Analysis

Here we provide a numerical analysis on the interior equilibria for varying values of total phosphorus, P. This follows the procedure used by Li *et al.* (2011) We fix all other parameters with values listed in Table 1 and the Holling type II function $f(x) = \frac{\hat{f}x}{a+x}$ for the grazer ingestion rate. The model below is parameterized for populations of algae and *Daphnia*

$$\frac{dx}{dt} = 1.2x \min\left\{1 - \frac{x}{1.5}, 1 - \frac{0.0038}{Q}\right\} - \min\left\{\frac{0.81x}{0.25+x}, \frac{0.0243}{Q}\right\} y \tag{4.25a}$$

$$\frac{dy}{dt} = \min\left\{\frac{0.648x}{0.25+x}, \frac{Q}{0.03}\frac{0.81x}{0.25+x}, \frac{0.0194}{Q}\right\} y - 0.25y \tag{4.25b}$$

$$\frac{dQ}{dt} = \frac{0.2(P - Qx - 0.03y)}{0.008 + P - Qx - 0.03y}\frac{2.5 - Q}{2.4962} - 1.2\min\left\{Q(1 - \frac{x}{1.5}), (Q - 0.0038)\right\}. \tag{4.25c}$$

The phase space is

$$\Omega = \left\{(x, y, Q) : 0 \le x \le \min\left\{1.5, \frac{P}{0.0038}\right\}, 0 \le y, 0.0038 \le Q \le 2.5, Qx + 0.03y \le P\right\}. \tag{4.26}$$

Now we investigate the phase portraits for varying values of P. Figure 4.3 depicts the interior nullsurfaces of System (4.25). Notice the parameter P is only in the differential equation (4.25c). Therefore varying P does not affect the x (blue) or y (yellow) nullsurface. Increasing P changes the Q (red) nullsurface. Equilibria are located where all three nullsurface intersect with each other.

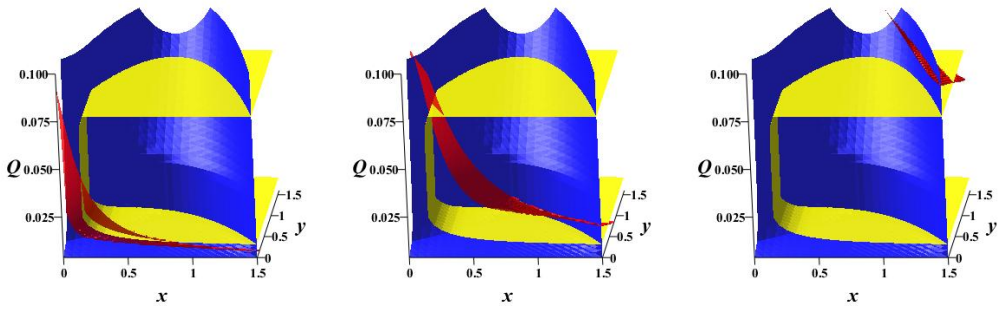

Figure 4.3: Phase portraits of the full model presented in System (4.25) performed using parameters found in Table 4.1 and varying values for P, (a) P=0.01 mg P / L, (b) P=0.03 mg P / L, (c) P= 0.14 mg P / L. The surfaces are the producer (blue), grazer (yellow), and producer P:C (red) nullsurfaces. The intersection of all three of these surfaces depict equilibria. Varying P only affects the Q nullsurface (red) and changes the position and number of interior equilibria.

The number of intersections, and thus the number of interior equilibria, depends on P. We break this analysis into the following cases.

- Case 1: $P < 0.0163$
- Case 2: $0.0163 \leq P < 0.0202$
- Case 3: $P = 0.0202$
- Case 4: $0.0202 < P < 0.0319$
- Case 5: $P = 0.0319$
- Case 6: $0.0319 < P < 0.0815$
- Case 7: $P = 0.0815$

- Case 8: $0.0815 < P < 0.0853$
- Case 9: $P = 0.0853$
- Case 10: $0.0853 < P < 0.1167$
- Case 11: $P = 0.1167$
- Case 12: $0.1167 < P \leq 0.122$
- Case 13: $P = 0.122$
- Case 14: $P > 0.122$

Case 1: $P < 0.0163$

No interior equilibria exists in this case. For an example phase portrait see Figure 4.3a, there is no interior intersection of all three nullsurfaces. All solutions go to the boundary equilibria E_1. Here there is not enough P to support the *Daphnia* population.

Case 2: $0.0163 \leq P < 0.0202$

There is one interior equilibrium in this case, E_1^*. The intersection of the nullsurfaces can be seen in Figure 4.4. Simulations suggest that this interior equilibrium is stable. Here P levels are high enough to support only a small *Daphnia* population since the food is of low quality, as the algal P:C is low.

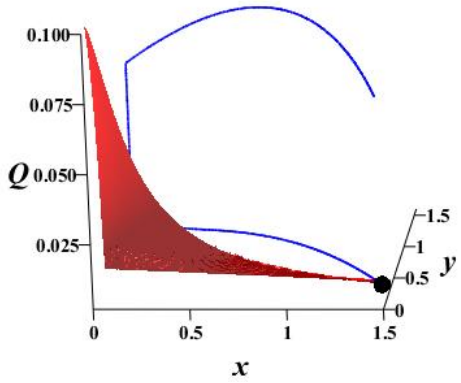

Figure 4.4: Nullsurface intersections for case 2 ($P = 0.0163$ mg P / L). The blue curve is the intersection of the x and y nullsurfaces, the red plane is the Q nullsurface, the black point is the intersection of all nullsurfaces and the stable interior equilibrium, E_1^*.

Case 3: $P = 0.0202$

There are two interior equilibria in this case, E_1^* and E_2^*. The intersection of the nullsurfaces can be seen in Figure 4.5. Simulations suggest that E_1^* is stable and E_2^* is unstable. As P increases, the algal P:C (Q) increases and a larger *Daphnia* population is able to exist.

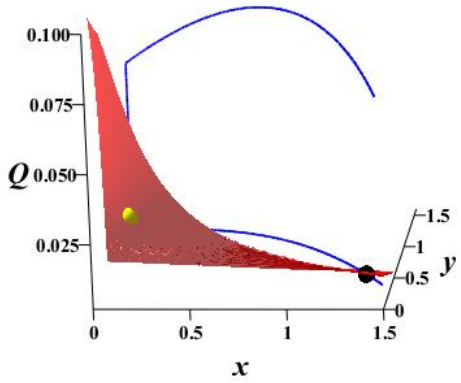

Figure 4.5: Nullsurface intersections for case 3 ($P = 0.0202$ mg P / L). The blue curve is the intersection of the x and y nullsurfaces, the red plane is the Q nullsurface, the black point is the stable interior equilibrium, E_1^*, and the yellow point is the unstable interior equilibrium, E_2^*.

Case 4: $0.0202 < P < 0.0319$

There are three interior equilibria in this case, E_1^*, E_2^*, and E_3^*. The intersection of the nullsurfaces can be seen in Figure 4.6. Simulations suggest that E_1^* is stable and E_2^* is an unstable spiral, and E_3^* is a saddle point. As P increases, the algal P:C (Q) increases and a larger *Daphnia* population is able to exist. Also, as P increases, the stable equilibrium and the saddle point approach each other.

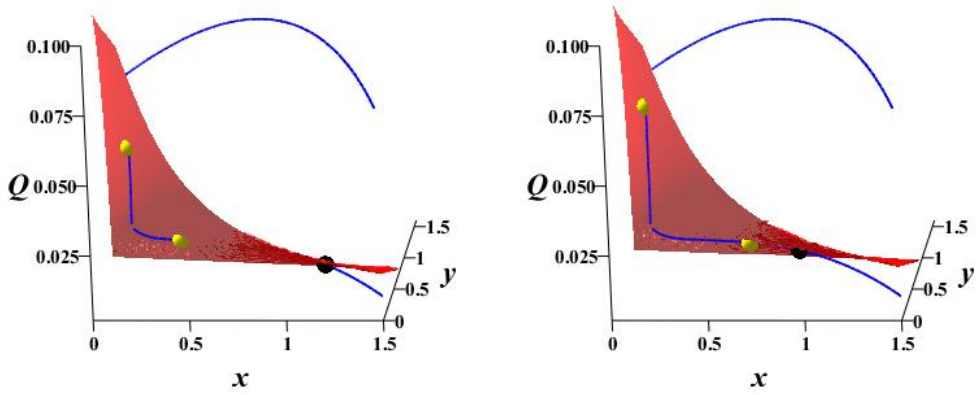

Figure 4.6: Nullsurface intersections for case 4 a.) $P = 0.028$ mg P / L and b.)$P = 0.0313$ mg P / L. The blue curve is the intersection of the x and y nullsurfaces, the red plane is the Q nullsurface, the black point is the stable interior equilibrium E_1^*, the left yellow point is the unstable spiral node E_2^*, and the right yellow point is the saddle point E_3^*. As P increases, the two equilibria E_1^* and E_3^* approach each other and eventually converge when $P = 0.0319$.

Case 5: $P = 0.0319$

When $P = 0.0319$ the two equilibria converge and disappear once P increases. Here there is a saddle-node bifurcation as a large-amplitude limit cycle appears to be created when these two equlibria coalesce at a saddle-node bifurcation.

Case 6: $0.0319 < P < 0.0815$

There is one interior equilibrium in this case, E_2^*. The intersection of the nullsurfaces can be seen in Figure 4.7. Simulations suggest that E_2^* is an unstable spiral inside a

limit cycle. Here the populations exhibit predator-prey cycling.

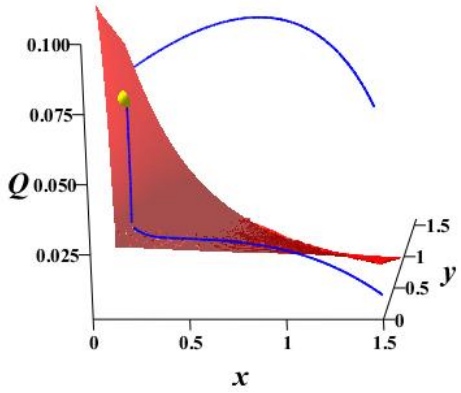

Figure 4.7: Nullsurface intersections for case 6 ($P = 0.032$ mg P / L). The blue curve is the intersection of the x and y nullsurfaces, the red plane is the Q nullsurface, the yellow point is an unstable spiral node, E_2^*.

Case 7: $P = 0.0815$

Here there is an unstable Hopf bifurcation that stabilizes interior equilibrium E_2^*. There is still only one interior equilibrium in this case, E_2^*, which is stable. The intersection of the nullsurfaces can be seen in Figure 4.8.

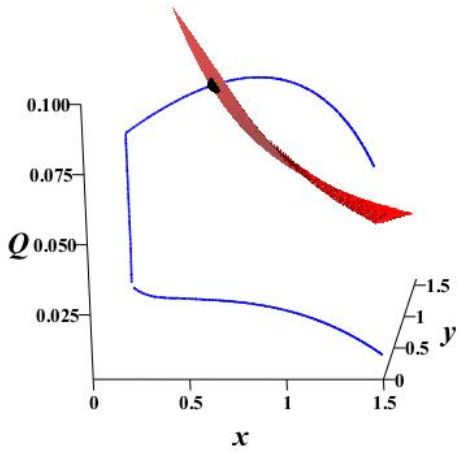

Figure 4.8: Nullsurface intersections for case 7 ($P = 0.0815$ mg P / L). The blue curve is the intersection of the x and y nullsurfaces, the red plane is the Q nullsurface, the black point is the stable equilibrium, E_2^*.

Case 8: $0.0815 < P < 0.0853$

There is still only one interior equilibrium in this case, E_2^*. Here there is a region of bistability. Simulations depict stable limit cycles around E_2^*. Numerical simulations show a region of bistability exists with the limit cycles and E_2^*, see Figure 4.9.

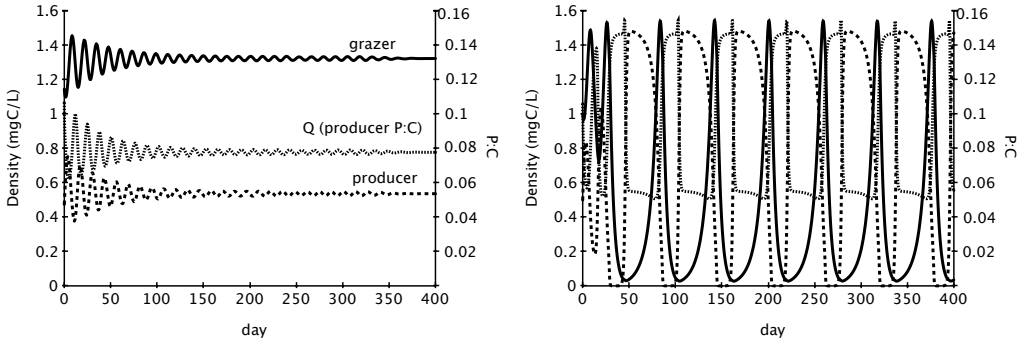

Figure 4.9: Numerical simulations for case 8 $P = 0.083$ mg P / L with initial conditions a.) $x_0 = 0.47$ mg C / L, $y_0 = 1.15$ mg C / L, $Q_0 = \frac{P-\theta y_0}{x_0}$, and b.) $x_0 = 0.5$ mg C / L, $y_0 = 1$ mg C / L, $Q_0 = \frac{P-\theta y_0}{x_0}$. Grazer and producer densities (mg C / L) are given by solid and big-dashed lines respectively and Q, producer cell quota (P:C), is given by small-dotted lines. Solutions tend to a.) E_2^* or to b.) the stable limit cycle. Here there is a region of bistability as the solutions tend to the limit cycle or E_2^* depending on the initial conditions.

Case 9: $P = 0.0853$

There is still only one interior equilibrium in this case, E_2^*. Here the stable and unstable periodic orbits coalesce in a periodic saddle-node bifurcation (sometimes called a "Blue-Sky" bifurcation).

Case 10: $0.0853 < P < 0.1167$

There is still only one interior equilibrium in this case, E_2^*, and it is stable.

Case 11: $P = 0.1167$

There are two interior equilibria in this case, E_2^* and E_4^*. Here there is a transcritical bifurcation that re-stabilizes boundary equilibrium E_1 and generates the unstable coexistence equilibrium, E_4^*.

Case 12: $0.1167 < P < 0.122$

There are two interior equilibria in this case, E_2^* and E_4^*. Simulations suggest that E_2^* is stable and E_4^* is a saddle. This is a region of bistability with equilibrium E_2^* and boundary equilibrium E_1. The intersection of the nullsurfaces can be seen in Figure 4.10. Similar to Case 4, as P increases in this case, the stable equilibrium and the saddle point approach each other. As P increases, *Daphnia* populations at equilibrium E_2^* decrease. Here P is in excess and we start to see the effects of the *stoichiometric knife edge*. These high levels of P, lead to large enough algal P:C to lower *Daphnia* density.

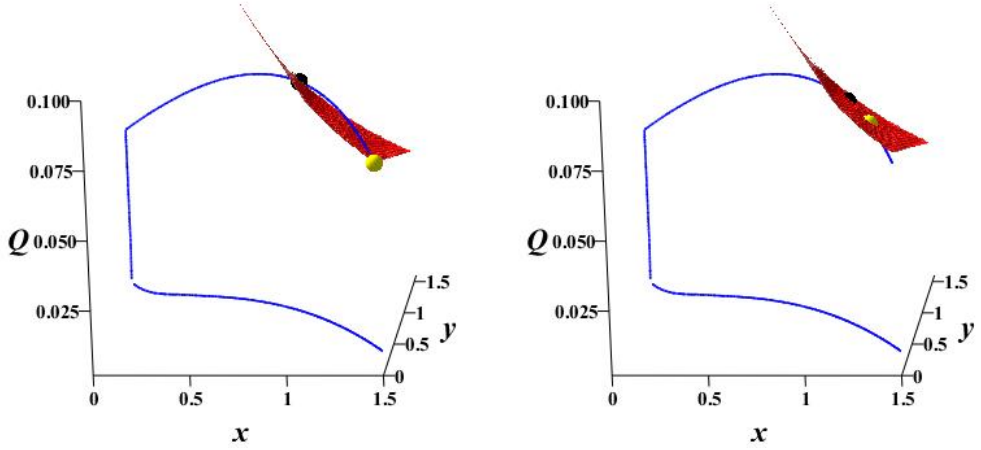

(a) (b)

Figure 4.10: Nullsurface intersections for Case 12 a.) $P = 0.1167$ mg P / L and b.)$P = 0.1215$ mg P / L. The blue curve is the intersection of the x and y nullsurfaces, the red plane is the Q nullsurface, the black point is the stable interior equilibrium E_2^*, the yellow point is the saddle E_4^*. As P increases, the two equilibria E_2^* and E_4^* approach each other and eventually converge when $P = 0.122$.

Numerical simulations show a region of bistability exists. See Figure 4.11. For y_0 small enough, solutions will tend to the boundary equilibrium E_1. However, for larger y_0, solutions will tend to the interior equilibrium E_2^*. If *Daphnia* population density starts off too low, the population will die out. On the other hand, for very large values of y_0, solutions will again tend to the boundary equilibrium E_1.

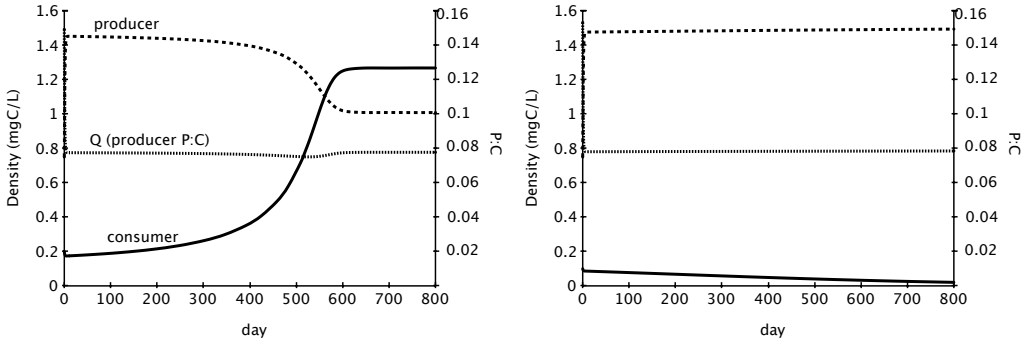

Figure 4.11: Numerical simulations for Case 12 $P = 0.118$ mg P / L with initial conditions a.) $x_0 = 0.75$ mg C / L, $y_0 = 0.2$ mg C / L, $Q_0 = \frac{P-\theta y_0}{x_0}$, and b.) $x_0 = 0.75$ mg C / L, $y_0 = 0.1$ mg C / L, $Q_0 = \frac{P-\theta y_0}{x_0}$. Grazer and producer densities (mg C / L) are given by solid and big-dashed lines respectively and Q, producer cell quota (P:C), is given by small-dotted lines. Here there is a region of bistability. For y_0 small enough, solutions will tend to the boundary equilibrium E_1. For larger y_0, solutions will tend to the interior equilibrium E_2^*. However, for very large y_0, solutions will again tend to the boundary equilibrium E_1 (not shown).

Case 13: $P = 0.122$

When $P = 0.122$ the two equilibria E_2^* and E_4^* converge and disappear once P increases. Here there is a saddle-node bifurcation when these two equilibria converge and then cease to exist.

Case 14: $P > 0.122$

No interior equilibria exists in this case. For an example phase portrait see Figure 4.3c, there is no interior intersection of all three nullsurfaces. All solutions go to the boundary equilibria E_1. Algal P:C is large enough to drive the *Daphnia* population to

extinction. These are drastic effects of the *stoichiometric knife edge* phenomenon.

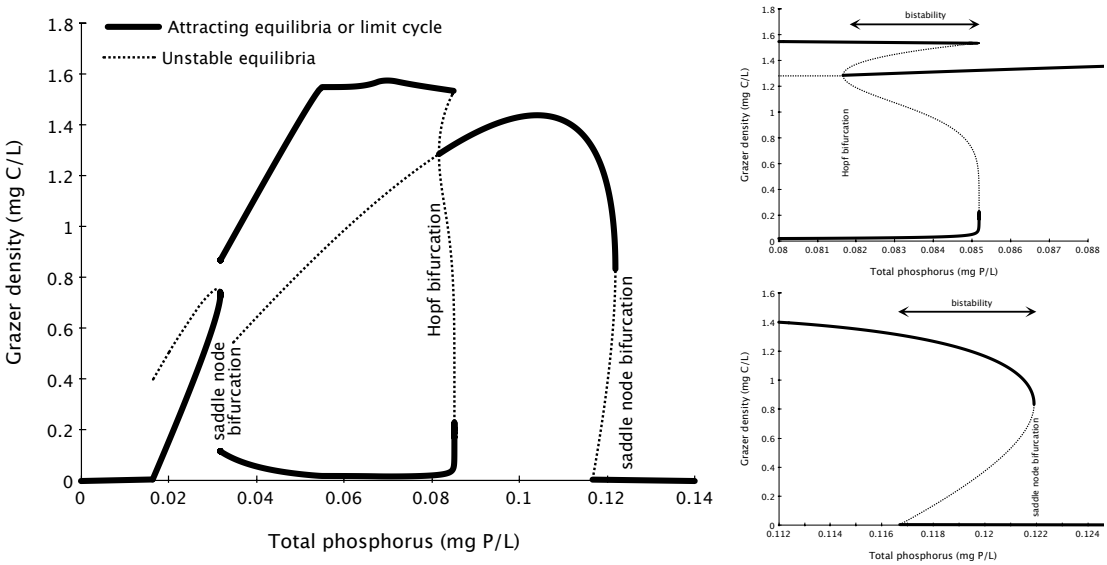

Figure 4.12: Bifurcation diagram for the full model (System 4.13) using parameter values listed in Table 4.1. The bifurcation parameter, P, varies from 0 to 0.14 mg P / L. There are two saddle node bifurcations, a Hopf bifurcation, and two regions of bistability. There is a stable equilibrium for low values of P. As P increases the grazer equilibrium increases until the stable equilibrium is lost at a saddle-node bifurcation. There is a large-amplitude limit cycle and as P increases the amplitudes of the oscillations increase. For P large enough, the oscillations are abruptly halted at a homoclinic bifurcation after the coexistence equilibrium is stabilized at a Hopf bifurcation. As P continues to increase, the grazer equilibria starts to decrease until it reaches the second saddle-node bifurcation and then suddenly the consumer is driven to extinction. The right panels show closer views of the two regions of bistability. These regions of bistability correspond to Cases 8 and 10. Data was generated using XPP-AUTO, details of which can be found in Appendix A.2.

4.5 Discussion

A bifurcation analysis of the full model (System 4.13) using bifurcation parameter P shows the rich dynamics of this model (Figure 4.12). This model supports two saddle node bifurcations, a Homoclinic bifurcation, a Hopf bifurcation, and two regions of bistability.

The full model (System (4.13)), that explicitly tracks free phosphorus, is an extension of the two dimensional knife edge model (System (3.1)) (Peace *et al.* (2013)). The two dimensional model (System (3.1)) assumes the producer is extremely efficient at taking up free nutrients from the environment and that there is no upper bound for Q, as seen in assumption (A3). If we apply these assumptions to the full model (System (4.13)) it converges to the previous model (System (3.1)). To show this, first we consider System (4.13) and assume the producer has an infinite uptake efficiency ($\hat{c} \to \infty$). The dynamics of the producer P content are much faster than the growth dynamics of the producer and of the grazer and a quasi-steady state argument may be applied to eq. (4.13c).

$$0 = \frac{dQ}{dt} = \frac{\hat{c}(P - Qx - \theta y)}{\hat{a} + P - Qx - \theta y}\frac{\hat{Q} - Q}{\hat{Q} - q} - bQ\min\left\{1 - \frac{x}{K}, 1 - \frac{q}{Q}\right\}$$

$$\implies (P - Qx - \theta y)\frac{\hat{Q} - Q}{\hat{Q} - q} = \frac{bQ\min\left\{1 - \frac{x}{K}, 1 - \frac{q}{Q}\right\}(\hat{a} + P - Qx - \theta y)}{\hat{c}}$$

Letting $\hat{c} \to \infty$ yields the following.

$$(P - Qx - \theta y)\frac{\hat{Q} - Q}{\hat{Q} - q} = 0$$

$$(P - Qx - \theta y)\frac{1 - \frac{Q}{\hat{Q}}}{1 - \frac{q}{\hat{Q}}} = 0$$

Now we assume Q has no upper bound and let $\hat{Q} \to \infty$.

$$P - Qx - \theta y = 0$$
$$\Longrightarrow Q = \frac{P - \theta y}{x}$$

Eq. (4.13a) can be written as

$$\begin{aligned}
\frac{dx}{dt} &= bx \min\left\{1 - \frac{x}{k}, 1 - \frac{q}{(P - \theta y)/x}\right\} - \min\left\{f(x), \frac{\hat{f}\theta}{Q}\right\} y \\
&= bx \min\left\{1 - \frac{x}{k}, 1 - \frac{x}{(P - \theta y)/q}\right\} - \min\left\{f(x), \frac{\hat{f}\theta}{Q}\right\} y \\
&= bx \left(1 - \frac{x}{\min\left\{k, (P - \theta y)/q\right\}}\right) - \min\left\{f(x), \frac{\hat{f}\theta}{Q}\right\} y
\end{aligned}$$

and System (4.13) becomes equivalent to System (3.1). Hence the two dimensional knife edge model can be regarded as the limiting case of the full model when $\hat{c} \to \infty$, $\hat{Q} \to \infty$. Figure 4.14 shows that the P bifurcation diagram of the full model converges to that of the two dimensional model when $\hat{c}$ and $\hat{Q}$ are large enough.

While the dynamics of these two models are similar, there are some important distinguishing features between these two models. A main qualitative difference between the knife edge model System (3.1) and the full model System (4.13) can be seen when comparing the bifurcation diagrams, Figure 4.13. Parameter values are in Table 1 where P varies from 0 to 0.14 mg P / L. In both diagrams, for very low values of P the grazer cannot persist due to starvation. As P increases the grazer equilibrium increases until the stable equilibrium loses its stability at a saddle-node bifurcation. There is a limit cycle and as P increases the amplitudes of the oscillations increase. For P large enough, the oscillations are abruptly halted at a homoclinic bifurcation after the coexistence equilibrium is stabilized at a Hopf bifurcation and another coexistence equilibrium emerges. As P continues to increase the grazer equilibrium starts to decrease and eventually is driven to extinction.

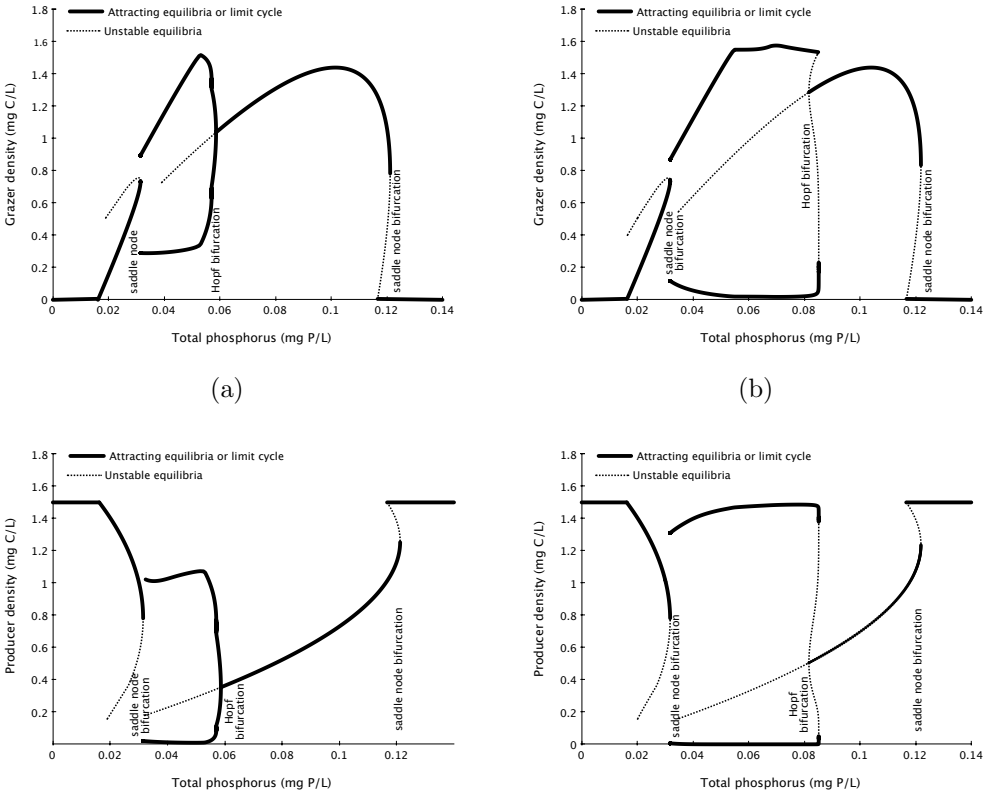

Figure 4.13: Bifurcation diagrams for the knife edge System (3.1) of the a.) grazer and c.) producer , and the Full model System (4.13) of the b.) grazer and d.) producer. Parameter values are listed in Table 4.1. The bifurcation parameter, P, varies from 0 to 0.14 mg P / L. Both diagrams have similar qualitative characteristics, however there are some important differences between the two. Oscillations of the full model exhibit much larger amplitudes than those of the knife edge model. Here the fate of the grazer population is more sensitive to stochastic extinction. The Hopf bifurcation of the knife edge model occurs at a lower value of P making the region where cycling occurs shorter and the region for stable coexistence longer. In the full model, the Hopf bifurcation occurs at a higher value of P giving the grazer population a wider region of the dangerous limit cycling. After the Hopf bifurcation, the grazer population has a shorter window for the coexistence stable equilibrium before eventually going to extinction. Data was generated using XPP-AUTO, details of which can be found in Appendix A.2.

Both models have two locally attracting coexistence equilibria; one before the oscillations and one after the oscillations. These coexistence equilibria have quite different characteristics. During the first stable coexistence region, prior to the saddle-node bifurcation, producers have a low P:C ratio. In this region, an increase of energy (light) will not increase the grazer density. This region exhibits the "paradox of energy enrichment" (Loladze *et al.* (2000); Diehl (2007)). Here an increase in producer productivity causes an increase in producer density but does not result in an increase in grazer density. The second stable coexistence equilibrium, post the Hopf bifurcation, exhibits another type of paradox, once the grazer density starts to decrease due to a high producer P:C ratio. Here a large amount of nutrient causes an increase in producer productivity which causes an increase in producer density but does not result in an increase in grazer density. We name this new type of paradox the "paradox of excess enrichment".

Differences between the two diagrams are first seen in the limit cycles. Oscillations in the full model (Figure 4.13b) exhibit much larger amplitudes than those in the 2D model (Figure 4.13a). These large limit cycles can be dangerous for the survival of the grazer. During these cycles, the grazer populations spend significant periods of time near low population values and are sensitive to stochastic extinction. Oscillations in both models are eventually halted by a Hopf bifurcation. The increase is food quantity accompanied by a decrease in food quality causes the flow of energy (C) from the producer to the grazer to decrease because the grazer is eating less biomass. Here low food quality, due to excess P, drives these systems through the Hopf bifurcations. The location of the Hopf bifurcation is another important difference between these two models. The Hopf bifurcation of the 2D model occurs at a lower value of P making the region where cycling occurs shorter and the region for stable coexistence longer. In the full model, the Hopf bifurcation occurs at a higher value of P giving the grazer

population a wider region of the dangerous limit cycling. After the Hopf bifurcation, the grazer population has a shorter window for the coexistence stable equilibrium before eventually going to extinction. The location of the Hopf bifurcation depends on the parameters in the producer phosphorus uptake function (Eq. 4.4). The sensitivity of the bifurcation diagram to $\hat{c}$ is shown in Figure 4.14. The Hopf bifurcation point decreases as $\hat{c}$ increases.

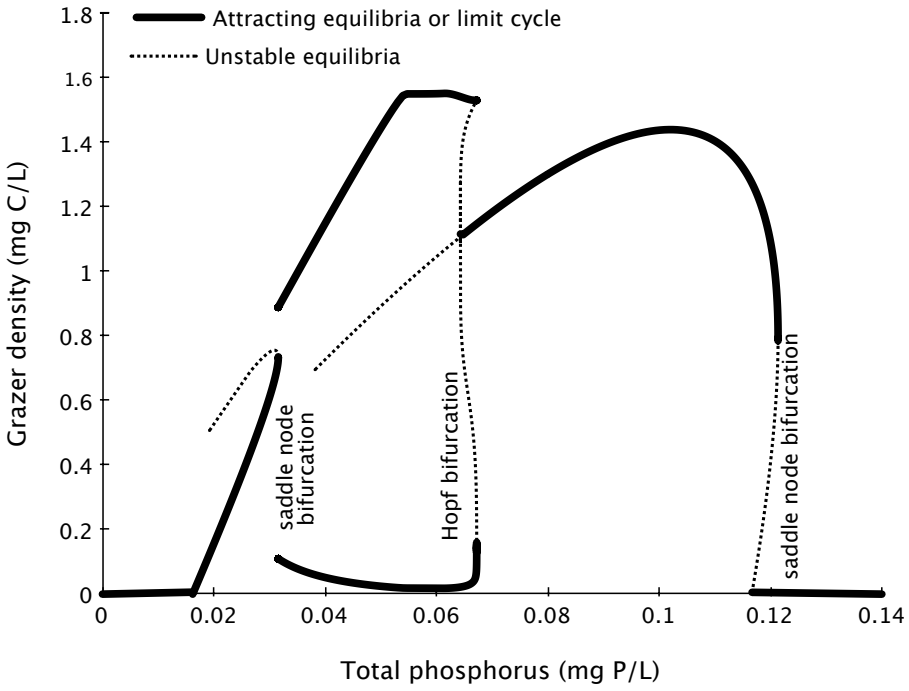

(a)

Figure 4.14: Bifurcation diagrams for Full model System (4.13) using P as the bifurcation parameter with $\hat{c} = 0.8$ mg P/ mg C/d. Compare to Figure 4.13b. Increasing $\hat{c}$ effectively shifts the Hopf bifurcation to left, which decreases the region of periodic cycling and increases the region of the stable coexistence equilibrium. Data was generated using XPP-AUTO, details of which can be found in Appendix A.2.

The full model (System (4.13)) is an extension of the nonsmooth stoichiometric

LKE model (System (2.3)). Through a robust global analysis of the LKE model, Li *et al.* (2011) demonstrated that the LKE model has complicated dynamics including supercritical and subcritical Hopf bifurcations, saddle-node bifurcation, and transcritical bifurcation as well as a region of bistability with an interior equilibrium and limit cycles. We have shown that the full model exhibits some similar bifurcations and regions of bistability. Further analysis of interior equilibria and a rigorous bifurcation analysis may provide further insight and interesting dynamical behaviors.

The full model gives us better insight to the true effects that excess nutrients can have on population dynamics of a food web. Since the previous model does not explicitly track free phosphorus, it underestimates the impacts that food quality can have on the growth of grazers. The full model shows that the fate of the grazer population is particularly sensitive to excess nutrient concentrations (Figures 4.2d, 4.13b). These results suggest that the *stoichiometric knife edge* phenomenon plays a larger role in the model than originally predicted (Peace *et al.* (2013)).

Chapter 5

CONCLUSION

Mathematical biology is not only concerned with how biology inspires new mathematics or how mathematics progresses biology, but how the two are interlaced and advance each other. Since the development of the Lotka-Volterra equations in the early 1900s, thousands of producer-grazer models have been formulated and analyzed and provided biological and mathematical insight into many ecological systems. Recent advances towards the understanding of ecological interactions have been made through the development of the theory of ecological stoichiometry. The stoichiometric ratios of elements, such as carbon and phosphorus, have complex dynamics as they vary within and across trophic levels. Stoichiometric imbalances between trophic levels affect population growth and community structures. Using the fact that all organisms are (ignoring reserves) structurally composed of multiple chemical elements combined in non-arbitrary proportions, ecological stoichiometry stresses the importance of incorporating the effects of food quality, as well as quantity, into ecological modeling.

A wide variety of stoichiometric producer-grazer models have been proposed and analyzed over the last two decades; a summary of selected models is presented in Chapter 2. These models make qualitatively different predictions about stability, coexistence, and the effects of environmental perturbations on population dynamics compared to models without stoichiometry (Andersen *et al.* (2004); Hessen *et al.* (2013)). Stoichiometric models can incorporate key feedbacks such as grazer-driven nutrient recycling and nonintuitive paradoxes such as the "*paradox of energy enrichment*" (Loladze *et al.* (2000); Diehl (2007)) and the coexistence of more than one grazer on a single producer (Loladze *et al.* (2004)). While these models vary in ecological settings,

mathematical complexity, and make different biological assumptions, each model uses stoichiometric principles to incorporate the effects of low nutrient food content on grazer dynamics.

While there is a clear understanding of why grazer growth is low when food nutrient content is low, there has been little insight into the consequences of reduced grazer growth when food nutrient content is high. The models presented here are the first to incorporate the *stoichiometric knife edge* phenomenon into grazer dynamics, where a reduction in animal growth occurs not only by food with low P content but also by food with excessively high P content.

The knife edge model of Chapter 3 (System 3.1) modifies the grazer's ingestion rate and conversion efficiency in order to capture the mechanisms of the *stoichiometric knife edge*. Analytical, numerical, and bifurcation analysis exhibit the dynamical consequences of excess nutrients on a producer-grazer system. These consequences on grazer growth can be seen in the theoretical knife edge curve of the grazer growth function, g. As a function of the producer phosphorus:carbon ratio, Q, the grazer growth function from the knife edge models takes the following form:

$$g(Q) = \min\left\{\hat{e}, \frac{Q}{\theta}\right\} \min\left\{f(x), \frac{\hat{f}\theta}{Q}\right\} \tag{5.1}$$

where $\hat{e}$ is the grazer's maximal production efficiency, θ is the grazer's constant P:C ratio, and $f(x)$ is the grazer's functional response with maximal ingestion rate $\hat{f}$. Function $g(Q)$ is plotted in Figure 5.1. The left side of the curve depicts growth limitation by P deficiency and the right side shows growth decreasing due to excess P, as growth becomes limited by C due to reduced feeding rates.

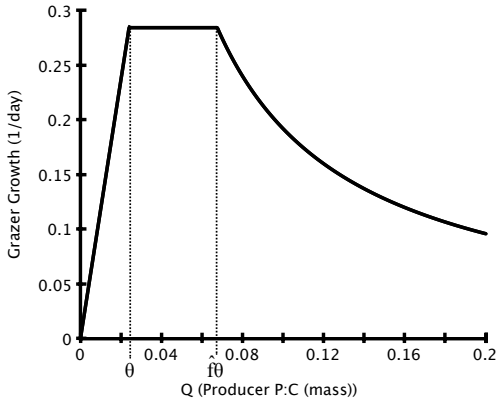

Figure 5.1: Theoretical knife edge curve showing predicted dependence of grazer growth rate on producer P content using parameter values from Table 3.1. The grazer growth rate is low both when food P content is low, where growth is limited by P, and when food P content is high, where P is in excess and growth is limited by C.

The extended full knife edge model of Chapter 4 (System 4.13), which mechanistically tracks P in the producer and free P in the environment, provides further investigations of the growth response of Daphnia to algae with varying P:C ratios. Bifurcation analysis and numerical simulations of the full model, which explicitly tracks phosphorus, lead to quantitatively different predictions than previous models which neglect to track free nutrients. The full model provides better insight tothe true effects that excess nutrients can have on the population dynamics of a food web. Since the previous model does not explicitly track free phosphorus, it underestimates the impacts that food quality can have on the growth of grazers. The full model shows that the fate of the grazer population is particularly sensitive to excess nutrient concentrations (Figure 4.13). These results suggest that the *stoichiometric knife edge* phenomenon may play a larger role than originally predicted in previous models, especially when the producer maximum P per C uptake rate is low.

These modeling efforts provide insight on the effects of excess nutrient content

on grazer dynamics and deepen our understanding of the effects of stoichiometry on the mechanisms governing population dynamics and the interactions between trophic levels. This research provides further evidence that the stoichiometric framework can help shed light on the mathematical and physical properties in many complex biological systems and phenomena. Figure 5.2 depicts how stoichiometric modeling has impacted the maturity of producer-grazer models over the years.

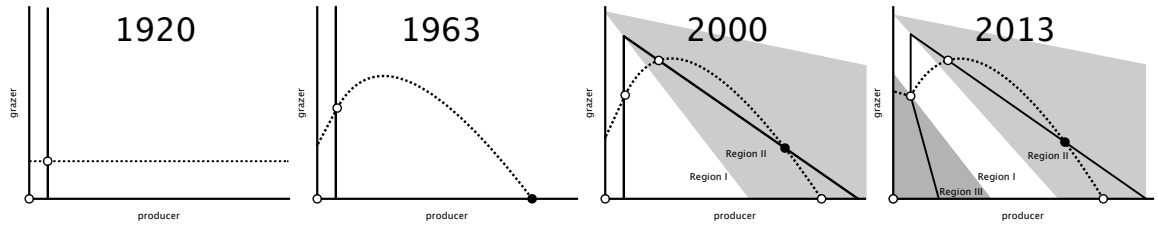

(a) Lotka-Volterra (b) Rosenzweig-MacArthur (c) LKE (d) Knife Edge

Figure 5.2: Phase planes for the (a) classical Lotka-Volterra model (Lotka (1920); Volterra (1926)), (b) Rosenzweig-MacArthur (Rosenzweig and MacArthur (1963)), (c) stoichiometric LKE model (Loladze *et al.* (2000)), and (d) *stoichiometric knife edge* model (Peace *et al.* (2013)). Here, see how the nullclines have matured over time. In 1920, the classical Lotka-Volterra grazer nullcline is a vertical line and the producer nullcline is a horizontal line. By 1963 the producer nullcline becomes hump-shaped in the Rosenzweig-MacArthur modification. In 2000 the LKE model breaks the grazer nullcline into two segments, diving the phase plane into two regions; region I, where grazer growth is determined by food quantity and region II, where grazer growth is determined by food with limiting nutrients. In 2013 the knife edge model takes into account excess food nutrient content. The grazer nullcline is divided into three segments, breaking the phase plane into three regions. This new region III is where grazer growth is limited by excess food nutrient content.

While the presented models are built on empirical work related to zooplankton and algae dynamics and use P as a key nutrient, they likely have broader applications. The *stoichiometric knife edge* has been observed in diverse situations (Hessen *et al.* (2013); Boersma and Elser (2006); Cease *et al.* (2012)), for example see Figure 1.3. This phenomenon of reduced performance on a nutrient-rich diet was also observed for locusts fed on nitrogen-fertilized plants in the study of Cease *et al.* (2012) which provides intriguing evidence that nitrogen excess is an important nutritional factor regulating plant-insect interactions. This study shows that understanding this knife-edge phenomenon may be critical for developing sustainable land management practices.

It is important to note that these models are a first attempt to capture the knife-edge in an analytically tractable form and to examine its underlying dynamical structure and implications. That is, it is an effort to examine the dynamical consequences of the knife edge for grazers. The mechanisms behind the *stoichiometric knife edge* are likely to be more complicated than a simple reduction in ingestion rate, the hypothesis we incorporated into assumption 4. A second hypothesis is that the feeding behavior does not change but excess P may cause the animal to decrease its C absorption rate. That is, once inside the animals, C and P might compete for absorption sites and excess P may hinder C absorption. An additional hypothesis is that excess P may increase metabolic costs. Respiration rate may increase due to the costs of egesting, metabolizing, and/or excreting extra P. Another hypothesis is that excess P may have a direct toxicity effect on grazers. Ultimately, the mechanisms behind the *stoichiometric knife edge* may reflect any combination of these different responses (Elser *et al.* (2012)). Further experiments on respiration and feeding rates can help evaluate the mechanisms underlying this observed reduction in growth rate. More empirical studies are needed to better understand the effects of ranges of resource

stoichiometry and the mechanism behind the reduction of grazer growth (Hessen *et al.* (2013)). Once we have a clearer understanding of the biology behind this phenomenon, we can modify the model to include the specific mechanisms that create it.

5.1 Future Directions

The presented models make the assumption that θ, the P:C ratio of the grazer, is constant (A2). This strict homeostatic assumption is based on the fact that, although grazer stoichiometries are variable, the range of variation is small compared to the range of producer stoichiometries. Wang *et al.* (2012) investigated how the strict homeostatic assumption used in stoichiometric algae-zooplankton models affects the dynamics. More work is needed to investigate the validity of (A2) and to determine how varying θ changes the dynamics and predictions of this model.

Another possible modification of the model is to include stage-structure. Food nutrient content potentially has a different effect on grazer growth during different stages of development. Early stages, characterized by high growth rates, may be especially affected by nutrient limitation due to low food P content (Andersen *et al.* (2004)). Stoichiometric constraints indeed affect grazer growth and ontogeny (Demott *et al.* (1998); Villar-Argaiz and Sterner (2002)). Reproductive tissues have high contents of N and P; thus, low food nutrient content may have strong effects on reproductive output (Færøvig and Hessen (2003)). It is not clear how excess food nutrient content might affect growth rates at the various stages of the developmental cycle. Such stage-specific effects will affect population dynamics, suggesting a stage-structured model will be more appropriate. To begin investigating how food nutrient content might affect growth rates at the various stages of the developmental cycle, one can simply consider two stages for the grazer, adults and non-reproductive juveniles, and incorporate these stages into the LKE model (System 2.3). We assume the algae

have no major structure compared to the stage structure in the life cycle of *Daphnia*, so only the grazer population exhibits structure.

The simplest approach to incorporate stage structure is with a compartmental ODE system. Define $x(t)$ as the density of the producer (algae) population. Assume the grazer (*Daphnia*) population is divided into two stage classes, juvenile $J(t)$ and adult $A(t)$. The initial iteration of a stoichiometric stage structured ODE model takes the following form:

$$\frac{dx}{dt} = bx\left(1 - \frac{x}{\min\left\{k, \frac{P-\theta_j J-\theta_a A}{q}\right\}}\right) - f_j(x)J - f_a(x)A \tag{5.2a}$$

$$\frac{dJ}{dt} = \underbrace{\min\left\{e_a, \frac{Q(x(t))}{\theta_a}\right\} f_a(x)A}_{\text{Reproduction Rate}} - \underbrace{\min\left\{e_j, \frac{Q(x(t))}{\theta_j}\right\} f_j(x)J}_{\text{Maturation Rate}} - d_j J \tag{5.2b}$$

$$\frac{dA}{dt} = \underbrace{\min\left\{e_j, \frac{Q(x(t))}{\theta_j}\right\} f_j(x)J}_{\text{Maturation Rate}} - d_a A \tag{5.2c}$$

where θ_j, θ_a are the constant P:C ratios, d_j, d_a are death rates, e_j, e_a are the maximum production efficiencies, and $f_j(x)$ and $f_a(x)$ are the grazer ingestion rates for $J(t)$ and $A(t)$, respectively. Including two grazer stage classes into this ODE allows one to investigate the effects of different feeding behaviors of adults versus juveniles on the overall dynamics of the producer and grazer populations. This initial iteration of a two stage population model makes some simplifying assumptions. The model assumes that all juvenile growth goes directly to maturation, thus all juvenile density growth simply increases the density of the adult population via maturation. On the other hand, all adult growth goes directly to reproduction of juveniles. The model does not allow for individual growth outside of maturation or reproduction. One will have to consider the consequences of these assumptions when analyzing, or more likely, when formulating the second iteration of the model.

Structured population models of ecological interactions can be used to predict

dynamics that lead to different types of fluctuations. Models that assimilate delays can be more effective and accurate compared to ordinary differential equation-based models when it is crucial to capture oscillation dynamics with specific periods and amplitudes (Kuang (2012)). Therefore, another approach is to use a system of delay differential equations (DDE) to incorporate a maturation rate into the stoichiometric LKE model. The maturation rate will depend on the quantity as well as the quality of the producer. The initial iteration of the DDE model follows the model development proposed by McCauley *et al.* (2008). Below, $x(t)$ is the density of the producer (algae) population. Assume the grazer (*Daphnia*) population is divided into two stage classes, juvenile $J(t)$ and adult $A(t)$. The first iteration of a stoichiometric stage structured DDE model takes the following form:

$$\frac{dx(t)}{dt} = \underbrace{bx(t)\left(1 - \frac{x(t)}{\min\{k, (P - \theta_j J(t) - \theta_a A(t))/q\}}\right)}_{\text{Producer Growth Rate}} - \underbrace{U_j(x(t))J(t)}_{\text{Juvenile Uptake Rate}} - \underbrace{U_a(x(t))A(t)}_{\text{Adult Uptake Rate}} \tag{5.3a}$$

$$\frac{dJ(t)}{dt} = \underbrace{R\Big(x(t), A(t)\Big)}_{\text{Reproduction Rate}} - \underbrace{M\Big(x(t), R(x(t-\tau(t)), A(t-\tau(t))\Big)}_{\text{Maturation Rate}} - \underbrace{d_j J(t)}_{\text{Juvenile Death Rate}} \tag{5.3b}$$

$$\frac{dA(t)}{dt} = \underbrace{M\Big(x(t), R(x(t-\tau(t)), A(t-\tau(t))\Big)}_{\text{Maturation Rate}} - \underbrace{d_a A(t)}_{\text{Adult Death Rate}} \tag{5.3c}$$

where θ_j, θ_a are the constant P:C ratios, d_j, d_a are death rates, and U_j, U_a are uptake functions for $J(t)$ and $A(t)$, respectively. These uptake functions depend on $x(t)$, and if the dynamics of the knife edge are considered, they will also depend on $Q(t)$. $R(x(t), A(t))$ is the rate of reproduction of neonates described as,

$$R(x(t), A(t)) = \frac{\chi}{\gamma} \min\left\{e_a, \frac{Q(x(t))}{\theta_a}\right\} U_a(x(t))A(t) \tag{5.4}$$

where χ is the proportion of utilized C allocated for reproduction, γ is the carbon required to produce one neonate, and e_a is the maximum production efficiency for

adults. $M(x(t), R(x(t-\tau(t)), A(t-\tau(t)))$ is the maturation function described as,

$$M\bigg(x(t), R(x(t-\tau(t)), A(t-\tau(t))\bigg) = R\bigg(x(t-\tau(t)), A(t-\tau(t))\bigg) S(t) \frac{g(x(t))}{g(x(t-\tau(t)))} \tag{5.5}$$

where $g(x(t))$ is the juvenile growth rate, $g(x(t)) = \min\left\{e_j, \frac{Q(x(t))}{\theta_j}\right\} U_j(x(t))$ and e_j is the maximum production efficiency for juveniles. $S(t)$ is the juvenile survival rate. $S(t) = \int_{t-\tau(t)}^{t} e^{-d_j s} ds$. $\tau(t)$ is the delay for the juvenile stage duration. τ is a function of time since the maturation rate is resource dependent, as it depends on both producer quantity and quality. Assume the grazer uptake functions take the following form:

$$U_j(x(t)) = \frac{c_j x(t)}{a + x(t)} \tag{5.6a}$$

$$U_a(x(t)) = \frac{c_a x(t)}{a + x(t)} \tag{5.6b}$$

Then the rate of reproduction can be written as

$$R(x(t), A(t)) = \frac{\chi}{\gamma} \min\left\{e_a, \frac{Q(x(t))}{\theta_a}\right\} \frac{c_a x(t) A(t)}{a + x(t)} \tag{5.7}$$

and the rate of maturation can be written as

$$M = R\bigg(x(t-\tau(t)), A(t-\tau(t))\bigg) S(t) \frac{\min\left\{e_j, \frac{Q(x(t))}{\theta_j}\right\} \frac{c_j x(t)}{a+x(t)}}{\min\left\{e_j, \frac{Q(x(t-\tau(t)))}{\theta_j}\right\} \frac{c_j x(t-\tau(t))}{a+x(t-\tau(t))}} \tag{5.8a}$$

$$= \frac{\chi}{\gamma} \min\left\{e_a, \frac{Q(x(t-\tau(t)))}{\theta_a}\right\} \frac{c_a x(t-\tau(t))}{a + x(t-\tau(t))} A(t-\tau(t)) \tag{5.8b}$$

$$S(t) \frac{\min\left\{e_j, \frac{Q(x(t))}{\theta_j}\right\} \frac{c_j x(t)}{a+x(t)}}{\min\left\{e_j, \frac{Q(x(t-\tau(t)))}{\theta_j}\right\} \frac{c_j x(t-\tau(t))}{a+x(t-\tau(t))}}$$

$$= \frac{\chi}{\gamma} \min\left\{e_a, \frac{Q(x(t-\tau(t)))}{\theta_a}\right\} c_a A(t-\tau(t)) S(t) \frac{x(t)}{a + x(t)} \frac{\min\left\{e_j, \frac{Q(x(t))}{\theta_j}\right\}}{\min\left\{e_j, \frac{Q(x(t-\tau(t)))}{\theta_j}\right\}} \tag{5.8c}$$

This results in the following stoichiometric delay differential equation model,

$$\frac{dx(t)}{dt} = bx(t)\left(1 - \frac{x(t)}{\min\{k, (P - \theta_j J(t) - \theta_a A(t))/q\}}\right) - \frac{c_J x(t)}{a + x(t)} J(t) - \frac{c_a x(t)}{a + x(t)} A(t) \tag{5.9a}$$

$$\frac{dJ(t)}{dt} = \frac{\chi}{\gamma} \frac{\min\left\{e_a, \frac{Q(x(t))}{\theta_a}\right\} c_a x(t) A(t)}{a + x(t)} - \frac{\chi}{\gamma} \frac{c_a A(t - \tau(t)) S(t) x(t) \min\left\{e_a, \frac{Q(x(t-\tau(t)))}{\theta_a}\right\} \min\left\{e_j, \frac{Q(x(t))}{\theta_j}\right\}}{(a + x(t)) \min\left\{e_j, \frac{Q(x(t-\tau(t)))}{\theta_j}\right\}} - d_j J(t) \tag{5.9b}$$

$$\frac{dA(t)}{dt} = \frac{\chi}{\gamma} \frac{c_a A(t - \tau(t)) S(t) x(t) \min\left\{e_a, \frac{Q(x(t-\tau(t)))}{\theta_a}\right\} \min\left\{e_j, \frac{Q(x(t))}{\theta_j}\right\}}{(a + x(t)) \min\left\{e_j, \frac{Q(x(t-\tau(t)))}{\theta_j}\right\}} - d_a A(t) \tag{5.9c}$$

System (5.9) is a state-dependent delay-differential equation system that is non-smooth. In order to tackle this problem, first one can make a transformation in the time variable in order to change the problem into a system of DDEs with a fixed delay following McCauley *et al.* (2008). Juvenile stage duration depends on x and Q. Let ω be the carbon required to complete the juvenile development process.

$$\omega = \int_{t-\tau(t)}^{t} \min\left\{e_j, \frac{Q(x(\xi))}{\theta_j}\right\} U_j(x(\xi)) d\xi \tag{5.10}$$

This provides an integral constraint to calculate the juvenile stage-duration. Equation (5.10) defines the delay $\tau(t)$. Define

$$\phi(t) = \int_{0}^{t} \min\left\{e_j, \frac{Q(x(\xi))}{\theta_j}\right\} U_j(x(\xi)) d\xi \tag{5.11a}$$

$$\frac{d\phi(t)}{dt} = \min\left\{e_j, \frac{Q(x(t))}{\theta_j}\right\} U_j(x(t)) \tag{5.11b}$$

then Equation (5.10) can be written as

$$\omega = \int_{t-\tau(t)}^{t} \frac{d\phi(\xi)}{d\xi} d\xi \tag{5.12a}$$

$$= \phi(t) - \phi(t - \tau(t)) \tag{5.12b}$$

and thus $\phi(t-\tau(t)) = \phi(t) - \omega$. With this transformation the system can be written in terms of ϕ with a fixed delay, ω.

This formulation would follow that of McCauley *et al.* (2008) with added stoichiometric minimum functions. There are some issues with this model formulation, in particular McCauley *et al.* (2008) made some approximation assumptions in the maturation rate function. We used the same approach when describing Equation (5.5). Here, maturation only depends on juvenile growth rates at two times, t and $t-\tau(t)$. This approximation may lead to serious consequences. A better approach to this model formation is to begin with an expression of the juvenile population at time t,

$$J(t) = \frac{\xi}{\gamma}\int_{-\tau(t)}^{0} e^{-d_j s} A(t+s) \min\left\{ e_a \frac{Q(x(t+s))}{\theta_a} \right\} U_a(x(t+s))ds \tag{5.13a}$$

$$\equiv \frac{\xi}{\gamma}\int_{-\tau(t)}^{0} f(t,s)ds \tag{5.13b}$$

From here one should differentiate to get an expression for $J'(t)$. This will require the following form of Leibniz's integral rule.

$$J(t) = \frac{\xi}{\gamma}\int_{-\tau(t)}^{0} f_t(t,s)ds - f(-\tau(t),s)(-\tau'(t)) \tag{5.14}$$

Future work may involve exploring this improved approach to the model formulation and seeing what directions are possible. The expression for $\tau'(t)$ may come out of Equation (5.10). Hopefully a similar transformation in the time variable will be possible in order to change this newly formulated problem into a system of DDEs with a fixed delay, similar to equation (5.11). One future direction is to continue investigating these stoichiometric stage-structured ODE and DDE models in order to address the questions on how food nutrient content and stoichiometric ratios might effect population growth dynamics at various stages of grazer growth and how incorporating stage structure alters the behavior of the overall populations. After developing these techniques, one can further extend any model to incorporate the

dynamics of the stoichiometric knife edge. We believe these approaches will lead to insight on how food quality affects grazer growth at various stages in the structured population.

We also note the opportunity to extend these knife edge models to include more species. Competition models have shown that stoichiometry, as incorporated into models via the effects of low nutrient food content, may play an important role in explaining biodiversity (Loladze *et al.* (2004)) as well as provide a mechanism for deterministic extinction (Miller *et al.* (2004)). It would be interesting to investigate the effects of not only low nutrient food content, but also high nutrient food content on systems with competing producers and/or competing grazers. For example, these models can be extended to include more than one grazer species and to examine subsequent impacts of coexistence and exclusion, as in the analysis of Loladze *et al.* (2004) and Lin *et al.* (2012). Expanding the models to include more than one producer and examining extinction effects, as in the analysis of Miller *et al.* (2004), would also be insightful.

In addition to extending these models to include competing species, one can expand the presented modeling techniques up the food chain, by incorporating higher trophic levels. Empirical evidence shows that the *stoichiometric knife edge* phenomenon is observed in primary grazers (*Daphnia*), but future studies and modeling efforts should explore the consequences of this phenomenon on secondary consumers. One can investigate the formulation of stoichometric food web models of three trophic levels to address the following questions: How does producer nutrient content (food quality) affect population growth and the flow of energy and nutrients up the food chain and across trophic levels? What roles do grazer and predator nutrient recycling rates play to alter ecosystem level nutrient availability and how does this affect population dynamics of the food web? How does the addition of a predation third trophic level into

well established two dimensional stoichiometric producer-grazer models (Loladze *et al.* (2000); Peace *et al.* (2013)) change the dynamics of species growth and population structure? In order to answer these questions, one can extend the LKE model (System 2.3) to include a predator or secondary grazer:

$$\frac{dx}{dt} = bx\left(1 - \frac{x}{\min(K, (P - \theta_y y - \theta_z z)/q)}\right) - f(x)y \tag{5.15}$$

$$\frac{dy}{dt} = \hat{e}_y \min\left(1, \frac{(P - \theta_y y - \theta_z z)/x}{\theta_y}\right) f(x)y - g(y)z - d_y y \tag{5.16}$$

$$\frac{dz}{dt} = \hat{e}_z \min\left(1, \frac{\theta_y}{\theta_z}\right) g(y)z - d_z z \tag{5.17}$$

Here $x(t)$, $y(t)$, and $z(t)$ are the biomass of the producer, consumer, and predator respectively, measured in terms of C. b is the maximum growth rate of the producer, K is the producer carrying capacity in terms of C and represents the light intensity, P is the total phosphorus in the system, θ_y and θ_z are the constant P:C ratios of the consumer and predator respectively, q is the producer minimal P:C, $\hat{e}_y$ and $\hat{e}_z$ are the maximum production efficiencies of the consumer and predator, d_y is the consumer loss rate, and d_z is the predator loss rate. The consumer's ingestion rate, $f(x)$ is taken to be a monotonic increasing and differentiable function, $f'(x) \geq 0$. $f(x)$ is saturating with $\lim_{x\to\infty} f(x) = \hat{f}$. The predator's ingestion rate, $g(y)$ has similar properties. The model above is just the first iteration. The next step is to study this model, investigate the consequences of the assumptions made, and to continue to update the model to gain biological insight in order to continue exploring how food quality affects population structures.

Indeed, ecological stoichiometric modeling provides quantitative and qualitative improvements in the predictive power of theoretical and computational population ecology. The framework offered by ecological stoichiometry is equally applicable to biological phenomena at the suborganismal level as well as phenomena at the biosphere level (Elser and Kuang (2012)). As human activities continue to alter environmental

balances and chemical cycles, it is becoming vital to understand how these changes can impact the environment and food web dynamics. Mathematically modeling the essential elements and their interactions through the theory of ecological stoichiometry is one of the best tools we have to better understand our world.

REFERENCES

Andersen, T., *Pelagic nutrient cycles; herbivores as sources and sinks.* (Springer,Berlin, 1997).

Andersen, T., J. J. Elser and D. O. Hessen, "Stoichiometry and population dynamics", Ecology Letters **7**, 9, 884–900 (2004).

Bennett, E. M., S. R. Carpenter and N. F. Caraco, "Human impact on erodable phosphorus and eutrophication: a global perspective", BioScience **51**, 3, 227–234 (2001).

Boersma, M. and J. J. Elser, "Too much of a good thing: on stoichiometrically balanced diets and maximal growth", Ecology **87**, 1325–1330 (2006).

Cease, A., J. J. Elser, C. Ford, S. Hao, L. Kang and H. J.F., "Heavy livestock grazing promotes locust outbreaks by lowering plant nitrogen content.", Science **335**, 467–469 (2012).

Demott, W., R. Gulati and K. Siewertsen, "Effects of phosphorus-deficient diets on the carbon and phosphorus balancance of *Daphnia magna*", Limnol Oceanogr **43**, 1147–1161 (1998).

Diehl, S., "Paradoxes of enrichment: Effects of increased light versus nutrient supply on pelagic producer-grazer systems", The American Naturalist **169**, 6, E173–E191 (2007).

Droop, M., "Vitamin b12 and marine ecology. iv. the kinetics of uptake, growth and inhibition in monochrysis lutheri", J. Mar. Biol. Assoc. UK **48**, 3, 689–733 (1968).

Droop, M., "The nutrient status of algal cells in continuous culture", Journal of the Marine Biological Association of the United Kingdom **54**, 04, 825–855 (1974).

Elser, J. J. and E. Bennett, "Phosphorus cycle: A broken biogeochemical cycle", Nature **478**, 29–31 (2011).

Elser, J. J., T. H. Chrzanowski, R. W. Sterner and K. H. Mills, "Stoichiometric constraints on food-web dynamics: a whole-lake experiment on the canadian shield", Ecosystems **1**, 1, 120–136 (1998).

Elser, J. J., D. R. Dobberfuhl, N. A. MacKay and J. H. Schampel, "Organism size, life history, and n: P stoichiometry", BioScience **46**, 9, 674–684 (1996).

Elser, J. J., W. F. Fagan, R. F. Denno, D. R. Dobberfuhl, A. Folarin, A. Huberty, S. Interlandi, S. S. Kilham, E. McCauley, K. L. Schulz *et al.*, "Nutritional constraints in terrestrial and freshwater food webs", Nature **408**, 6812, 578–580 (2000).

Elser, J. J., K. Hayakawa and J. Urabe, "Nutrient limitation reduces food quality for zooplankton: *Daphnia* response to seston phosphorus enrichment", Ecology **82**, 898–903 (2001).

Elser, J. J. and Y. Kuang, *Encyclopedia of theoretical ecology*, chap. Ecological Stoichiometry, no. 4 (University of California Pr, 2012).

Elser, J. J., I. Loladze, A. L. Peace and Y. Kuang, "Lotka re-loaded: Modeling trophic interactions under stoichiometric constraints", Ecological Modelling (2012).

Elser, J. J., J. Schampel, M. Kyle, J. Watts, E. Carson, T. Dowling, C. Tang and P. Roopnarine, "Reponse of grazing snails to phosphorus enrichment of modern stromatolitic microbial communities", Freshwater Biology **50**, 1826–1835 (2005).

Elser, J. J. and J. Urabe, "The stoichiometry of consumer-driven nutrient recycling: theory, observations, and consequences", Ecology **80**, 3, 735–751 (1999).

Elser, J. J., J. Watts, J. Schampell and J. Farmer, "Early Cambrian food webs on a trophic knife-edge? a hypothesis and preliminary data from a modern stromatolite-based ecosystem", Ecology Letters **9**, 295–303 (2006).

Færøvig, P. and D. Hessen, "Allocation strategies in crustacean stoichiometry: the potential roleof phosphorus in the limitation of reproduction", Freshwater Biol. **48**, 1782–1792 (2003).

Fan, M., I. Loladze, Y. Kuang and J. J. Elser, "Dynamics of a stoichiometric discrete producer-grazer model", Journal of Difference Equations and Applications **11**, 4-5, 347–364 (2005).

Frost, P., J. Benstead, W. Cross, H. Hillebrand, J. Larson, M. Xenopoulos and T. Yoshida, "Threshold elemental ratios of carbon and phosphorus in aquatic consumers", Ecology Letters **9**, 774–779 (2006).

Gause, G., *The struggle for existence* (Williams & Wilkins Baltimore (reprinted in 1964 and 1969 by Hafner, NY and in 1971 by Dover, New York), 1934).

Gaxiola, R. A., M. Edwards and J. J. Elser, "A transgenic approach to enhance phosphorus use efficiency in crops as part of a comprehensive strategy for sustainable agriculture", Chemosphere **84**, 6, 840–845 (2011).

Grover, J. P., "Stoichiometry, herbivory and competition for nutrients: simple models based on planktonic ecosystems", Journal of theoretical biology **214**, 4, 599–618 (2002).

Grover, J. P., "The impact of variable stoichiometry on predator-prey interactions: a multinutrient approach", The American Naturalist **162**, 1, 29–43 (2003).

Grover, J. P., "Predation, competition, and nutrient recycling: a stoichiometric approach with multiple nutrients", Journal of theoretical biology **229**, 1, 31–43 (2004).

Hardin, G., "The competitive exclusion principle", Science **131**, 1292–1297 (1960).

Hessen, D. O., J. J. Elser, R. W. Sterner and J. Urabe, "Ecological stoichiometry: An elementary approach using basic principles", Limnol. Oceanogr **58**, 6, 2219–2236 (2013).

Kooijman, S. A. L. M., "The synthesizing unit as model for the stoichiometric fusion and branching of metabolic fluxes", Biophysical chemistry **73**, 1, 179–188 (1998).

Kooijman, S. A. L. M., *Dynamic energy and mass budgets in biological systems* (Cambridge University Press, 2000).

Kooijman, S. A. L. M., *Dynamic energy budget theory for metabolic organisation* (Cambridge university press, 2009).

Kooijman, S. A. L. M., T. Andersen and B. W. Kooi, "Dynamic energy budget representations of stoichiometric constraints on population dynamics", Ecology **85**, 5, 1230–1243 (2004).

Kooijman, S. A. L. M., J. Grasman and B. Kooi, "A new class of non-linear stochastic population models with mass conservation", Mathematical biosciences **210**, 2, 378–394 (2007).

Kuang, Y., *Encyclopedia of theoretical ecology*, chap. Delay Differential EQuations, no. 4 (University of California Pr, 2012).

Kuang, Y., J. Huisman and J. J. Elser, "Stoichiometric plant-herbivore models and their interpretation", Mathematical biosciences and engineering **1**, 2, 215–222 (2004).

Levin, S. A., "Community equilibria and stability, and an extension of the competitive exclusion principle", American Naturalist pp. 413–423 (1970).

Li, X., H. Wang and Y. Kuang, "Global analysis of a stoichiometric producer–grazer model with holling type functional responses", Journal of mathematical biology **63**, 5, 901–932 (2011).

Lin, L. H.-R., B. B. Peckham, H. W. Stech and J. Pastor, "Enrichment in a stoichiometric model of two producers and one consumer", Journal of Biological Dynamics **6**, 2, 97–116 (2012).

Loladze, I., Y. Kuang and J. J. Elser, "Stoichiometry in producer-grazer systems: Linking energy flow with element cycling", Bull. Math Bio. **62L**, 1137–1162 (2000).

Loladze, I., Y. Kuang, J. J. Elser and W. F. Fagan, "Competition and stoichiometry: coexistence of two predators on one prey", Theoretical Population Biology **65**, 1, 1–15 (2004).

Lotka, A. J., "Undamped oscillations derived from the law of mass action.", Journal of the american chemical society **42**, 8, 1595–1599 (1920).

Lotka, A. J., *Elements of physical biology* (Williams & Wilkins Baltimore, 1925).

MacArthur, R. and R. Levins, "Competition, habitat selection, and character displacement in a patchy environment", Proceedings of the National Academy of Sciences of the United States of America **51**, 6, 1207 (1964).

Makarenkov, O. and J. S. Lamb, "Dynamics and bifurcations of nonsmooth systems: A survey", Physica D: Nonlinear Phenomena (2012).

Markus, L., "Ii. asymptotically autonomous differential systems", Contributions to the theory of nonlinear oscillations p. 17 (1956).

McCauley, E., W. A. Nelson and R. M. Nisbet, "Small-amplitude cycles emerge from stage-structured interactions in daphnia–algal systems", Nature **455**, 7217, 1240–1243 (2008).

Miller, C. R., Y. Kuang, W. F. Fagan and J. J. Elser, "Modeling and analysis of stoichiometric two-patch consumer–resource systems", Mathematical biosciences **189**, 2, 153–184 (2004).

Moe, S. J., R. S. Stelzer, M. R. Forman, W. S. Harpole, T. Daufresne and T. Yoshida, "Recent advances in ecological stoichiometry: insights for population and community ecology", Oikos **109**, 1, 29–39 (2005).

Muller, E. B., R. M. Nisbet, S. A. L. M. Kooijman, J. J. Elser and E. McCauley, "Stoichiometric food quality and herbivore dynamics", Ecology Letters **4**, 6, 519–529 (2001).

Nisbet, R., E. McCauley, A. De Roos, W. Murdoch and W. Gurney, "Population dynamics and element recycling in an aquatic plant-herbivore system", Theoretical Population Biology **40**, 2, 125–147 (1991).

Nisbet, R., E. Muller, K. Lika and S. A. L. M. Kooijman, "From molecules to ecosystems through dynamic energy budget models", Journal of animal ecology **69**, 6, 913–926 (2000).

Peace, A., Y. Zhao, I. Loladze, J. J. Elser and Y. Kuang, "A stoichiometric producer-grazer model incorporating the effects of excess food-nutrient content on consumer dynamics", Mathematical biosciences (2013).

Plath, K. and M. Boersma, "Mineral limitation of zooplankton: stoichiometric constraints and optimal foraging", Ecology **82**, 5, 1260–1269 (2001).

Rosenzweig, M. L. and R. H. MacArthur, "Graphical representation and stability conditions of predator-prey interactions", American Naturalist **97**, 895, 209 (1963).

Sanchez, L. A., "Convergence to equilibria in the lorenz system via monotone methods", Journal of Differential Equations **217**, 2, 341–362 (2005).

Smith, V. and D. Schindler, "Eutrophication science: where do we go from here?", Trends Ecol. Evol. **24**, 201–207 (2009).

Stech, H., B. Peckham and J. Pastor, "Enrichment effects in a simple stoichiometric producer-consumer population growth model", Communications in Applied Analysis **16**, 4, 687 (2012a).

Stech, H., B. Peckham and J. Pastor, "Enrichment in a general class of stoichiometric producer–consumer population growth models", Theoretical population biology **81**, 3, 210–222 (2012b).

Stech, H., B. Peckham and J. Pastor, "Quasi-equilibrium reduction in a general class of stoichiometric producer–consumer models", Journal of biological dynamics **6**, 2, 992–1018 (2012c).

Sterner, R., T. Andersen, J. J. Elser, D. Hessen, J. Hood, E. McCauley and J. Urabe, *Scale-dependent carbon : nitrogen : phosphorus seston stoichiometry in marine and freshwaters*, vol. 53 (2008).

Sterner, R. W. and J. J. Elser, *Ecological stoichiometry: the biology of elements from molecules to the biosphere* (Princeton University Press, 2002).

Sui, G., M. Fan, I. Loladze and Y. Kuang, "The dynamics of a stoichiometric plant-herbivore model and its discrete analog", Mathematical Biosciences and Engineering **4**, 1, 29 (2007).

Tett, P. and M. Droop, *CRC handbook of laboratory model systems for microbial ecosystems. 2 (1988)*, vol. 2, chap. 7, pp. 177–233 (CRC Press, 1988).

Thieme, H. R., "Convergence results and a poincaré-bendixson trichotomy for asymptotically autonomous differential equations", Journal of mathematical biology **30**, 7, 755–763 (1992).

Thingstad, T. F., "Utilization of n, p, and organic c by heterotrophic bacteria. i. outline of a chemostat theory with a consistent concept of maintenancemetabolism", Mar. Ecol. Prog. Ser **35**, 1-2, 99–109 (1987).

Urabe, J., J. J. Elser, M. Kyle, T. Yoshida, T. Sekino and Z. Kawabata, "Herbivorous animals can mitigate unfavourable ratios of energy and material supplies by enhancing nutrient recycling", Ecology Letters **5**, 2, 177–185 (2002).

Urabe, J. and R. W. Sterner, "Regulation of herbivore growth by the balance of light and nutrients", Proceedings of the National Academy of Sciences **93**, 16, 8465–8469 (1996).

Verhulst, P., "Notice sur la loi que la population suit dans son accroissement", Corr. Math. et Phys. **10**, 113-121 (1838).

Verhulst, P., "Recherches mathématiques sur la loi d'accroissement de la population", Mém. Acad. Roy. **18**, 1-38 (1845).

Villar-Argaiz, M. and R. Sterner, "Life history bottlenecks in *Diaptomus clavipes* induced by phosphorus-limited algae", Limnol Oceanogr **47**, 1229–1233 (2002).

Volterra, V., "Fluctuations in the abundance of a species considered mathematically", Nature **118**, 558–560 (1926).

Wang, H., Y. Kuang and I. Loladze, "Dynamics of a mechanistically derived stoichiometric producer-grazer model", Journal of Biological Dynamics **2**, 3, 286–296 (2008).

Wang, H., R. W. Sterner and J. J. Elser, "On the strict homeostasis assumption in ecological stoichiometry", Ecological Modelling **243**, 81–88 (2012).

Xie, C., M. Fan and W. Zhao, "Dynamics of a discrete stoichiometric two predators one prey model", Journal of Biological Systems **18**, 03, 649–667 (2010).

APPENDIX A

BIFURCATION DIAGRAMS WITH MATLAB AND XPP-AUTO

A.1 DATA COMPUTED WITH MATLAB

The bifurcation diagram of the presented models can be created using MATLAB 8.2, using built in ODE solvers. MATLAB's ODE solvers can handle the nonsmooth dynamics of the minimum functions. It is important to note that all the equilibria data computed this way uses the same initial conditions. Therefore this method will not detect any regions of bistability.

A.2 DATA COMPUTED WITH XPP-AUTO

The bifurcation diagrams of models (3.1) and (4.13) presented in Figures 4.12, 4.13, 4.14 were created using XPP-AUTO and parameter values in Table 4.1. Unlike the method described in section A.1, AUTO can detect regions of bistability. AUTO is better for computing bifurcation diagrams, however, it can not handle the nonsmooth dynamics of the minimum functions as well as MATLAB. Since these systems are nonsmooth one must be cautious about trusting AUTO. To address these concerns we formulated smooth analogs of our models and compared the bifurcation diagrams between the two. We used the following approach to construct smooth analogs to the minimum functions in our models. Consider the smooth approximation to the maximum function of two values a and b,

$$\max\{a, b\} \approx \frac{a^{n+1} + b^{n+1}}{a^n + b^n} \tag{A.1}$$

for n large. We then used the fact that $\max\{a, b\} + \min\{a, b\} = a + b$ to write an expression for the minimum function,

$$\min\{a, b\} = a + b - \max\{a, b\} \tag{A.2a}$$

$$\min\{a, b\} \approx a + b - \frac{a^{n+1} + b^{n+1}}{a^n + b^n} \tag{A.2b}$$

We used this above expression (with large n) to replace all the minimum functions in order to create smooth analogs to our models. Bifurcation diagrams of the smooth analog models were created using AUTO and compared to the bifurcation diagrams of the full nonsmooth models. The behaviors of the bifurcation diagrams created by AUTO were similar when changing the minimum functions to their smooth analogs, see figure A.1. Thus, we feel that none of the observed dynamics are artifacts of the nonsmoothness.

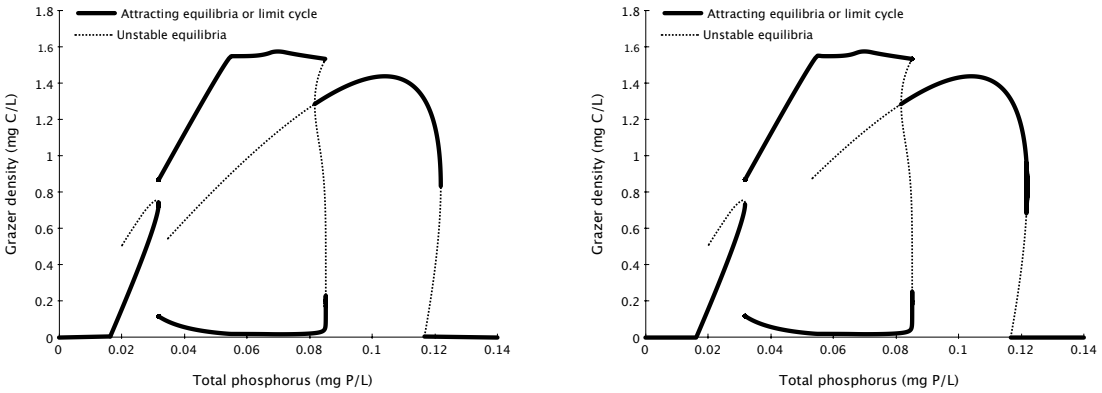

Figure A.1: Bifurcation diagrams of a.) nonsmooth model System (4.13) and it's b.) smooth analog using the approximation in equation (A.2) with $n = 50$. Both diagrams used the same parameter values. Data was generated using XPP-AUTO. The qualitative and quantitative behaviors of both digrams are similar.